Final Report
NASA Grant NAG-1-281

An Experimental Investigation of AS4/2220-3 Graphite Epoxy Woven Fabric Composite Bolted Joints

Dale W. Wilson
R. Byron Pipes

University of Delaware
Center for Composite Materials
201 Spencer Lab
Newark, Delaware 19716

Submitted to
Mr. Benson Dexter
NASA Langley Research Center
Mail Stop 188A
Hampton, Virginia 23665

January 1986

1. Report No.	2. Government Accession No.	3. Recipient's Catalog No.
4. Title and Subtitle An Experimental Investigation of AS4/2220-3 Graphite Epoxy Woven Fabric Composite Bolted Joints		5. Report Date January 1986
		6. Performing Organization Code
7. Author(s) Dale W. Wilson and R. Byron Pipes		8. Performing Organization Report No. CCM-86-07
		10. Work Unit No.
9. Performing Organization Name and Address University of Delaware Center for Composite Materials 201 Spencer Laboratory Newark, DE 19716		11. Contract or Grant No. NASA Grant NAG-1-281
		13. Type of Report and Period Covered
12. Sponsoring Agency Name and Address NASA Langley Research Center Mail Stop 188A Hampton, VA 23665		14. Sponsoring Agency Code
15. Supplementary Notes		

16. Abstract

The influence of design parameters on the strength and failure mode behavior of bolted joints in AS4/2220-3 plain weave fabric graphite epoxy laminates has been investigated. The effects of fastener size, laminate thickness, fastener half spacing and fastener torque were experimentally characterized for two stacking sequence configurations of quasi-isotropic laminates. Qualitative characterization of failure mechanisms and joint strength was performed for laminates configured with varying percentages of angle plies. The experimental data was used to assess the effectiveness of a composite bolted joint strength model based on the application of a quadratic interaction failure criterion on a "critical distance" plane around the loaded portion of the hole. The strength model was found to work when properly calibrated to data for the material system and range of geometric parameters considered.

Evidence suggested that the strength model should not be applied generally without proper calibration in the range of geometry of interest.

17. Key Words (Suggested by Author(s))	18. Distribution Statement
Composite Material, Bolted Joints, Woven Fabric, Failure Analysis	

19. Security Classif. (of this report)	20. Security Classif. (of this page)	21. No. of Pages	22. Price

N-305

FINAL REPORT
NASA Grant NAG-1-281

An Experimental Investigation of AS4/ 2220-3 Graphite Epoxy Woven Fabric Composite Bolted Joints

Dale W. Wilson
R. Byron Pipes

University of Delaware
Center for Composite Materials
201 Spencer Lab
Newark, Delaware 19716

Submitted to
Mr. Benson Dexter
NASA Langley Research Center
Mail Stop 188A
Hampton, Virginia 23665

TABLE OF CONTENTS

RESEARCH OBJECTIVES

The objective of the research reported herein was to experimentally investigate the strength and failure mode behavior of woven fabric composite bolted joints. Experimental studies were conducted on single fastener bolted joints fabricated from Hercules AS4/2220-3 plane weave fabric laminates configured in a quasi-isotropic layup. A careful study of the failure strengths and modes was performed in order to identify the mechanisms involved in the failure process which could then be used in the formulation of an analytical failure model for the analysis of strength in woven fabric bolted joints. The specific research tasks performed in accomplishing the research objectives is summarized below:

1. The basic mechanical properties (E_1, E_2, G_{12}, S_1, S_2, S_6 and ν_{12}) and notched strength properties for the AS4/2220-3 plan weave graphite/epoxy material system were determined.
2. An experimental investigation of the bolted joint strength and failure mode behavior as a function of laminate stacking sequence, fastener diameter, fastener half spacing, bolt torque and laminate thickness was conducted for the AS4/2220-3 plain weave graphite/epoxy material system.
3. Based upon the failure behavior observed in the

experiments a failure model was formulated as a basis for an analytical strength analysis.

4. The failure model was coupled with a stress analysis to form a bolted joint strength model and analytically predicted woven joint behavior compared with experimental results.

LIST OF FIGURES

LIST OF TABLES

1.0 Background

The performance of composite bolted joints is controlled by a complex interaction of discrete failure mechanisms; a condition arising from the heterogeneous anisotropic characteristics of laminated composite systems. Because of this complexity there is still significant reliance upon experimental characterization of bolted joint behavior in the design and analysis of composite bolted joints. While considerable research attention has been devoted to both the experimental and analytical study of bolted joint behavior in continous fiber, nonwoven laminates, little has been published on the performance and behavior of laminates constructed from woven materials. It is worth reviewing the state of the art in composite bolted joints and what the basis for the anticipated differences in woven fabric joint behavior is. In this introductory section the problem description will be given followed by a historical summary of what approaches have been used to date.

1.1 Bolted Joint Mechanics

It is worth describing the full complexity of bolted joint mechanics in order to place the approximate nature of currently used analyses into perspective. The principle elements of the bolted joint geometry are summarized in figure 1.1-1 In the most general case an array

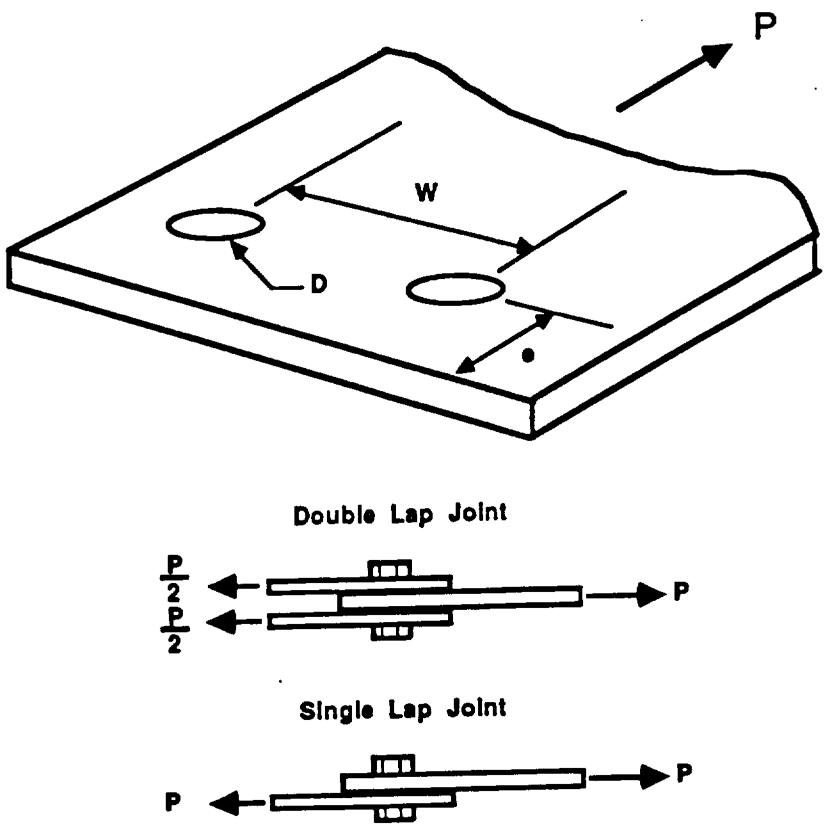

Figure 1.1-1 Description of Bolted Joint Geometry and Loading.

of fasteners with interacting stress fields must be considered. Each fastener in this array interacts with the adherand laminates by tranferring loads through several mechanisms. Within the plane of the laminate normal loads and tangent friction loads are tranferred as shown in figure 1.1-2a which may or may not be constant through the thickness (figure 1.1-1b) depending upon joint configuration (single or double lap) and fastener deformation. Bypass stresses arising from non bolt bearing interactions are also superimposed on the system. For torqued fasteners an additional frictional surface traction transfers load through shear into the inplane stress system. The fastener torque or preload generates an out of plane stress which can be skewed by load eccentricity (single lap joints). The interaction of the fastener with the laminate defines a nonlinear contact problem which is significantly affected by fastener to hole fit as well as load. The composite laminate has anisotropic, inhomogeous properties while the fastener typically possesses isotropic properties. As described the problem translates to a nonlin-ear, laminated, 3-D anisotropic multibody contact problem including friction.

Ultimate failure strength and mode of the joint system is dominated by the material properties, laminate configuration and geometry. For continous fiber constructed

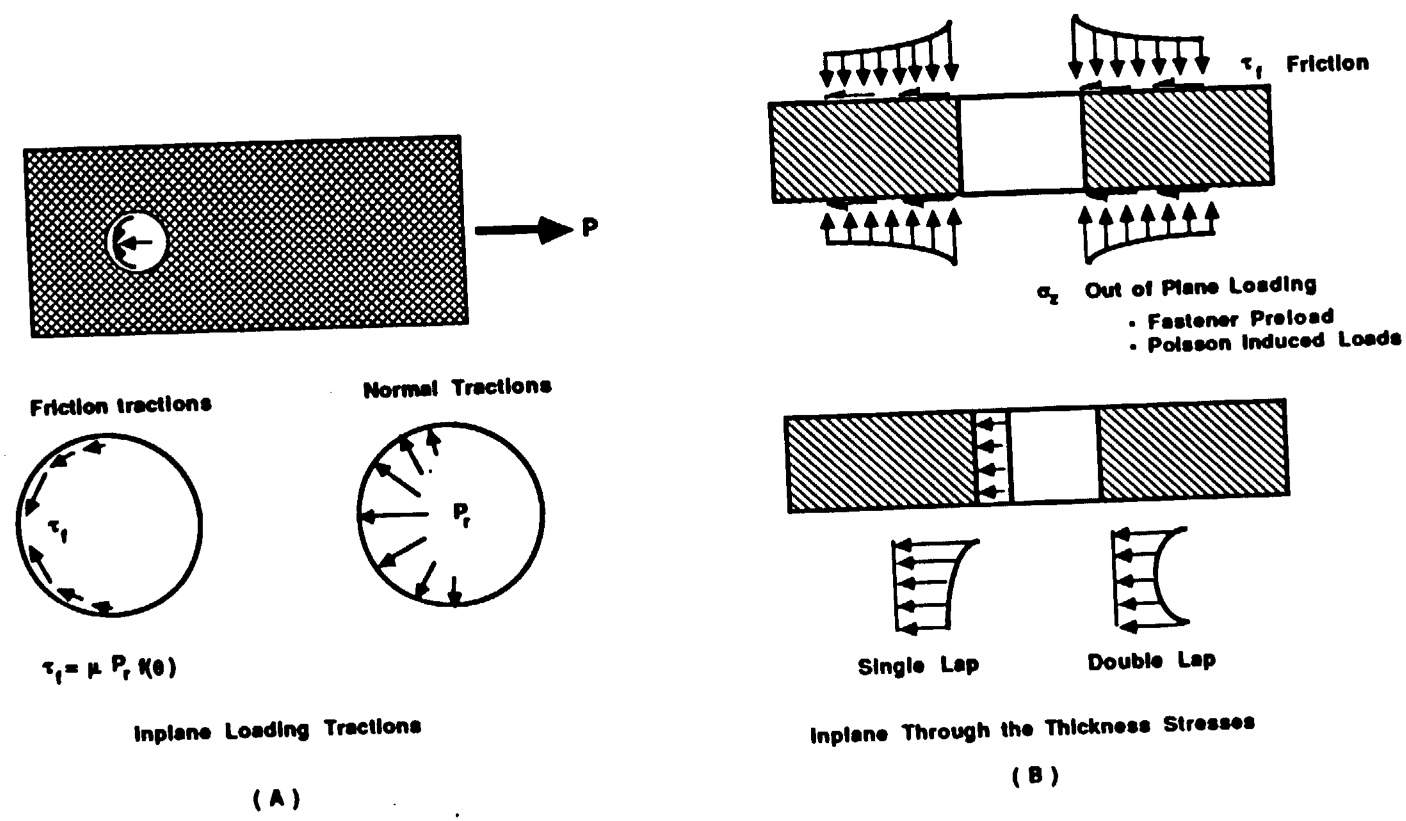

Figure 1.1-2. Descriptions of the loading tractions important in bolted joint analysis.

laminates typical stiffness anisotropy ratios, (E_1/E_2) are 15-20 and strength ratios of 25. Because of this orthotropy, stacking sequence effects can lead to detrimental interlaminar stresses which contribute to lower effective joint strengths. The small inplane anisotropy ratios, stiffness and strength, of fabric plies and the geometric undulation of the fibers have been shown to influence the elastic and strength properties of woven fabric laminates under general inplane loading conditions. While the fabric construction lowers the specific strength and stiffness properties slightly in comparison to unidirectional continuous fiber materials, the interlaminar stresses generated at free edges are smaller which translates to better strength properties for certain laminate configurations and stacking sequences. Additionally, the bidirectional strength integrity of each ply and the lower stiffness may play a role inhibiting damage propagation from the loaded edge of the fastener.

A composite bolted joint strength analysis is composed of a stress analysis, a strength model and a failure hypothesis. Due to the complexity of the joint mechanics, the stress analysis and the strength model only approximate the real system; as a result the failure hypothesis is normally manipulated empirically to corellate with experimentally measured behavior. These semi-empirical approaches are useful in preliminary design but are limited in generality of application requiring appropriate empirical data bases for calibration.

1.2 Summary of Bolted Joint Analysis Techniques

The strength and failure mode behavior of composite bolted joints has been investigated for almost 20 years without the development of an acceptable general strength and failure mode analysis. Early approaches to composite bolted joint design were empirical extensions of basic strength of materials calculations used for metal [1-3]. The analyses identified three distinct failure modes bearing, shearout and net tension with associated failure strengths determined from reduced section stresses. Often ratios between failure strengths and ultimate unnotched tension strengths were used to define stress concentration factors for practical ranges of joint geometry, material system and laminate configuration. Empircal analysis is accurate (provided the experimental data is accurate) and simple to use but requires unacceptably large data bases which are expensive and time consuming to develop and maintain.

For several years investigators attempted to develop more sophisticated strength analyses by improving the stress analysis and employing strength criteria which rely upon basic mechanical properties [4-17]. Early efforts looked at approximate analytical methods, the most significant being an orthotropic 2-D linear elastic plane stress analysis based on a complex variable elasticity solution credited to Leknitski [15]. This analytical solution is for a loaded hole in an infinite plate with finite width correction. Several versions of the analysis have been documented differing mainly in how the boundary conditions are imposed; Waszczak [7] employed a cosine normal stress distribution while Oplinger [5] employed a collocation procedure for spec-ifying the displacements. Collocation procedures have been recently reported by Zhang [16] which incorporated friction between the fastener and hole boundary and Hyer and Clang [17] which incorporated friction, fastener deformation, and contact area effects. In order to obtain more accurate stresses finite element analysis began to dominate the reported research. Still the analyses were predominantly restricted to 2-D linear elastic plane stress solutions assuming perfect fastener fit [4-6, 12, 14, 18, 19]. Again the main differences arise in the choice of boundary conditions. The cosine pressure distribution and fixed displacements along the partial hole boundary dominate the literature. There are three notable exceptions where new approaches have been reported. Matthews, et al [19] developed a special 3-D finite element to analyze stresses in laminated composite bolted joints but did not couple the analysis to a 3-D failure analysis. Springer and Chang [14] have developed a nonlinear finite element model to analyze composite joints and coupled that analysis to the critical distance models described below. Tsujimoto and Wilson [20] developed an elasto-plastic finite element model and coupled it to a damage density criterion.

Several failure models have been coupled to the 2-D stress analyses; Eisenmann and Waddoups employed a linear elastic fracture mechanics (LEFM) criterion. Waszczak used the Tsai-Hill criterion [7] along the hole boundary on a laminate basis and Oplinger the Hoffman criterion [5] on the hole boundary on a ply-by-ply, first ply failure basis. Garbo and Ogonowski [11] incorporated the ability to use maximum stress, maximum strain, Tsai-Hill, Tsai-Wu and Hoffman criteria at constant critical distances from the hole boundary. Their analysis suppressed first ply matrix failure. Soni employed a tensor polynomial strength model with the failure hypothesis that failure occurred at the first location in which the strongest ply at that location failed. The point and average stress criteria have been used by several investigators. Wilson, et al [8,9] and Ramkumar [10] applied the models along specific failure planes corresponding to failure locations for the three primary modes. Chang, Scott and Springer extended the point stress concept to a characteristic curve around the loaded half plane of the fastener and employed the Yamada-Sun strength model in a ply based first ply failure analysis. These semi-empirical strength models can be calibrated to the bolted joint behavior of a given laminate class and material system and have been shown to provide reasonable accuracy for nonwoven laminates. Only basic mechanical property data and bolted joint strength data for two fastener sizes is needed for the calibration of the model. Limitations on the applicability of the semi-empirical models have been shown for certain combinations of laminate configuration and geometry [21] but these models represent an improvement over the previous generation of failure models.

It is the intent of the research reported in this publication to describe the influence of special woven fabric characteristics on the behavior of mechanically fastened joints in plain weave AS4/2220-3 rubber toughened graphite-epoxy material and to develop a suitable strength analysis. The applicability of the new models has not been tested for woven fabric composite systems. In order to develop an analytical failure model to describe the strength and failure mode behavior of composite bolted joints the behavior of bolted joints in a woven fabric system must be experimentally characterized. The relationships between strength, failure mode and geometry determined from experiment along with an understanding of the basic failure mechanisms provide the basis for development of a semi-empirical model for the woven fabric system. Details of the experimental method, the stress analysis, failure model and strength analysis are given in the sections which follow along with a comprehensive discussion of the results.

2.0 Experimental Program

The experimental program which was proposed in this research grant was designed to compliment a much larger comprehensive program which was to be performed at NASA Langley Research Center. The primary objectives of this program's proposed tests were to characterize geometry dependent strength and failure mode behavior and to identify the failure mechanics of the fabric based system.

The experimental program consisted of three basic tasks: 1) the measurement of strength and stiffness properties for the AS4/2220-3 woven fabric system; 2) the characterization of tensile notched strength behavior (unloaded holes); and 3) characterization of bolted joint strength and failure behavior. The test programs are outlined in tables 2.0-1 and 2.0-2. The extent of the proposed test matrix reflects intent of the principal investigators interact with the NASA program to round out the data base. Unfortunately the NASA part of the project was cancelled hence only a partial data base developed for the material.

2.1 Material

At the request of NASA Hercules AS4/2220-3 rubber toughened graphite epoxy prepreg material was chosen for the program. The material was a plain weave fabric woven from

Table 2.0-1

Notched Strength Test Program

Laminate	Thickness	Notched Size	
(0/90/+45/+45/0/09)2s	0.127in(3.2mm)	0.125in(3.2mm)	3
	0.127in(3.2mm)	0.250in(6.4mm)	3
	0.127in(3.2mm)	0.375in(9.5mm)	3
	0.127in(3.2mm)	0.500in(12.7mm)	3
(0/90/+45/+45/0/90)6s	0.382in(9.7mm)	0.125in(3.2mm)	3
	0.382in(9.7mm)	0.250in(6.4mm)	3
	0.382in(9.7mm)	0.375in(9.5mm)	3
	0.382in(9.7mm)	0.500in(12.7mm)	3
(+45/0/90/0/90/+45)2s	0.116in(2.95mm)	0.125in(3.2mm)	3
	0.116in(2.95mm)	0.250in(6.4mm)	3
	0.116in(2.95mm)	0.375in(9.5mm)	3
	0.116in(2.95mm)	0.500in(12.7mm)	3
(+45/0/90/0/90/+45)6s	0.391in(9.93mm)	0.125in(3.2mm)	3
	0.391in(9.93mm)	0.250in(6.4mm)	3
	0.391in(9.93mm)	0.375in(9.5mm)	3
	0.391in(9.93mm)	0.500in(12.7mm)	3

Table 2.0-2

Bolted Joint Test Program

Test Variable	Configuration
Laminate Stacking Sequence	I_x = (0/90/+45/+45/0/90)Ns
	II_x = (+45/0/90/0/90/+45)Ns
	N = 1-6 x - a-g
Fastener Diameter	0.500in(12.70mm)
	0.375in (9.53mm)
	0.188in(4.80mm)
Edge Distance (e/D)	4.0
Fastener Half Spacing (w/D)	3.0
	6.0
Fastener Torque/Clamping Pressure	25, 50, 100in.lb/500psi
	50,100, 100in.lb/1000psi
Laminate Thickness (t/D)	0.33
	0.66
	1.00

3K fiber tows in a standard density of 12 yarns per inch. The first batch of the plain weave fabric was defectively prepreged and in the interim period of waiting for the replacement material (which turned out to be 18 months) a plain weave material of similar construction with Hercules 3501-6 resin was used to perform some testing to evaluate failure mechanics and mechanisms. The cured ply thickness for both prepregs was approximately 0.011 in./ply.

Laminates were made using standard procedures with manual compaction of the plies after the addition of each new ply. The standard processing cycle recommended by Hercules for AS4/2220-3 continuous fiber unidirectional (nonwoven) composites was tried and found to be inadequate in curing the woven fabric panels. Excessive bleeding of the resin from the top surface resulted in poor surface finish and in come cases an excessively dry top surface. A modification to the Hercules cure cycle and bagging procedure was developed to obtain the desired laminate quality and surface smoothness. It is a side bleed technique using caul plates on the top and bottom surfaces. The modified cure schedule is outlined below.

Cure Cycle

Hercules AS4/2220-3 Woven Fabric

1. Place prepreg in vacuum bag and draw vacuum of 30 in. Hg.
   Place system under vacuum in the autoclave.

2. Apply pressure (70-80 psi).

3. Vent vacuum to atmosphere at approximately 20 psi pressure.

4. Begin heating at 3-5°F/min.

5. Hold temperature at 350°F for 2 hours.

6. Cool down to 200°F under pressure (pressure may decay as temperature decreases).

7. Release pressure and remove from the autoclave.

The side bleed bagging arrangement is shown in figure 2.1-1. This arrangement worked well for both fabric based systems. Any bleeder material used on fabric surfaces tends to wick out the resin between the fiber crossover points and result in rough surface characteristics. In order to achieve satisfactory surface smoothness the side bleed bagging technique was employed on the AS4/3501-6 system in combination with the normal cure schedule for the 3501-6 resin system.

2.2 Specimen Fabrication

All of the test specimens were fabricated from panels layed-up and cured according to the procedures described above. Ultrasonic c-scan evaluation was used to evaluate laminate integrity prior to cutting test coupons from the panels. Specimens were not fabricated from flawed panels or portion of panels with flaws.

Since the properties in the warp and fill directions of fabrics are not necessarily the same, the

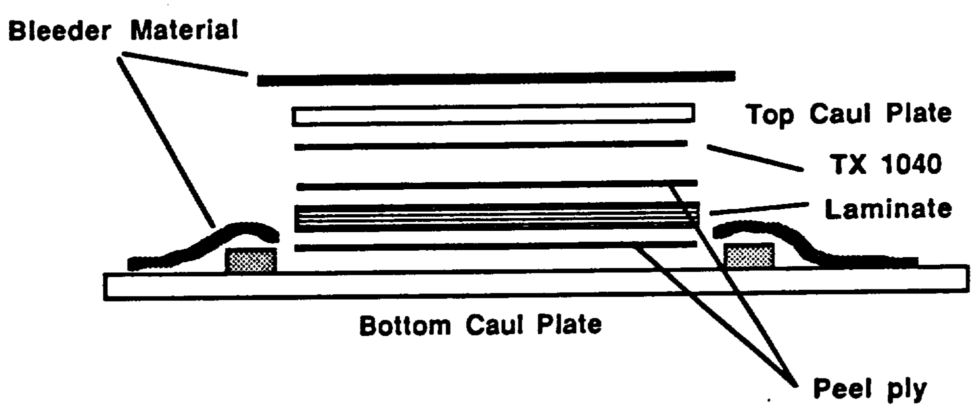

Figure 2.1-1   Processing Bag Arrangement For Side Bleed Cure.

following laminate convention was adopted and used consistently throughout the research program. The warp direction is designated the 1 direction (the direction along the fabric roll) and the fill direction the 2 direction. Each ply of the fabric material therefore consisted of an interwoven (0/90) unit where the 0° degree direction corresponds to the 1 direction. When rotated in the plane 45° the lamina unit becomes a (±45) unit. When fabricating composite laminates care was taken to always maintain the proper orientations of the plies, therefore a $[0/90]_2$ laminate always had the warp direction aligned along the same axis of the laminate and is distinctly different from a [(0/90)/(90/0] laminate in which the warp direction rotates 90°.

For the basic characterization tests a series of $[0/90]_{2S}$ laminates were employed. Specimens were cut from the panels parallel and perpendicular to the warp direction. The tension test specimens, standard 1 in. x 9 in. coupons were cut from the panels using a diamond wafing saw. Each tension specimen was instrumented with a 0/90 strain rosette (Micro-measurements EA-06-125TQ-350) using M-Bond 200 adhesive. Shear properties were measured by the two rail shear test and employed a 3-1/4 in. x 6 in. specimen. The six clearance holes were bored using a diamond core bit. The rail shear coupons were instrumented with a 0/90 strain rosette (same as above) rotated 45° and positioned along the midplane of the test section. Compression properties were measured using a 1/2 in. x 5 in. IITRI specimen with a 5/8 in. gage length. Single longitudinal strain gages (EA-06-062EN-350) were mounted on each surface.

All laminates for the notched strength and bolted joint test programs were of a quasi-isotropic configuration in one of two stacking sequences, $[(0/90)/(\pm45)/(\pm45)/(0/90)]_{ns}$ or $[(\pm45)/(0/90)/(0/90)/(\pm45)]_{ns}$. Different laminate thicknesses were achieved by increasing the number (n) of symmetrically repeated units. Specimens for the notched strength program were fabricated in two thicknesses, 0.128 in. and 0.384 in. All specimens were made 2 in. x 9 in. with the hole located in the center of the test section as shown in figure 2.2-1. Holes of 0.125, 0.250, 0.375 and 0.500 in. were drilled with diamond core bits and inspected both visually and ultrasonically for damage. Three replicates were fabricated for each set of test conditions for a total of 48 specimens.

A sequence of 12 laminates were fabricated for the bolted joint test program. Table 2.2-1 summarizes the laminate configurations and approximate cured thicknesses obtained for each. Single fastener bolted joint specimens were fabricated by curring 12 in. long tensile coupons in two at midspan of the test section. The width of the coupons, size of the fastener holes and location of the fastener holes from the specimen end were made to match the

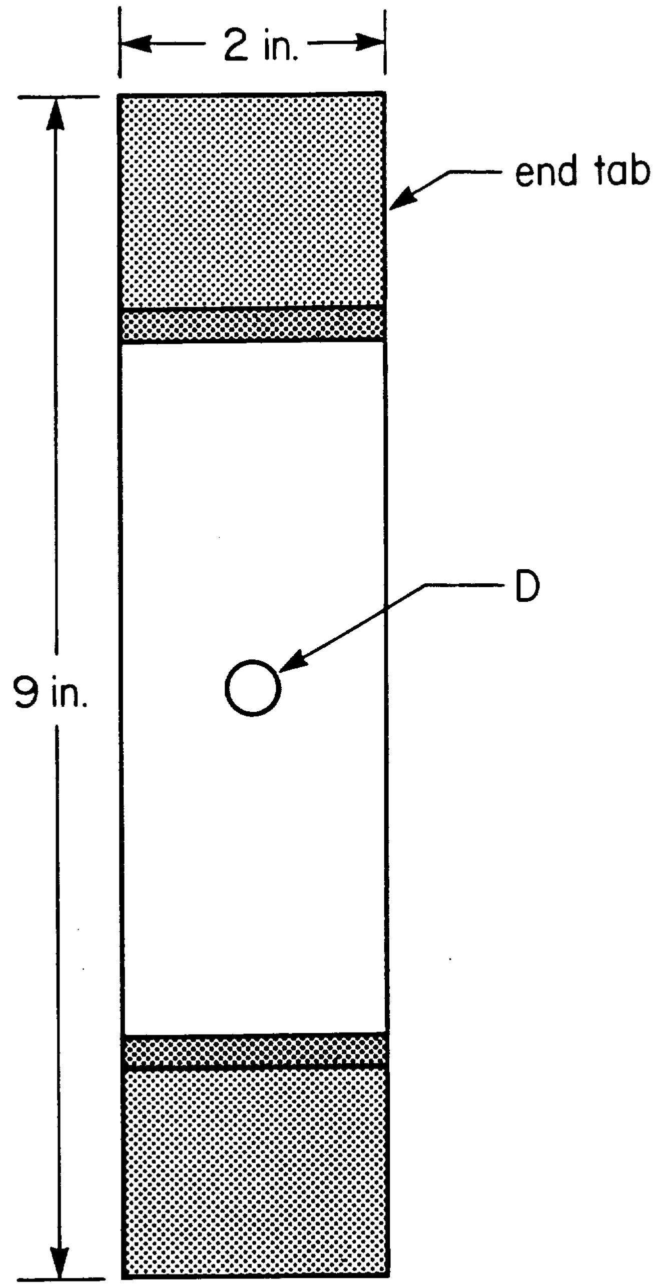

Figure 2.2-1 Test Coupon Geometry For The Notched Strength Tests.

Table 2.2-1

Stacking Sequenc/Cured Thickness

Laminate Code	Stacking Conf.	Cured Thickness
I_a	$[0/90/\pm45/\pm45/0/90]_2$	0.064
I_b	$[0/90/\pm45/\pm45/0/90]_{2s}$	0.128
I_c	$[0/90/\pm45/\pm45/0/90]_{2s}$	0.192
I_d	$[0/90/\pm45/\pm45/0/90]_{4s}$	0.256
I_e	$[0/90/\pm45/\pm45/0/90]_{5s}$	0.320
I_f	$[0/90/\pm45/\pm45/0/90]_{6s}$	0.384
II_a	$[\pm45/0/90/0/90/\pm45]_s$	0.064
II_b	$[\pm45/0/90/0/90/\pm45]_{2s}$	0.128
II_c	$[\pm45/0/90/0/90/\pm45]_{3s}$	0.192
II_d	$[\pm45/0/90/0/90/\pm45]_{4s}$	0.256
II_e	$[\pm45/0/90/0/90/\pm45]_{5s}$	0.320
II_f	$[\pm45/0/90/0/90/\pm45]_{6s}$	0.384

fastener holes from the specimen end were made to match the requirements of the test matrix outlined in table 20-2. The coupon geometry and key dimensional parameters are described in figure 2.2-2. The holes were drilled with diamond core bits and inspected both visually and ultrasonically for damage. Coupons having holes with delamination damage were rejected from the test program. A total of three coupons were fabricated for each test conditons for a total of 216 coupons.

Note that all laminates with thicknesses greater than 24 plies were not tabbed with beveled glass fabric end tabs to introduce the load. Through a small series of tests it was found that the fabric specimens could be griped with emory paper using standard wedge action tension grips with no detrimental effects on the measured failure loads or locations. Results for the untabbed specimens were the same as those of tabbed specimens. Thus, all specimens fabricated with greater than 24 plies were untabbed.

Prior to testing the thickness, width, hole diameter and hole location information for each test specimen was recorded. The important dimensional parameters have been included in the data tables in Appendices A and B.

2.3 Experimental Procedures

Standardized test methods were used in measuring the basic mechanical properties of the AS4/2220-3 woven fabric

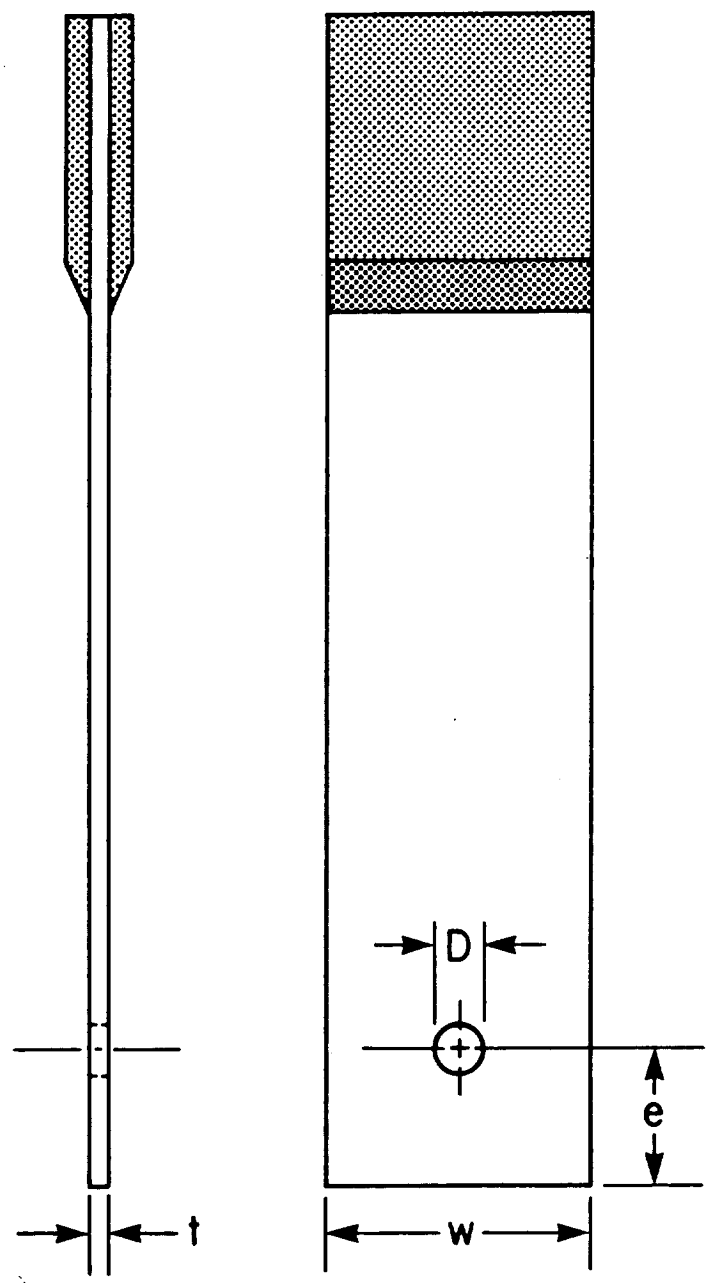

Figure 2.2-2 Bolted Joint Test Coupon Description

material system but special test methods had to be developed for the bolted joint test program. Details of these methods are summarized below.

Materials Characterization

The basic property characterization tests were only carried out for the AS4/2220-3 material system, not the 3501-6 system. Tension tests employed the method specified by ASTM Standard D3039. The compression tests were carried out using the methods specified by ASTM Standard D3410 and the shear tests were carried out using the method prescribed in ASTM Standard D4255. Although these methods do not specifically cover woven fabrics they were applied under the assumption that the fabric material is similar to a 0/90 laminate. The tests were carried out on an Instron Model 1125 Universal Test Machine and a Daytronic Model 3000 strain conditioning system was used to record the strains.

Notched Strength Tests

The notched strength tests were carried out on a 200K Tinius Olsen Test Machine. Specimens were loaded monotonically to failure and the ultimate failure load recorded. Failed specimens were tagged and saved for possible later fractographic analysis.

Bolted Joint Tests

The bolted joint tests were carried out in a single fastener double lap configuration. A special fixture was designed to accomodate the wide range of thicknesses and geometries demanded by the test program. The fixture is shown in figure 2.3-1 and has interchangeable inserts for each fastener size which keep the ratio of the fastener size to the outer diameter of the washer contraint constant at 2.2. High strength steel fasteners obtained from SPS Fasteners in Philadelphia were used to bolt the specimen into the test fixture. Fasteners were torqued to one of the two specified values using a torque wrench. The fit between the fastener and the fastener hole in the laminate was quantitatively documented for each specimen. The joint was monotonically loaded to failure while recording load versus extension behavior. Ultimate load carried by the laminate as well as first load drop off (load at which damage first initiated) values were recorded and reported in the data tables. All failed specimens were saved for possible fractographic analysis.

A set of tests were carried out to measure the corellation between torque and clamping pressure. The bolted joint tests were carried out at constant clamping pressure since the different fastener sizes exert different clamping pressures under conditions of constant torque. Calibration curves were developed for each of the three fastener sizes using the fixture shown in figure 2.3-2. The fasteners were strain gaged on opposing sides of the shaft. Strains were measured for a range of torques and converted to clamping pressures by knowing the modulus and cross sectional area of the bolt.

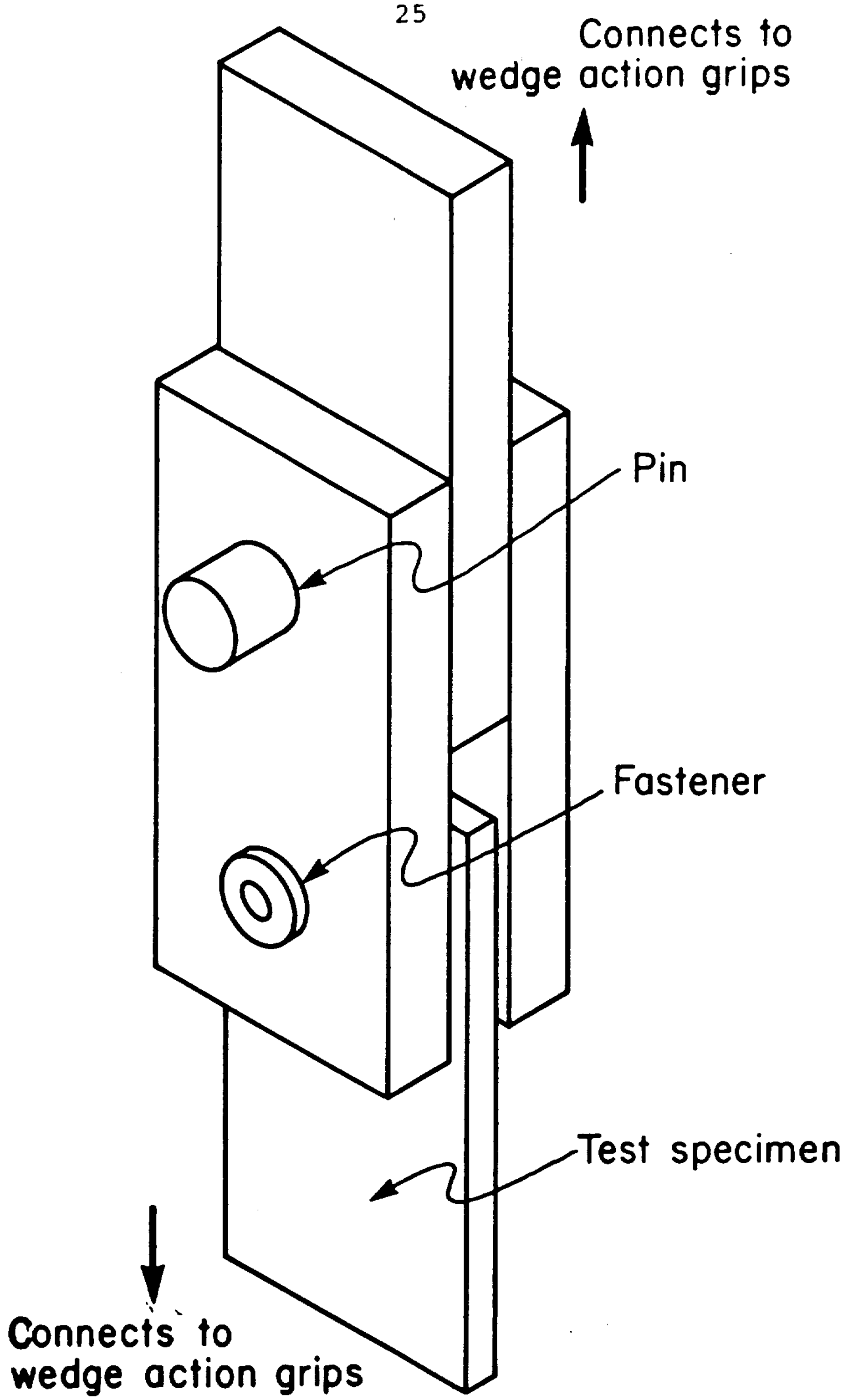

Figure 2.3-1 Bolted Joint Test Fixture.

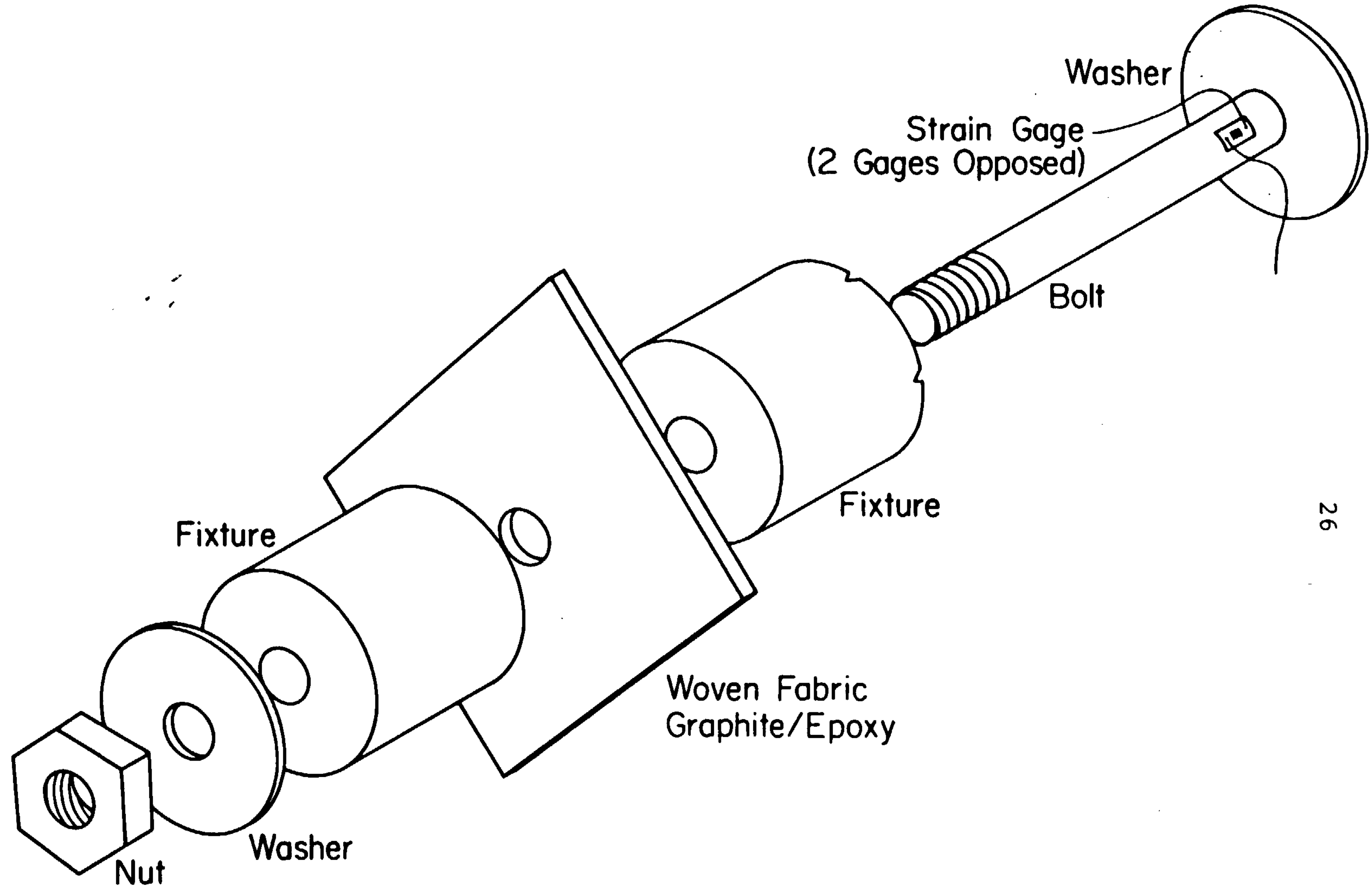

Figure 2.3-2 Fixture Used To Measure The Clamping Pressure As A Function Of Torque.

Some post failure studies were conducted on failed bolt bearing specimens. This was done by sectioning through the suspected damage areas and using optical microscopy. Visual inspection of the damage was also useful in identifying failure modes and locations.

A series of tests were run on AS4/3501 plain weave fabric if similar specifications (two size and years per inch) to study the bearing failure characteristics in woven fabric laminates. The influence of orienting varying percentages of plies at 45° to the loading axis and the influence on load of fastener size on load carrying efficiency was studied as well as characteristics of failure for the laminates of different ply ratios.

A modified IITRRI fixture was used to perform the bolt bearing tests in compression. A figure of the fixture arrangement is shown in figure 2.3-3. Three fastener sizes were investigated, 1/4, 3/8, and 1/2 inches and the bolts were torqued to 150 in. lbs. Load deflection behavior was recorded and the test carried out past the first indications of failure based on load drops or changes in the load-deflection slope. Ultrasonic c-scan techniques followed by sectioning and microscopy were used to characterize the bearing damage at failure.

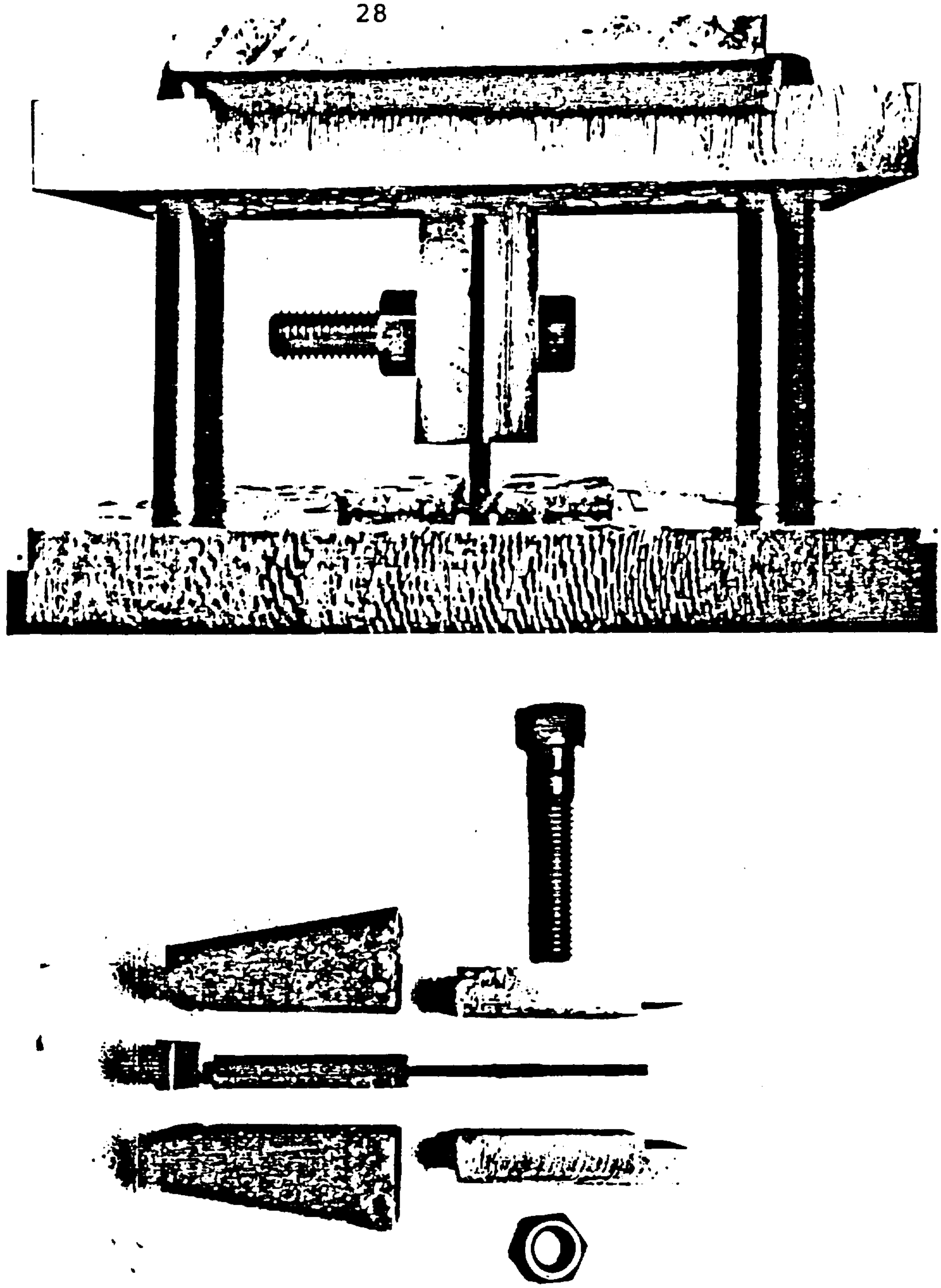

Figure 2.3-3 Fixture Used To Measure Bolt Bearing Strength In Compression.

ORIGINAL PAGE IS
OF POOR QUALITY

3.0 STRENGTH ANALYSIS FORMULATION

The bolted joint strength analysis formulated for the laminated woven fabric composites investigated in this research program was based on a 2-D linear elastic stress analysis employing a point stress failure hypothesis coupled to a quadratic interaction strength model. This analysis is consistant with the proposed experimental program which provides all of the necessary empirical paramters for the development of the strength model. A brief outline of the stress analysis derivation and strength model development is summarized below.

3.1 Stress Analysis

The stress analysis employed is a 2-D linear elastic plane stress formulation based upon the superposition of complex variable elasticity solutions of loaded and unloaded holes in infinite orthotropic plates. It is similar to the analysis employed by Waszcazk [7] modified to include a finite width correction, but no correction for finite length. Loading along the hole boundary was approximated by a cosine stress distribution which ignored friction tractions and assumed perfect fastener fit. The detailed derivation of this stress analysis is well documented but is briefly outlined here.

A stress function F is chosen such that equilibrium and compatibility requirements are met when the generalized biharmonic equation for an anisotropic plate is satisfied

$$S_{22} \frac{\partial^4 F}{\partial x^4} - 2S_{26}\, \partial x^3 \partial y + (2S_{12} + S_{66}) \frac{\partial^4 F}{\partial x^2 \partial y^2} - 2S_{16} \partial^4 F/\partial x \partial y^3$$
$$- 2S_{11} \frac{\partial^4 F}{\partial t^4} = 0 \qquad (3.1\text{-}1)$$

where the S_{ij} are the laminate compliances. The mathematical form of F depends upon the roots of the characteristic equation generated by the biharmonic equation (1) which is given below:

$$S_{11}R^4 - 2S_{16}R^3 + (2S_{12} + S_{66})\, R^2 - 2S_{26}R + S_{22} = 0 \quad (3.1\text{-}2)$$

The solution of the characteristic equation yields a set of complex conjugate roots, R_1, R_2, R_1, R_2 from which the stress function can be expressed as

$$F = 2\ \mathrm{Re}\ [F_1(a_1) + F_2(z_2)] \qquad (3.1\text{-}3)$$

where $F_1(z_1)$ and $F_2(z_2)$ are analytic functions of the complex coordinates $z_1 = X + R_1\, y$ and $z_2 = x + R_2\, y$ respectively. To simplify the expression, the following functions are defined:

$$\phi_1\ (z_1) = \frac{\partial F(z_1)}{\partial z_1} \qquad \phi_2\ (z_2) = \frac{\partial F(z_2)}{\partial z_2} \qquad (3.1\text{-}4)$$

The stresses and displacements written in terms of these functions are:

$$\sigma_x = \partial^2 F/\partial y^2 = 2\ \mathrm{Fe}\ [R_1{}^2 \phi_1{}'(z_1) + R_2{}^2 \phi_2{}'(z_2)]$$

$$\sigma y = \partial^2 F/\partial x^2 = 2 \text{ Fe } [\phi_1'(z_1) + \phi_2'(z_2)]$$

$$\tau_{xy} = \partial^2 F/\partial x \partial y = -2 \text{ Re } [R_1 \phi_1' (z_1 = R_2 \phi_2'(z_2)]$$

$$u = 2 \text{ Re } [P_1 \phi_1 (z_1) + P_2 \phi_2 (z_2)] \qquad (3.1\text{-}5)$$

$$v = 2 \text{ Re } [Q_1 \phi_1 (z_1) + Q_2 \phi_2 (z_2)]$$

where

$$P_1 = S_{11} R_1^2 + S_{12} - S_{16} R_1$$

$$P_2 = S_{11} R_2^2 + S_{12} - S_{16} R_2$$

$$Q_1 = S_{22}/R_1 + S_{12} R_1 - S_{26} \qquad (3.1\text{-}6)$$

$$Q_2 = S_{22}/R_2 + S_{12} R_2 - S_{26}$$

Rigid body rotations and displacements have been neglected in equations (5). By employing the mapping function

$$\xi_k = \frac{z_k \pm \sqrt{^2 z \; ^2_{-} a \; - R_k^2 a}}{a(1 - i R_k)} \qquad k=1,2 \qquad (3.1\text{-}7)$$

the circular boundary of the fastener hole of radius a in the z_k plane is mapped onto a unit circle in the ξ_k plane (k=1,2) which effectively nondimensionalizes hole size in the problem. For a given value of z_k two values of ξ_k are obtained, the one which maps into the region outside the unit circle is the one of interest.

In order to solve for the stresses a solution must be obtained for the stress functions $\phi(z_i)$ where i-1,2.

Requiring that all the stress components be real and single valued for a loaded hole in an infinite plate with stress free boundaries results in solutions for ϕ_i of the following form:

$$\phi_1(z_1) = B_1 z_1 + A_1 \ln \xi_1 + \sum A_{1m} \xi_1^{-m} \quad , \text{ for } m = 1,\infty$$

$$\phi_2(z_2) = B_2 z_2 + A_2 \ln \xi_2 + \sum A_{2m} \xi_2^{-m} \quad , \text{ for } m = 1,\infty \qquad (3.1\text{-}8)$$

The linear z_1 and z_2 terms are necessary for a uniform stress at infinity and the ln ξ_i terms contribute only when the applied stress on the hole bondary is nonzero. The series of coefficients under the summation are determined from the boundary conditions.

The solution for an infinite plate with an unloaded hole subjected to a far field stress oriented at some arbitrary angle α to the axis defined for the plate results in the following stress functions:

$$\phi_1(z_1) = \frac{iPa^2(1-iR_1)}{4(R_1-R_2)} \left[\frac{R_2\sin 2\alpha+2\cos^2\alpha+i(2R_2\sin^2\alpha+\sin 2\alpha}{z_1+\sqrt{z^2-a^2-R_1^2a^2}}\right]$$

$$\phi_2(z_2) = \frac{iPa2(1-iR^2)_2}{4(R_1-R_2)} \left[\frac{R_1\sin 2\alpha+2\cos^2\alpha+i(2R_1\sin^2\alpha+\sin 2\alpha}{z_2+\sqrt{z^2-a^2-R_2^2a^2}}\right] \qquad (3.1\text{-}9)$$

The solution for a loaded hole in an infinite plate was obtained by specifying a cosine stress distribution along the load bearing surface of the hole. At infinity the boundary of the plate is stress free thus the linear terms are dropped. The displacements along the hole boundary must be single valued since stress equilibrium requirements are not met. The coefficients of the terms are then found from the following set of simultaneous equations.

$$A_1-\bar{A}_1+A_2-\bar{A}_2 = \frac{P_y}{2\pi i}$$

$$R_1A_1-\bar{R}_1\bar{A}_1 + R_2A_2-\bar{R}_2\bar{A}_2 = \frac{-P_x}{2\pi i}$$

$$R_1{}^2A_1-R_1{}^2\bar{A}_1+R_2{}^2A_2R_2{}^2\bar{A}_2 = -S_{12}P_Y-\frac{S_{26}P_x}{2\pi iS_{22}} \tag{3.1-10}$$

$$A_1/R_1-\bar{A}_1/\bar{R}_1+A_2/R_2-\bar{A}_2/\bar{R}_2 = S_{12}P_x+\frac{S_{26}P_y}{2\pi iS_{22}}$$

The terms P_x and P_y are the net force resultants on the internal boundary of the hole in the x and y directions respectively. Similarly, by expressing the radial stresses on the hole boundary in terms of Fourier series and equating with the series terms in the stress function solution the coefficients A_{1m} and A_{2m} were obtained. The results are:

$$A_{12} = aPi\ (1+iR_2)/[16(R_2-R_1)]$$

$$A_{22} = aPi\ (1+iR_1)/[16(R_2-R_1\ ] \tag{3.1-11}$$

$$A_{1m} = A_{2m} = 0 \qquad \text{for } m = 2,46....$$

$$A_{1m} = -aP_i(-1)^{(m-1)/2}(2+imR_2)/[\pi m^2(m^2-4)(R_2-R_1)]$$

$$A_{2m} = -aP_i(-1)^{(m-1)/2}(2+imR_1)/[\pi m^2(m^2-4)\ (R_2-R_1)] \tag{3.1-12}$$

for $i = 1,3,5....$

This completes the solution for the linear elastic stresses in an infinite, two-dimensional, anisotropic materials with a circular loaded or unloaded hole. This solution assumes homogeneity but remains valid for symmetric laminates by using effective laminate elastic contants determined by classical laminated plate theory. Assuming the plate strains, determined from the midplane displacements, to be constant through the laminate thickness, classical lamination theory is invoked to find the stresses in each layer and lamina strains along the principal material directions. The total state of stress is obtained by the superposition of the loaded and unloaded hole solutions.

The constitutive relationship for an orthotropic sheet which defines the stresses in terms of the lamina stiffnesses and midplane strains is:

$$\{\sigma_i\}^k = [Q'_{ij}]^k\{\varepsilon_j'\}^k \qquad (3.1\text{-}13)$$

where the $\{\sigma'_i\}^k$, $[Q'_{ij}]^k$ and $\{\varepsilon_j'\}^k$ are the stresses, stiffnesses, and strains respectively, for the k^{th} ply in the laminate coordinate system. Stresses in the lamina coordinate system, were obtained through the normal transformation relations for orthogonal materials

$$\{\sigma_i\}^k = [T]^k\{\sigma_i'\}^k \qquad (3.1\text{-}14)$$

$$\{\varepsilon_j\}^k = [T^*]^k\{\varepsilon_j'\}^k$$

where $[T]^k$ and $[T^*]^k$ represent the stress and strain transformation matricies respectively and the primes denote components in the laminate coordinate system.

Finite width effects are significant for some combinations of orthotropy and geometry which are in the range of realistic designs hence a correction factor is developed for finite width effects. The correction is developed by performing a superposition of loaded and unloaded hole solutions with the following boundary conditions: for the loaded hole the bolt load, P, is reacted by tensile and compressive loads of P/2 at $+\infty$ and $-\infty$ respectively; the unloaded hole is given tensile stresses per unit thickness of P/2 at $\pm\infty$. The net result is that the bolt load is reacted by a stress at infinity which more closely approximates the finite width solution; the correction however does not produce an exact solution since the normal and shear stresses do not go to zero on the edges of the plate. Comparisons with finite element results showed that for the laminates analyzed the stresses predicted by this analysis for geometries in the range $2 < w/D < 8$ were reasonably accurate.

The properties used in this study were those measured for the AS4/2220-3 graphite epoxy woven fabric material. Since the stress solution was for a homogeneous orthotropic material, the effective laminate properties for each laminate configuration were determined using laminate analysis for input into the stress analysis.

3.2 Failure Model

The failure model is composed of the failure hypothesis and strength model. The failure hyothesis employed in this study was the point stress hypothesis developed by Nuismer and Whitney [22] and later modified by Pipes, et al [23]. In essence the hypothesis is that failure of a notched laminate occurs when the stress at a critical distance, d_o, from the notch edge along the net tension failure plane reaches the unnotched strength of the laminate. The critical distance parameter, d_o, is a function of notch radius, R, and is defined in the following form [23]

$$d_o = 1/C(R)^m \tag{3.2-1}$$

where the two empirical parameters m and C above are determined by experiment. The above definition of failure corresponds to the coupling of the point stress hypothesis with the maximum stress failure criterion and is based on a single mode (tensile) failure through the notch. It has been successfully applied on a laminate basis and for 0 and 90° lamina but has not been verified for cases of off-axis angle plies which exhibit mixed mode fracture resulting from multiaxial states of stress. It has also not been shown to be valid for bolted joints in woven fabric composites laminates.

An extension to the point stress concept has been proposed [8-11] which defines d_o as a function of θ, the polar position around the loaded half of the fastener hole. This extension along with the assumption of ply-by-ply analysis violate the original assumptions of single mode failure. Several variations of strength criteria have been employed to handle the stress interactions and their contributions to mixed mode failure. The Tsai-Hill criterion was used in this program since the approximate equivilence of the quadratic interaction criteria in combination with a point stress hypothesis has been shown for bolted joint strength analysis [21].

In two dimensions the mathematical form of this criterion is summarized below:

$$\sigma \pm \frac{(\sigma_1)^2}{F_1} + \frac{(\sigma_2)}{F_2^2} + \frac{(\tau_{12})^2}{F_{12}} - \frac{\sigma_1 \sigma_2}{F_1^2} = 1 \qquad (3.2\text{-}2)$$

where

F_{12} = lamina sheer strength

F_1, F_2 = lamina strength in the 1 and 2 directions respectively, where tension and compression allowables are employed depending on the sign of the stresses. The stress components are the ply stresses determined at the critical distance, d_o. Thus, the strength model developed by combining the critical distance hypothesis with the Tsai-Hill criterion is

$$\sigma_{ij}(r,\theta)\Big|_{r=r_o+d_o} = \sigma \qquad (3.2\text{-}3)$$

which says that failure will occur when the stresses at some position r,θ result in a value of $\sigma > 1$. The critical distance parameter d_o is a function of θ for continuous fiber composite laminates and thus was assumed to be of the following mathmatical form based on findings from unidirectional research.

$$d_o = f(R,\theta) \qquad (3.2\text{-}4)$$

This hypothesis was tested and the function $F(R,\theta)$ determined from the experimental data and a series of parameter studies which analyzed the relationship of strength to constant critical distance parameter.

A modified ply-by-ply strength analysis similar to that of Garbo and Ogonowski [8] was employed which predicts failure based on first ply failure excepting matrix tension failure. The elimination of matrix tension failure was accomplished by forming failure ratios R_x, R_y, and R_{xy} which quantify the contribution of each respective stress component in the failure criterion. The general form of these relations are

$$R_x = \frac{\sigma_1}{X_{1\sigma}} \qquad R_x = \frac{\sigma_1}{X_{2\sigma}} \qquad R_x = \frac{\tau_{12}}{X_{12\sigma}} \qquad (3.2\text{-}5)$$

where σ= the value determined from the quadratic interaction criterion employed. If $R_y/(R_x+R_y+R_{xy})>0.5$ or $R_y>R_x$, R_y then failure is considered a matrix tension failure. When a matrix tension failure occurs, the transverse allowable, $X_2{}^t$, is increased by a factor of 1.1 and calculations repeated until $X_2{}^t = X_2{}^c$ after which matrix tension failure is permitted.

The stresses within each ply may be determined and failure criterion applied at any location r,θ around the fastener hole to plot ply-by-ply failure maps for the joint for a specified applied load or the load may be iterated until first failure is predicted and the failure stress and location determined. The failure maps do not account for stress redistribution due to the damage and thus are only approximate.

3.3 Bearing Failure Model

To model the bearing strength, a semi-empirical approach developed by Collings [24] for continuous fiber laminates which utilizes a ply bearing factor K_0 that is dependent upon the laminate configuration was modified for application to fabrics. The ply bearing factor is defined as

$$K_0 = \frac{\sigma_c}{\sigma_{b090}} \tag{3.3-1}$$

where a σ_{090} is the average bearing stress in the (0/90) plies at failure and is σ_c the ultimate compression strength of the basic 0/90 fabric lamina. In a laminate which is composed of (0/90) plies and ($\pm$45) plies the following linear relationshp is used to define K_0 as a function of the percentage of $\pm$45° plies

$$K_0 = \frac{[\sigma_c(100-\phi)+\phi\sigma_{b090}}{100\ \sigma_{b090}} \qquad (3.3\text{-}2)$$

where ϕ is the percentage of $\pm$45° plies in the laminate. The bearing strength is then determined as a funciton of the ratio of (0/90) and ($\pm$45) plies from

$$\sigma b = \frac{1}{t} \left[\frac{t_{090}\sigma_c}{K_0} + t_{45}\sigma_{b45}\right] \qquad (3.3\text{-}4)$$

where σ_{b45} is the bearing strength for an all $\pm$45 laminate. This simple model was compared with experimental results for three fastener sizes.

4.0 RESULTS AND DISCUSSION

4.1 Materials Characterization

Basic lamina mechanical properties are necessary as input for stress analysis and for the normalizaiton of the bolted joint strength results. The basic mechanical properties of an AS4/2220-3 woven fabric composite lamina were measured using standard testing procedures. The results of these tests were given in table 1-1. Each entry in table 4.1-1 is the average of three data points and as shown the variation in the data was low. The inplane tensile moduli are almost identical in the warp and fill directions while there is a small (4%) difference in strength. The measured compression modulus is 14% lower than the tensile modulus and the strength is 20% lower in compression while the difference between the compression properties in the warp and fill directions is negliable.

These results for the plain weave fabric composite verify that the material is approximately isotropic in the mutually perpendicular directions aligned with the fibers in the plane. It is important to note that the material response appears to be bimodular; it exhibits different moduli in tension and compression. Also, as expected, the compression strength is lower than the tension strength. The difference in compression strength is not significantly more than that often measured for unidirectional composites

Table 4.1-1

Summary of Mechanical Properties

for Hercules AS4/2220-3 Fabric

Property	English		S.I.	
	Ave.	St.D	Ave.	St.D
E_1^T	9.29 Msi	0.4	64.0 GPa	2.8
E_1^C	7.96 Msi	0.05	54.9 GPa	0.65
E_2^T	9.28 Msi	0.2	64.0 GPa	1.32
E_2^C	7.87 Msi	0.08	54.1 GPa	0.55
ν_{12}	0.05 Msi	0.01	0.05	0.01
ν_{21}	0.04 Msi	0.01	0.04	0.01
G_{12}	0.69 Msi	0.06	4.73 GPa	0.3
S_1^T	119.9 Ksi	3.4	826.6 MPa	23.1
S_1^C	98.2 Ksi	0.9	677.3 MPa	64.7
S_2^T	124.3 Ksi	1.9	857.9 MPa	13.3
S_2^C	86.9 Ksi	7.0	599.3 MPa	48.1
S_6	16.8 Ksi	1.3	116.0 MPa	8.0

and is not necessarily a result of the fiber undulations. There was no obvious knee in the stress-strain curve for the tension tests but there is some indication of nonlinearity in the compression stress-strain curve. The slight difference in strength between the warp and fill directions may be due to the handling of the fibers and/or tension differences in the two directions during the weaving process.

A less extensive set of properties was measured for the AS4/3501-6 system used for a small number of bearing strength characterization studies and the results are summarized in table 4.1-2. For this material the difference in properties in the warp and fill directions is more pronounced but the difference between tension and compression properties is much lower. It is important to point out that the magnitudes of the properties are comparable to those measured for the AS4/2220-3 material.

4.2 Notched Strength Results

The notched strength behavior was measured because it provides an indication of the materials sensitivity to failure initiation at stress concentration sites under much better defined conditions than bolt loaded holes. The data also provides a mechanism for comparing tension field notch sensitivity to loaded hole strength behavior. The identification of a relationship between loaded and

Table 4.1-2

Summary of Mechanical Properties

for Hercules AS4/3501-6 Fabric

Property	English	S.I.
E_1^T	8.86 Msi	61.1 GPa
E_2^C	8.37 Msi	57.7 GPa
E_2^T	7.90 Msi	54.5 GPA
E_2^C	7.65 Msi	52.7 GPa
G_{12}	0.98 Msi	6.8 GPa
S_1^T	101.1 Ksi	697.1 MPa
S_1^C	96.5 Ksi	665.4 MPa
S_2^T	72.9 Ksi	502.6 MPa
S_2C	68.9 Ksi	475.1 MPa
S_6	13.7 Ksi	71.5 MPa

unloaded notched strength, if such a relationship exists, would help to simplify the data requirements for bolted joint design and analysis.

Notched strength tests were run for two laminate stacking sequences and two laminate thicknesses (refer to table 2.0-1). The notched strength data are presented in figure 4.2-1 for all four test specimen configurations. From the results it is apparent that both laminate thickness and stacking sequence influenece notched strength. For both stacking sequences there was approximately an 8-10% difference in measured strength at small notch radii while the difference is smaller, if not negligable, at the larger radii. The stacking sequence effect appeared nonexistant for the thin laminates but became significant for the thicker laminate pair. The smallest notch size (3.2mm) reduced the laminate strength to 45-50% of the unnotched strength after which increasing notch size further decreased strength.

The values of the notch sensitivity parameter, C and the exponential factor, m are given in figure 4.2-1. (With the exception of laminate 1_b the values of m are similar suggesting that the slopes of the curves are similar. These parameters along with $K_{T\infty}$ were used to generate the notched strength curves (solid line) shown in the figure according to the relationship

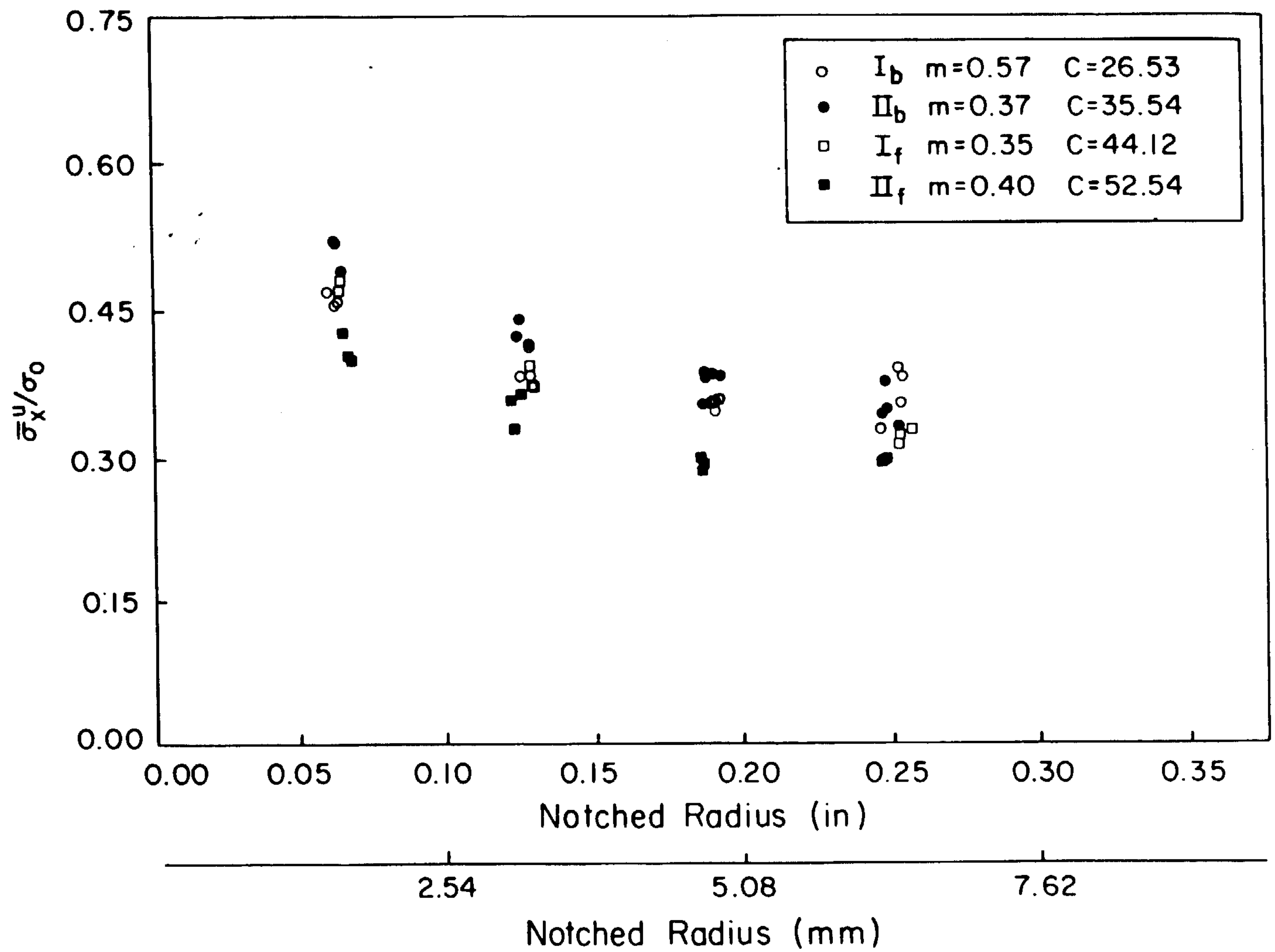

Figure 4.2-1 Ultimate Strength As A Funciton Of Hole Size, Unloaded Holes.

$$d_0 = 1/C\ (R^m) \qquad (4.2\text{-}1)$$

$$\sigma_N/\sigma_0 = 2\{2+(1+C^{-1}R^{m-1})^{-2}+3(1+C^{-1}R^{m-1})^{-4}$$
$$-(K_T^\infty-3)[5(1+C^{-1}R^{m-1})^{-6}-7(1+C^{-1}R^{m-1})^{-8}]\}^{-1} \qquad (4.2\text{-}2)$$

where $K_T^\infty = 1+\{2[(E_y/E_x)^{0.5}-\nu_{xy}]+E_y/G_{xy}\}$ (4.2-3)

and the terms E_x, E_y, ν_{xy} and G_{xy} are the effective engineering elastic constants for the material.

4.3 Bolted Joint Strength Results

The bolted joint program was designed to measure the strength and failure mode behavior as a function of t/D, W/D, fastener diameter, laminate stacking sequence and fastener torque. In addition, a series of special compression tests were run to characterize the mechanics of the bearing failure mode and investigate the applicability of Collings' [ ] proposed failure model to fabric based laminates.

Over the range of geometries tested in this program only net tension and bearing failure modes were observed. No shearout failures occurred, possibly due to the 0/90 construction of the fabric. Figure 4.3-1 shows typical net tension and bearing failure modes for the fabric specimens. In Appendix A a complete tabulation of all the test data from the bolted joint tests is given. Figures

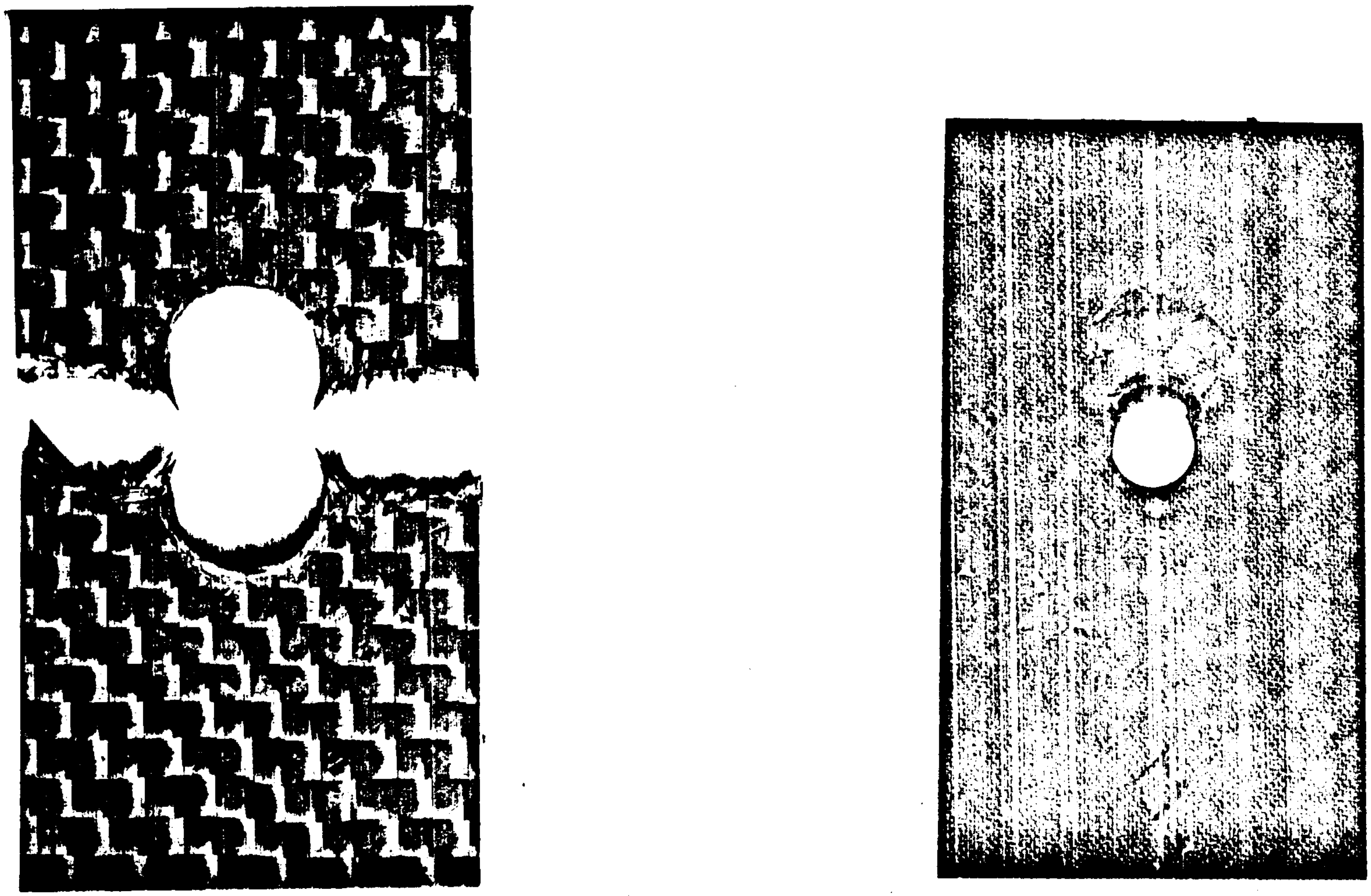

Figure 4.3-1   Photograph Of Bearing And Net Tension Failure Modes In Bolted Joint Specimens.

summarizing some of the important trends and relationships are used in the discussion of results which follows.

Influence of Fastener Diameter

Figures 4.3-2 through 4.3-5 show the influence of fastener diameter on ultimate far field stress (which will be termed strength) developed in the test coupons under conditions of constant thickness to fastener diameter and fastener half spacing, t/D and w/D, respectively. Note that with t/D=0.33 for both stacking sequences clamping pressures, strength decreased linearly with increasing fastener diameter. The apparent deviation from linearity seen in figure 4.3-2 is an artifact of fastener fit which arises for the net tension failure mode. The 0.25 in. and 0.50 in. fasteners had 0.005 in. more clearance than the 0.375 in. fastener. For net tension failure for the larger clearance fastener diameters, the failure location shifted from the minimum cross section and the resulting increase in load carrying cross sectional area allowed larger failure strengths. The effect was not noticed for the w/D=6.0 results since the failure mode was bearing. The results for t/D=0.66 generally agree with those of the smaller t/D.

A comparison of the results reveals that different stacking sequences and clamping pressures do not appear to have a significant influence upon joint strength or the relationship of strength to fastener diameter.

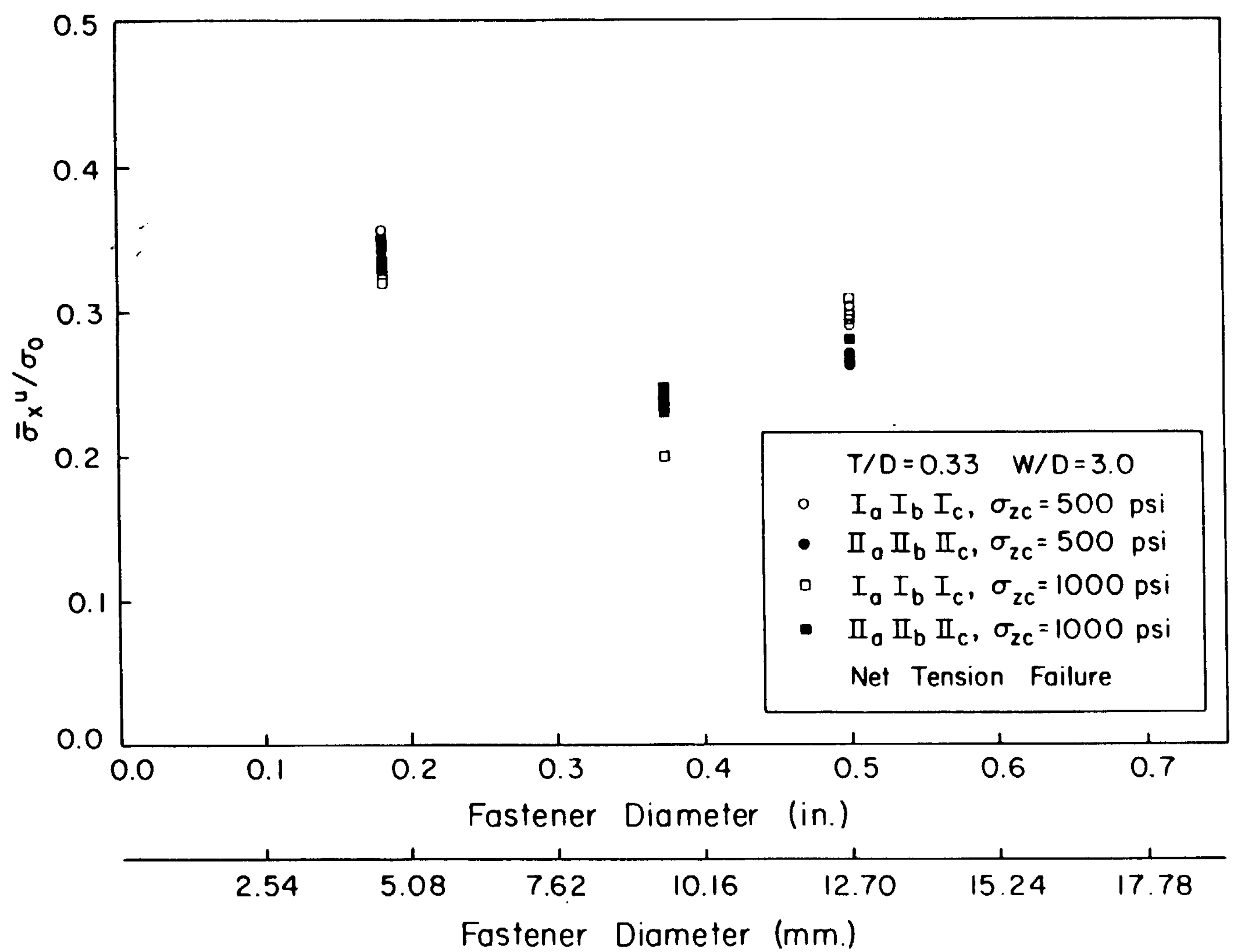

Figure 4.3-2 Influence Of Fastener Size On Bolted Joint Strength, t/D=0.33, w/D=3.

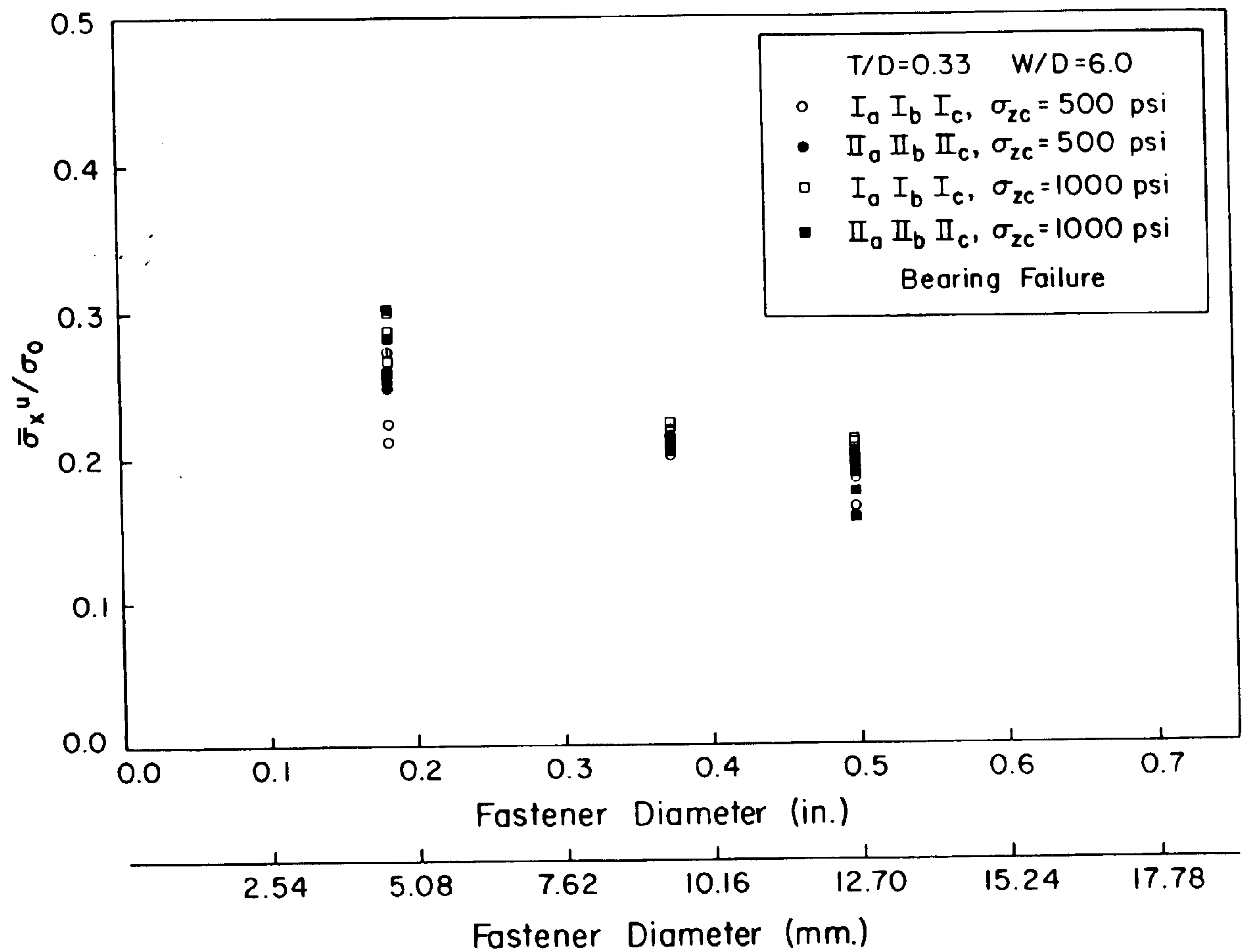

Figure 4.3-3 Influence Of Fastener Size On Bolted Joint Strength, t/D=0.33, w/D=6.

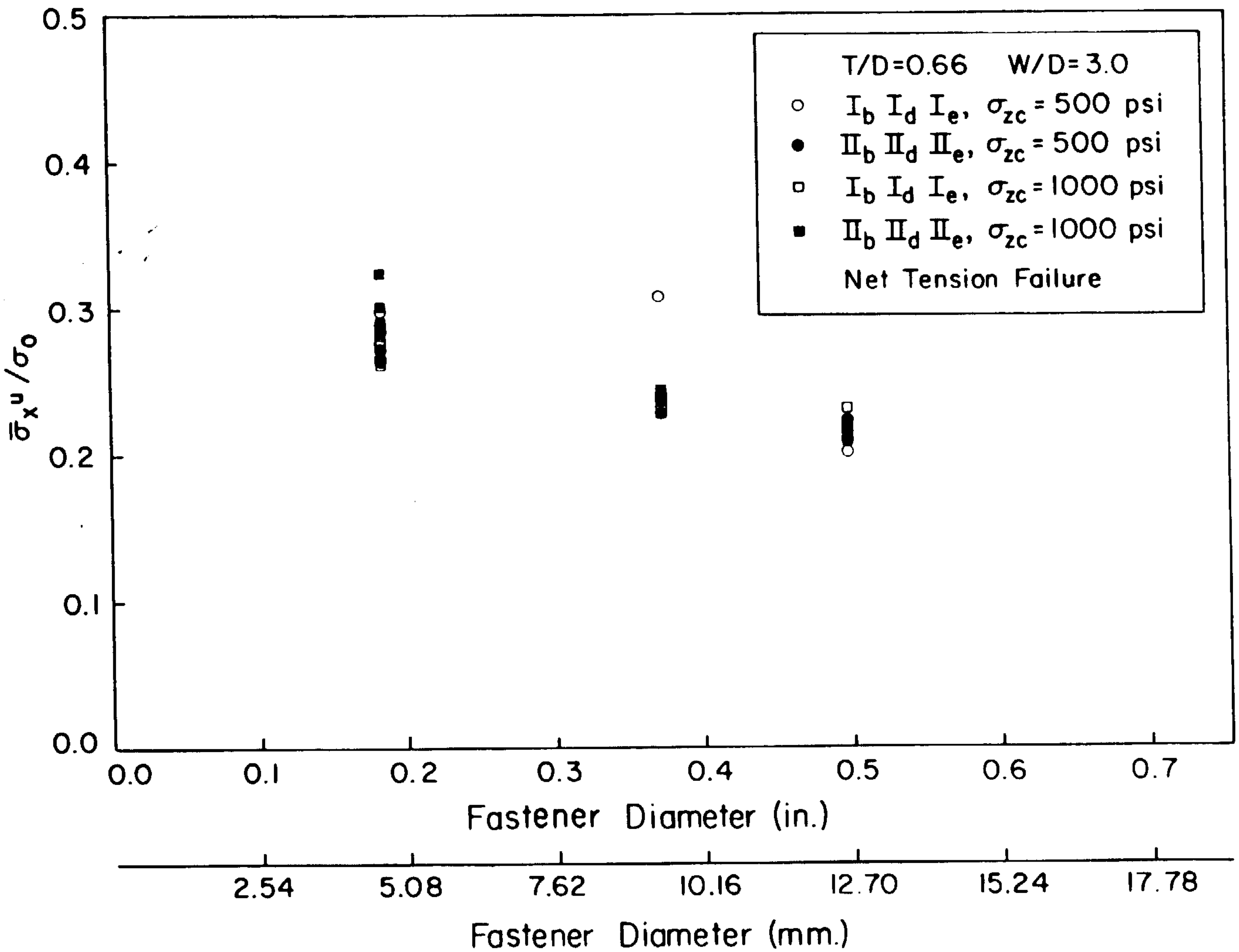

Figure 4.3-4 Influence Of Fastener Size On Bolted Joint Strength, t/D=0.66, w/D=3.

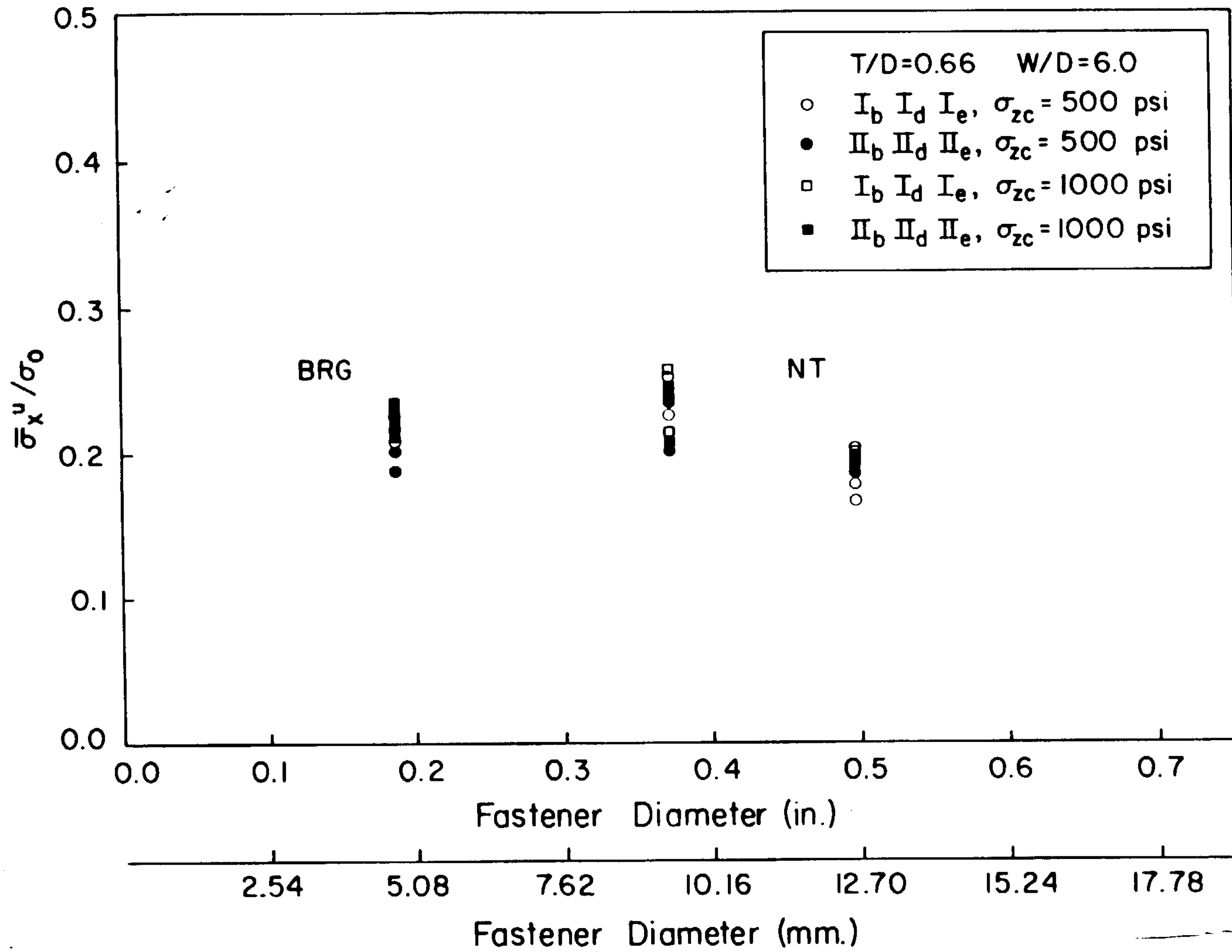

Figure 4.3-5 Influence Of Fastener Size On Bolted Joint Strength, t/D=0.66, w/D=6.

Influence of Fastener Half Spacing

Results summarizing the influence of fastener half spacing upon strength and failure mode are presented for three fastener sizes with constant t/D ratios of 0.33 and 0.66. Figures 4.3-6 through 4.3-11 show the results for fastener diameters, D=3/16 in., 3/8 in. and 1/2 in. respectively. Over the range of w/D-2.0 to 4.0 there is very little influence of stacking sequence and clamping pressure upon joint strength. While the data for the 3/16 and 1/2 inch diamenter fasteners for t/D=0.33 suggest a decrease in strength with w/D the relation is an artifact of fastener fit. The plot for the 3/8 in. fastener shows the true relationship. The results for t/D=0.66 agree with those for the smaller t/D except that the larger thickness appears to reduce the influence of fastener fit. A shift from the net tension to the bearing failure mode was consistantly observed for all three fastener sizes.

Influence of Clamping Pressure

The influence of torque or clamping pressure on the strength is presented in figures 4.3-12 to 4.4-17 for the three fastener sizes with t/D ratios of 0.33 and 0.66. For the woven fabric laminates investigated constant strength was measured over the range of torques investigated except for the bearing failure mode specimens tested for the 3/16 in. fastener diameter with t/D=0.33 where a slight increase in strength was observed with increasing torque.

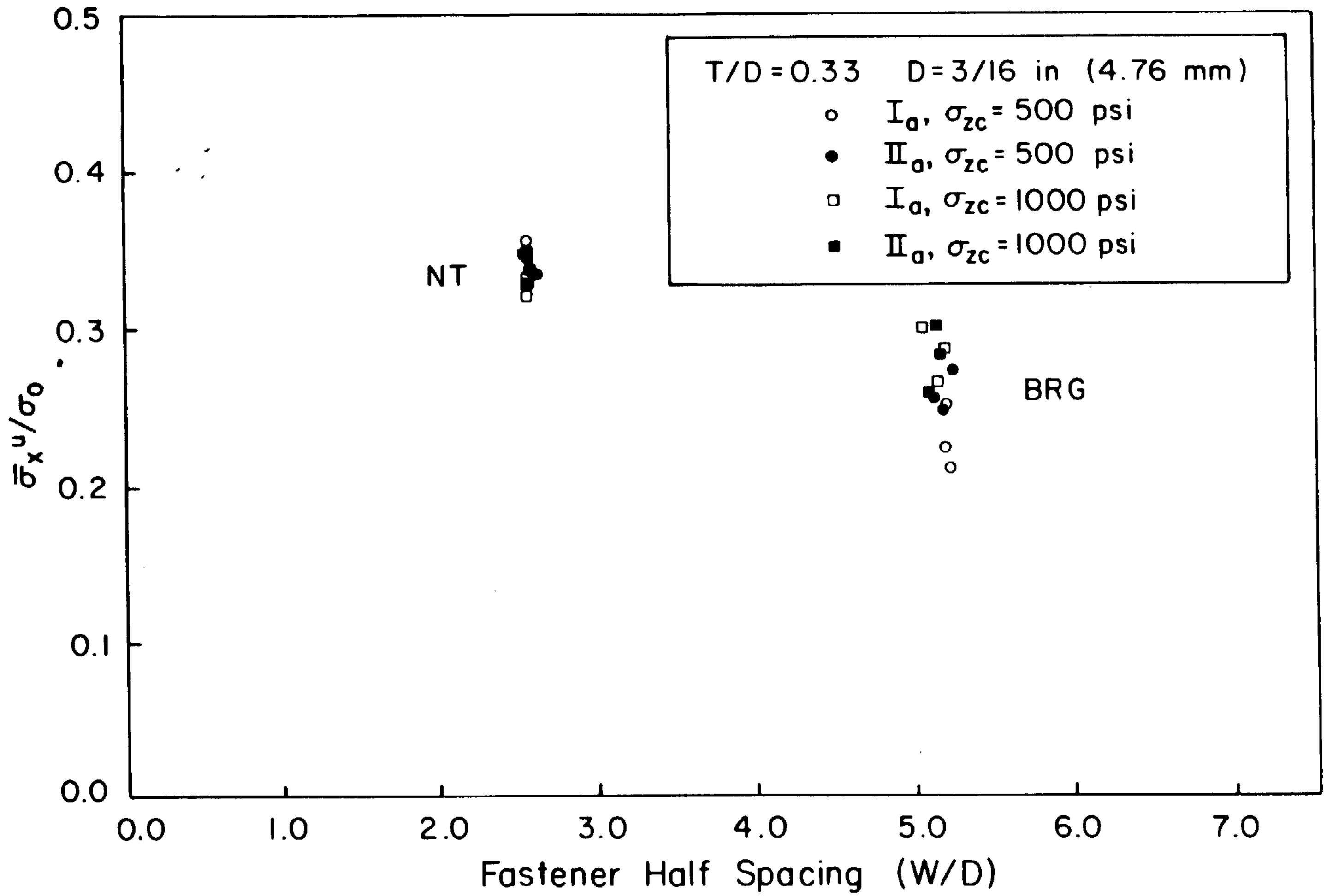

Figure 4.3-6 Plot Of Strength Versus Fastener Half Spacing For t/D=0.33, D=3/16 in.

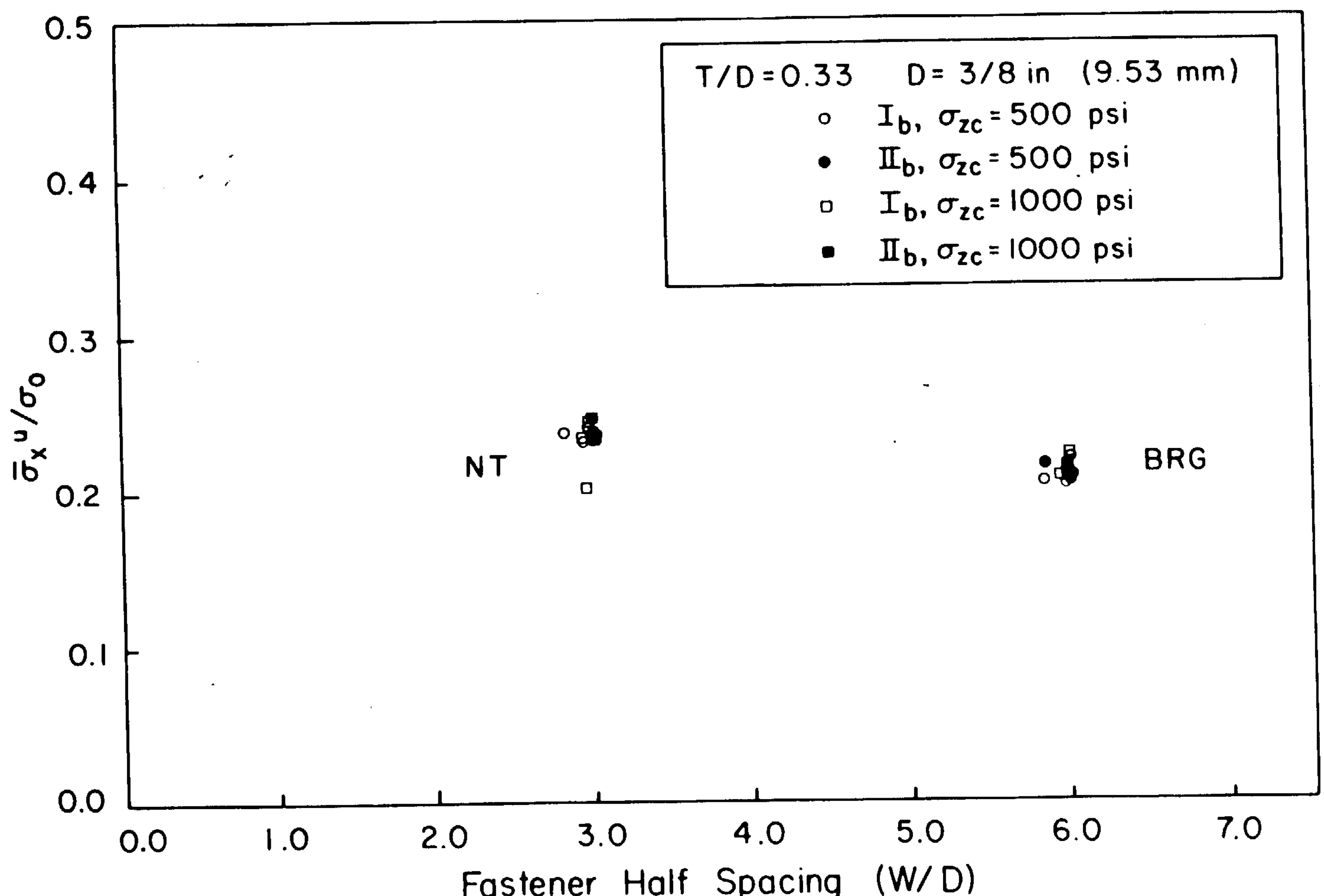

Figure 4.3-7 Plot Of Strength Versus Fastener Half Spacing For t/D=0.33. D=3/8 in.

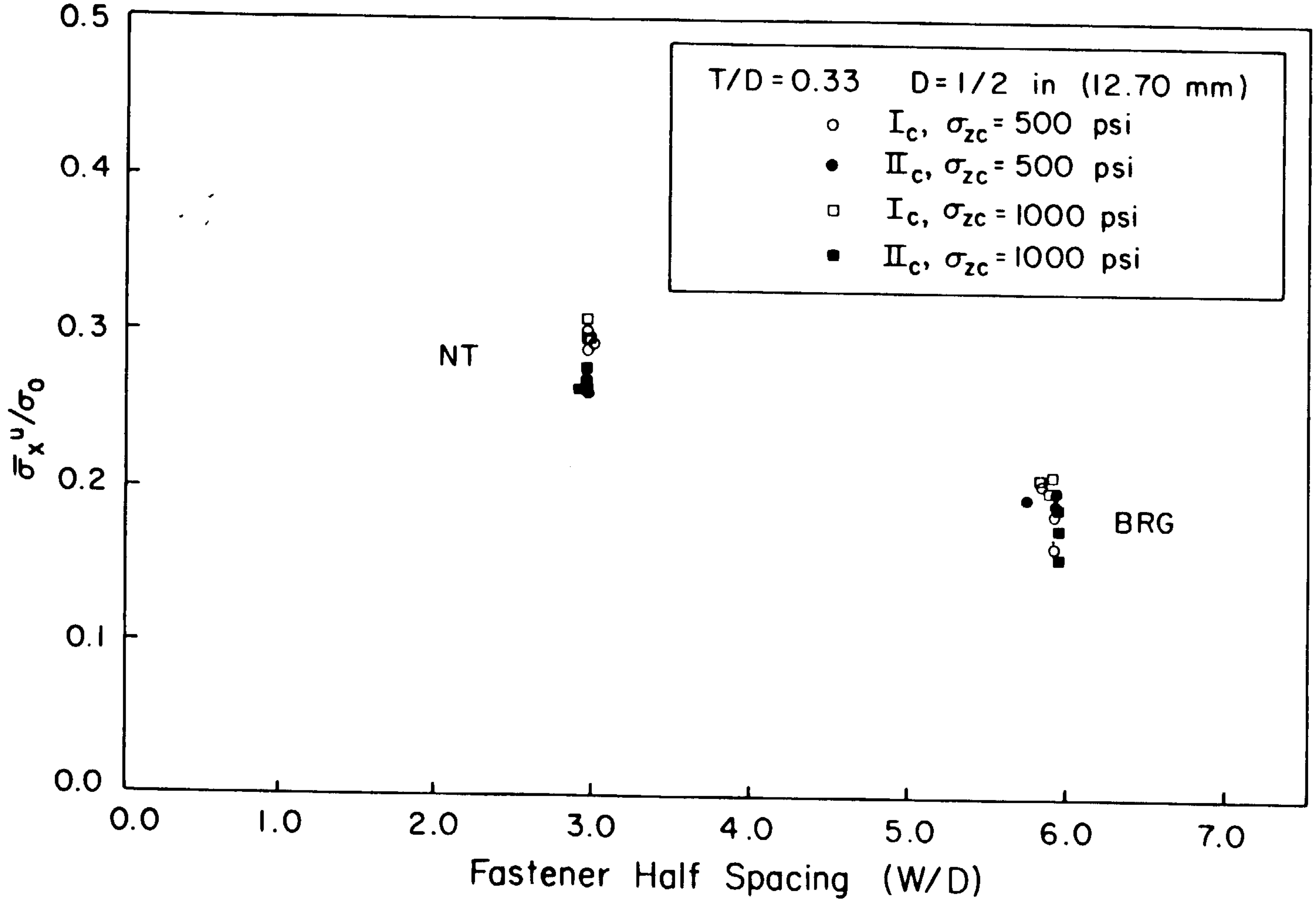

Figure 4.3-8 Plot Of Strength Versus Fastener Half Spacing For t/D=0.33, D=1/2 in.

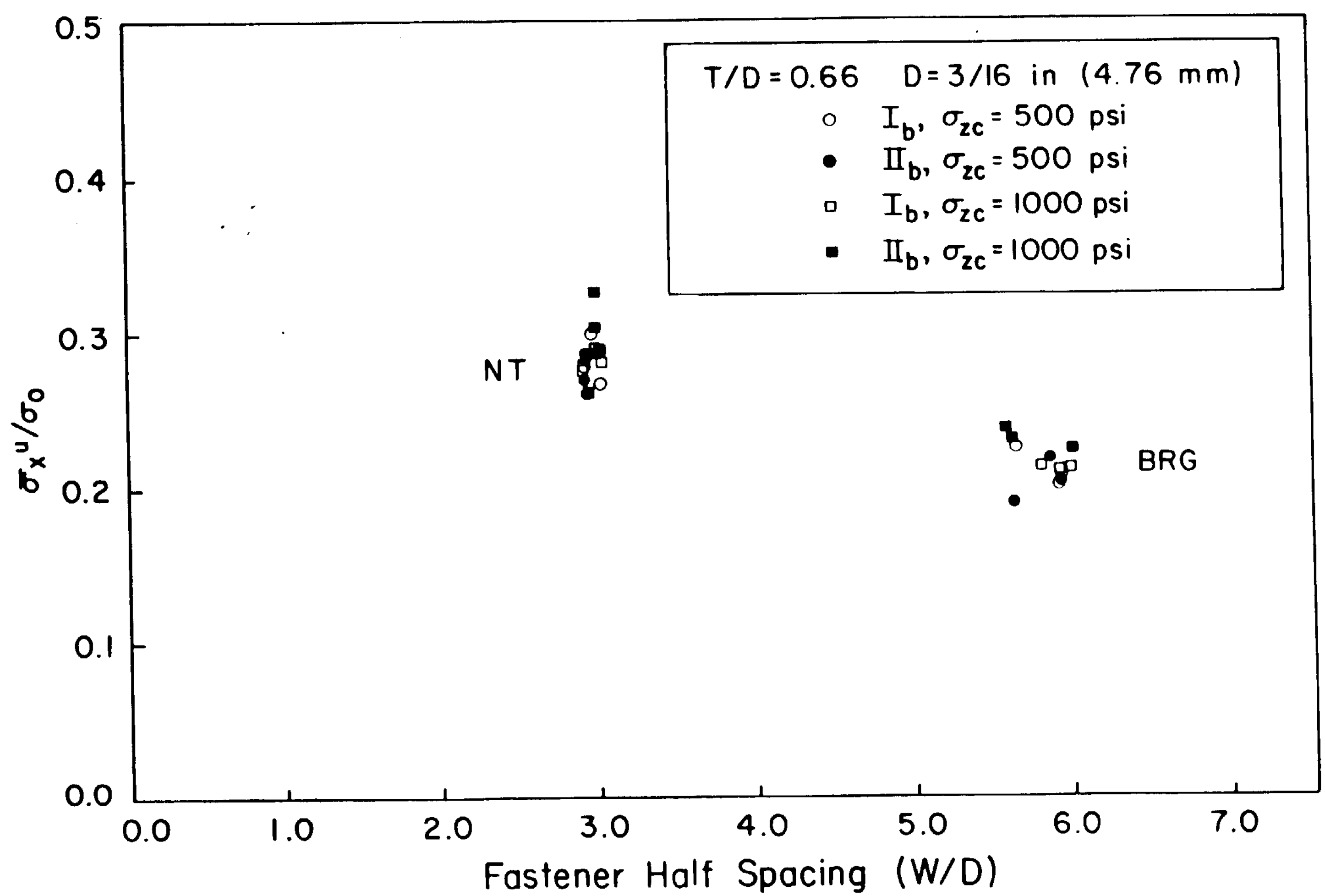

Figure 4.3-9 Plot Of Strength Versus Fastener Half Spacing For t/D=0.66, D=3/16 in.

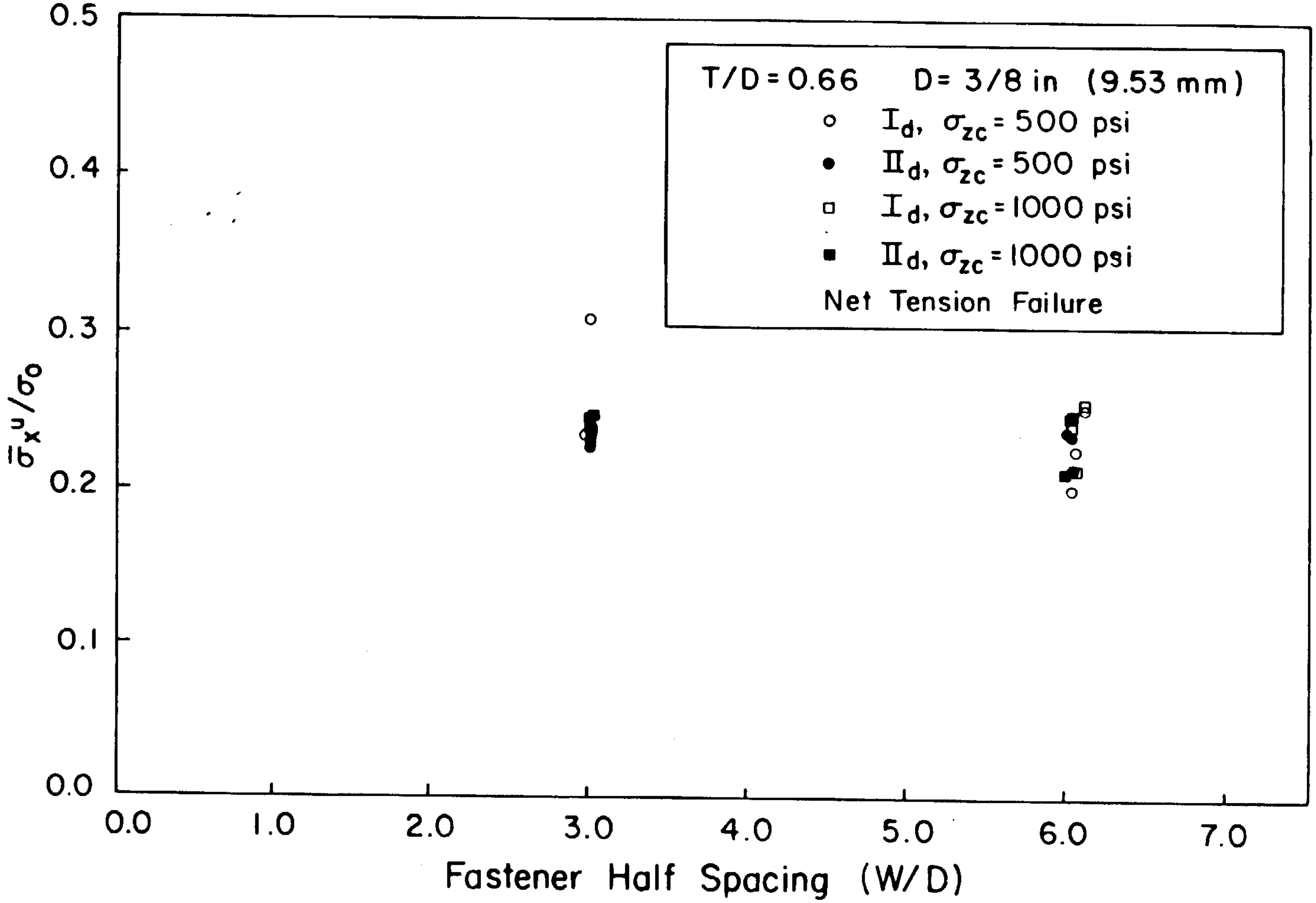

Figure 4.3-10 Plot Of Strength Versus Fastener Half Spacing For t/D=0.66, D=3/8 in.

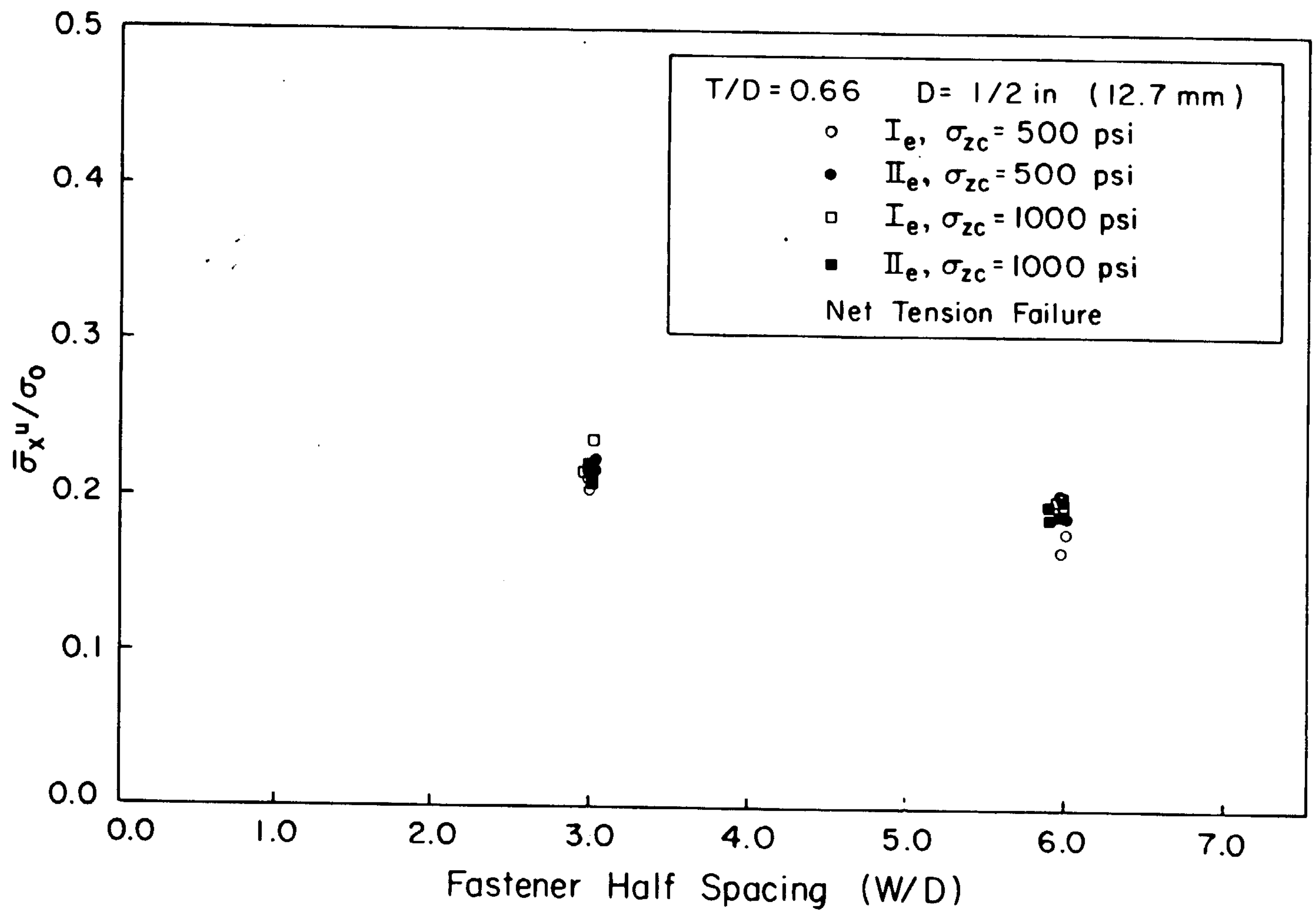

Figure 4.3-11 Plot Of Strength Versus Fastener Half Spacing for t/D=0.66, D=1/2 in.

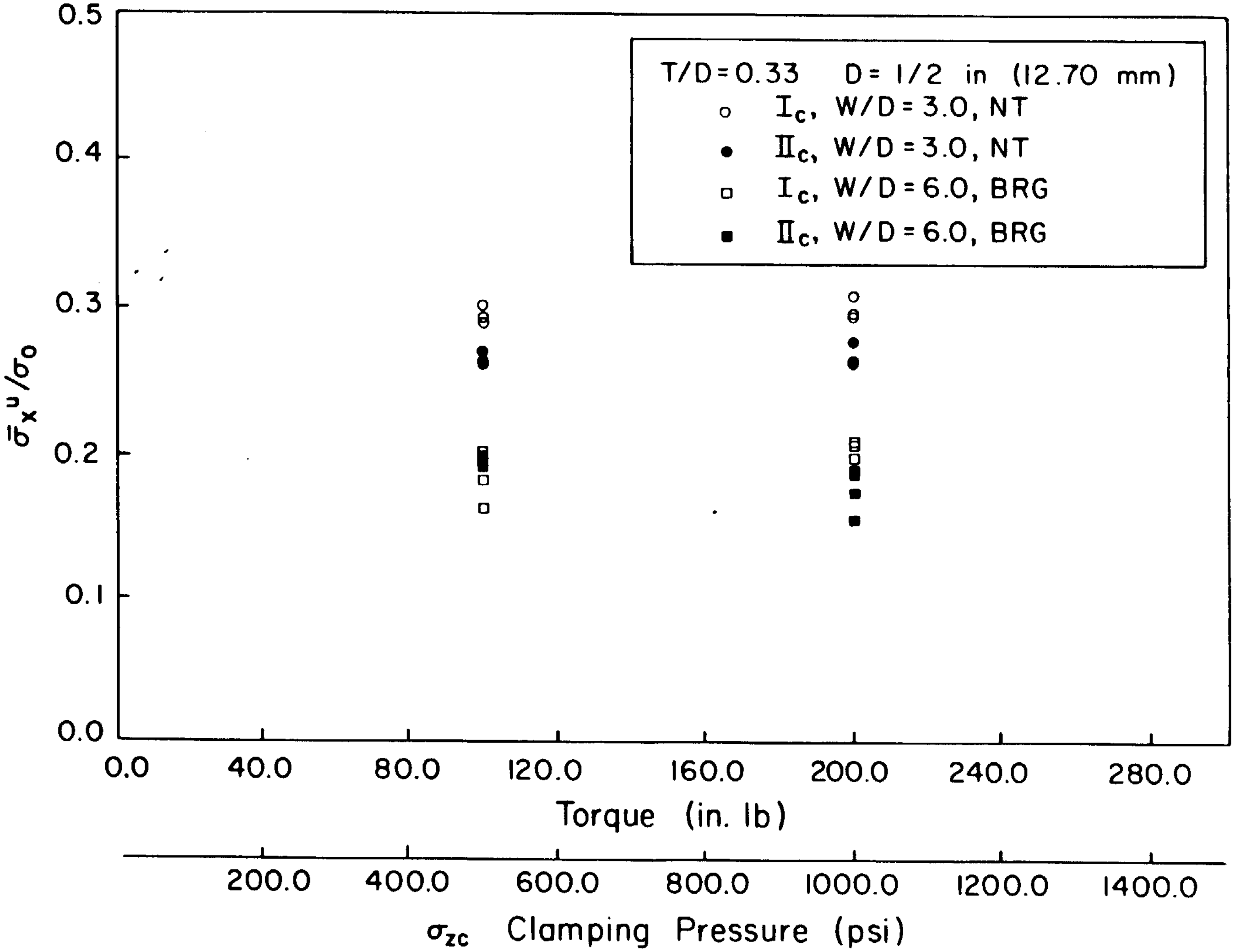

Figure 4.3-12 Influence Of Clamping Pressure Upon Joint Strength, t/D=0.33, D=1/2 in.

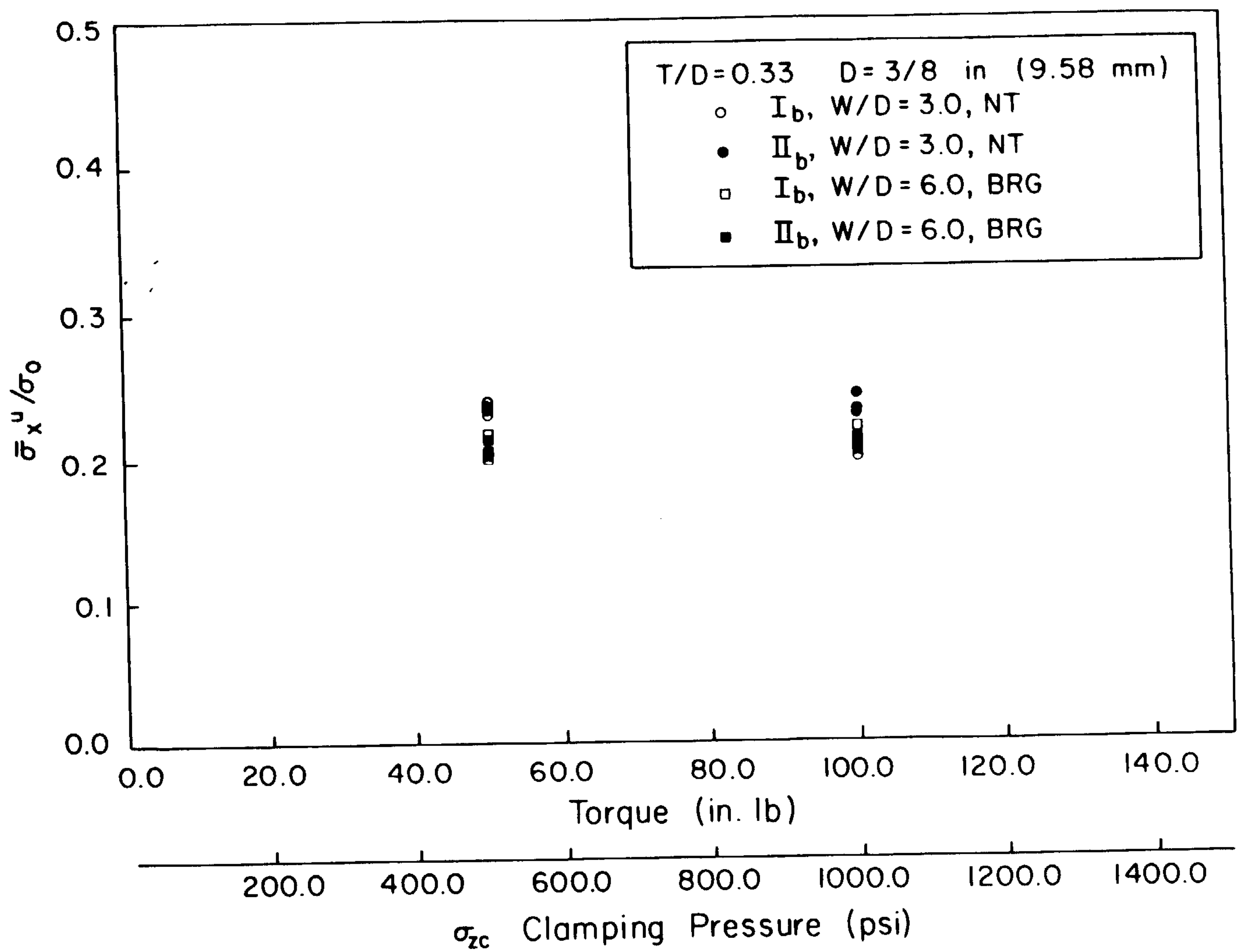

Figure 4.3-13 Influence Of Clamping Pressure Upon Joint Strength, t/D=0.33, D=3/8 in.

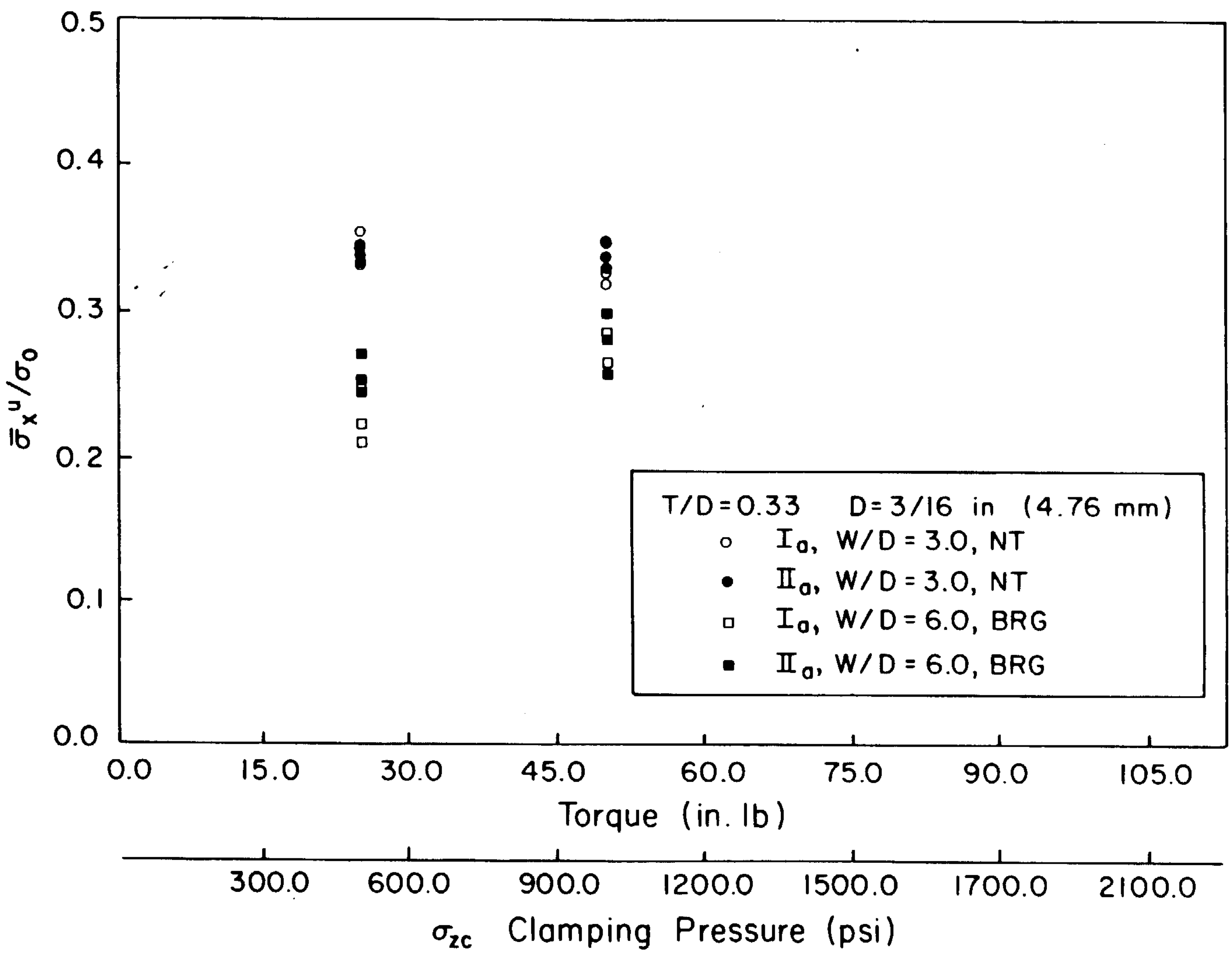

Figure 4.3-14 Influence Of Clamping Pressure Upon Joint Strength, t/D=0.33, D=3/16 in.

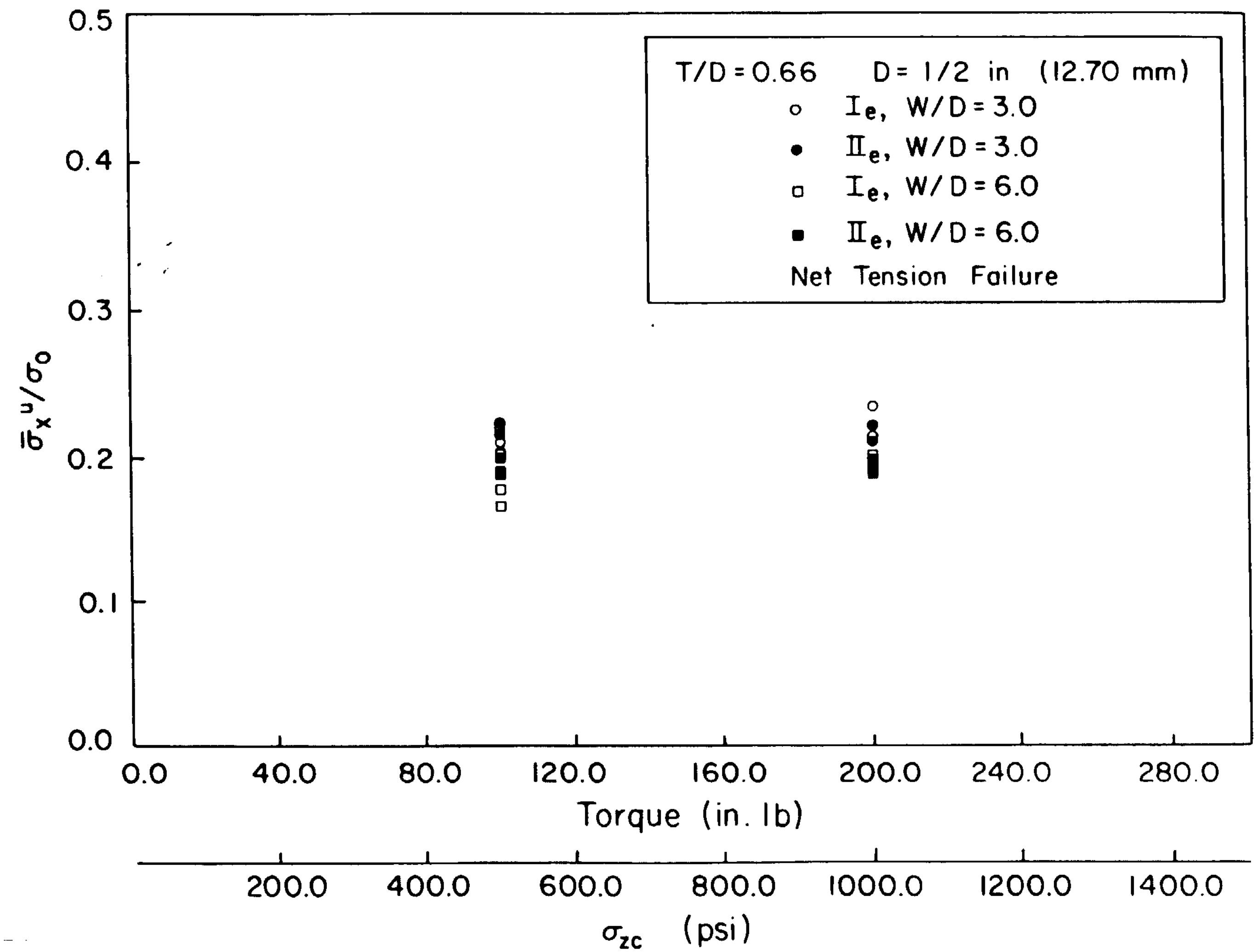

Figure 4.3-15 Influence Of Clamping Pressure Upon Joint Strength, t/D=0.66, D=3/16 in.

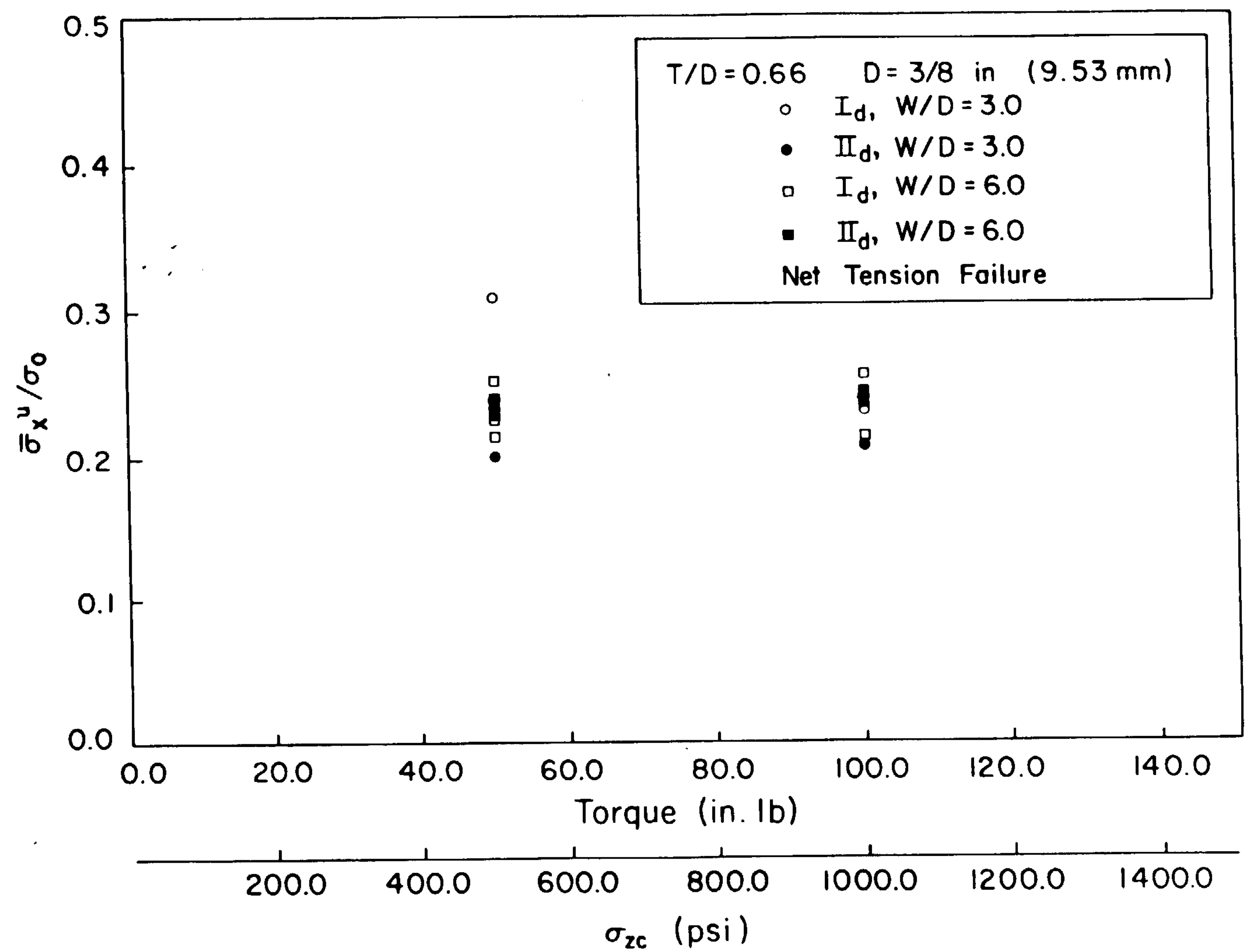

Figure 4.3-16 Influence Of Clamping Pressure Upon Joint Strength, t/D=0.66, D=3/8 in.

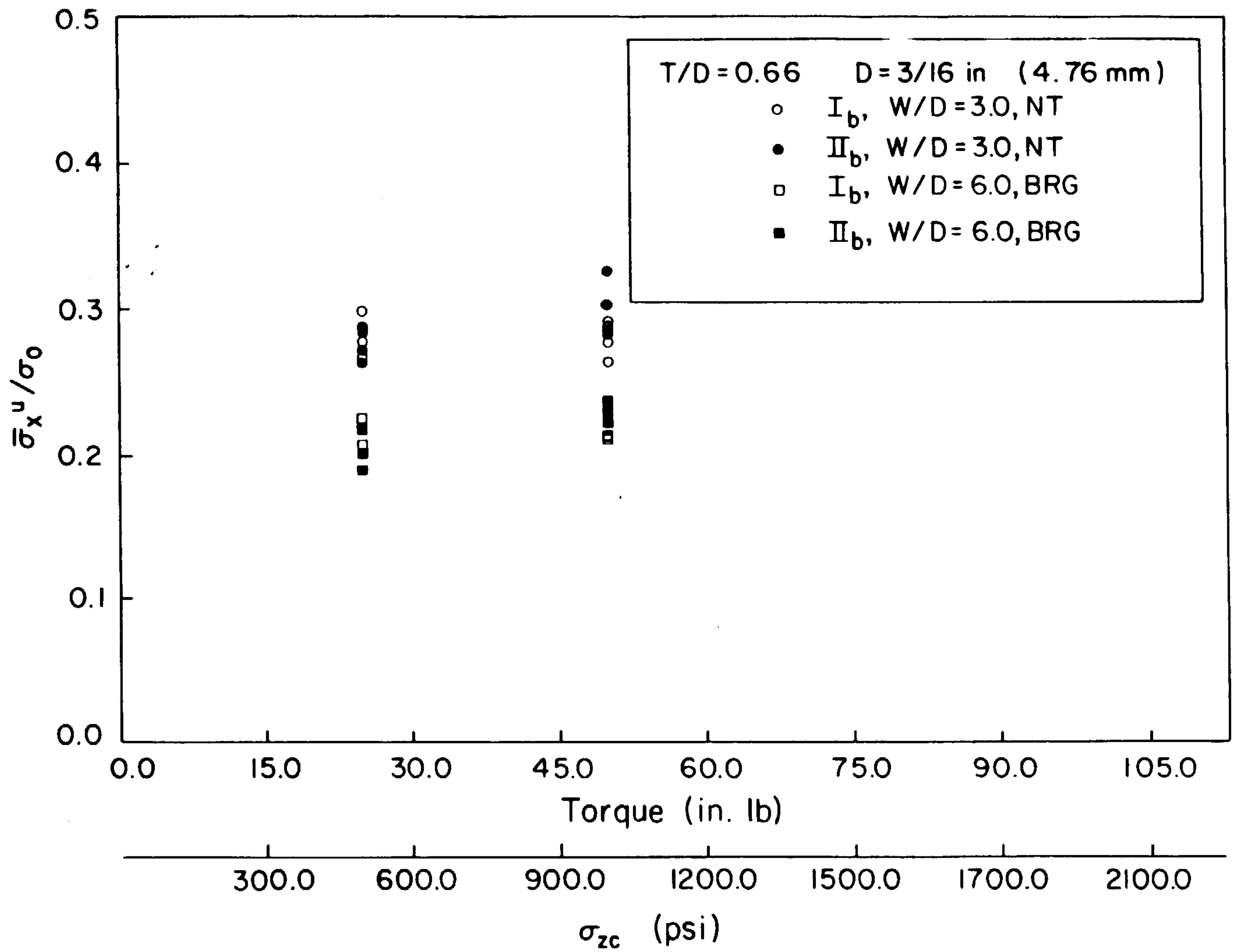

Figure 4.3-17 Influence Of Clamping Pressure Upon Joint Strength, t/D=0.66, D=3/16 in.

These results are different than results for continuous fiber laminate composites which exhibit a nonlinear increase in strength with fastener torque up to some value of torque above which strength is constant with increasing torque until laminate crushing results from the torque [25]. Recently, Jurf [26] has shown that the restraining force developed at failure through the thickness is constant over a range of fastener torques from finger tight to 50 ft. lbs. This finding infers that strength should be independent of fastener preload since all fasteners develop the same clamping forces at failure for any material, not just fabrics. One plausible explanation is the effects of frictional load transfer between the washer and composite plate. The surface roughness of woven fabric plates is very large compared to the relative smoothness of the typical continuous fiber laminate. Thus, frictional effects would be much less for the rough woven fabric plates since the contact area is less. This theory is now under investigation.

Influence of Plate Thickness

Figures 4.3-18 to 4.3-23 show the influence of laminate thickness on joint strength for pairings of constant fastener size and fastener half spacing. In general the strength remains constant with laminate thickness nondimensionalized by fastener size. The results for the half inch fastener are the exception where a clear

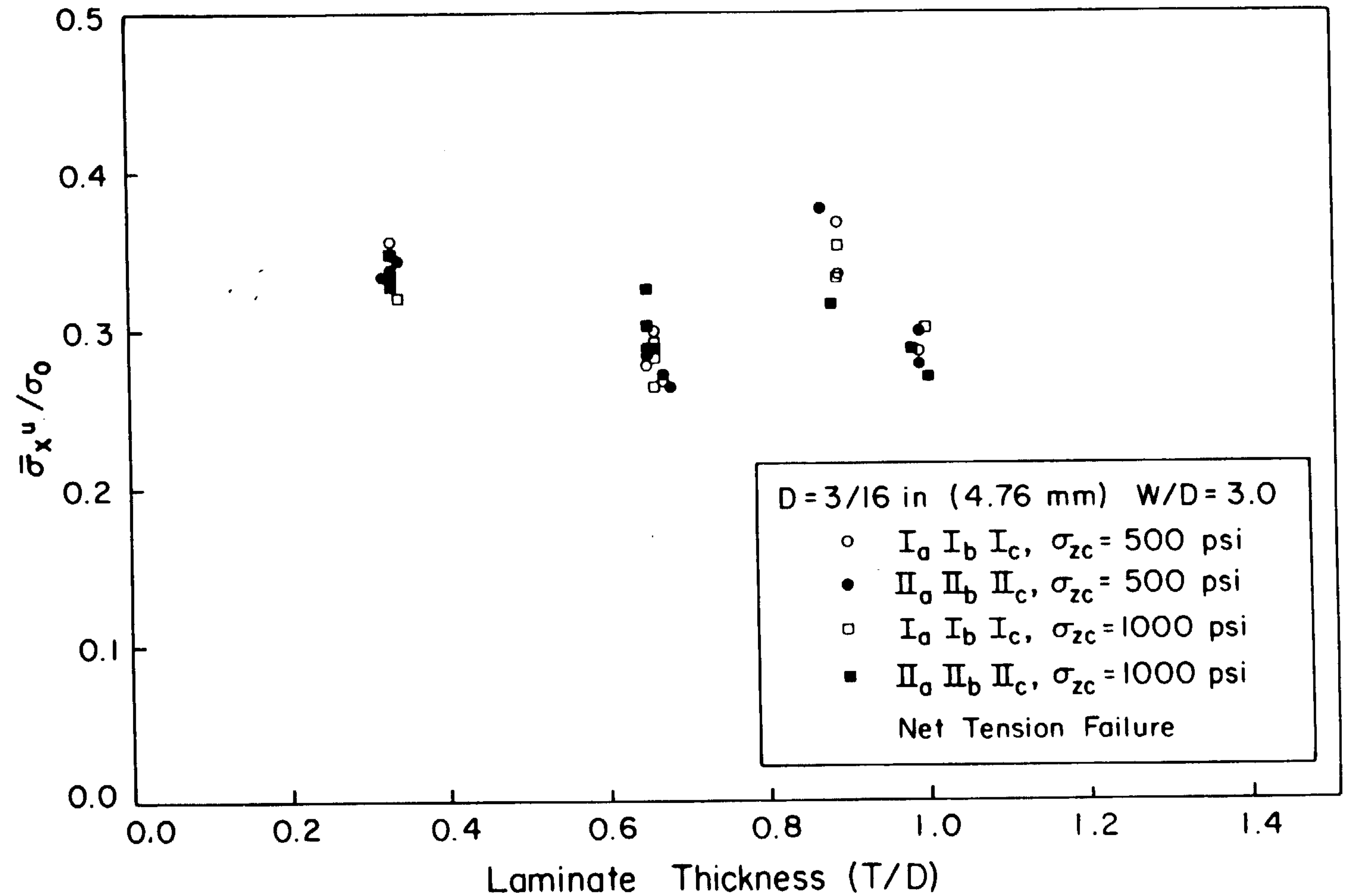

Figure 4.3-18 Plot Of Strength Versus Laminate Thickness For D=3/16, w/D=3.0.

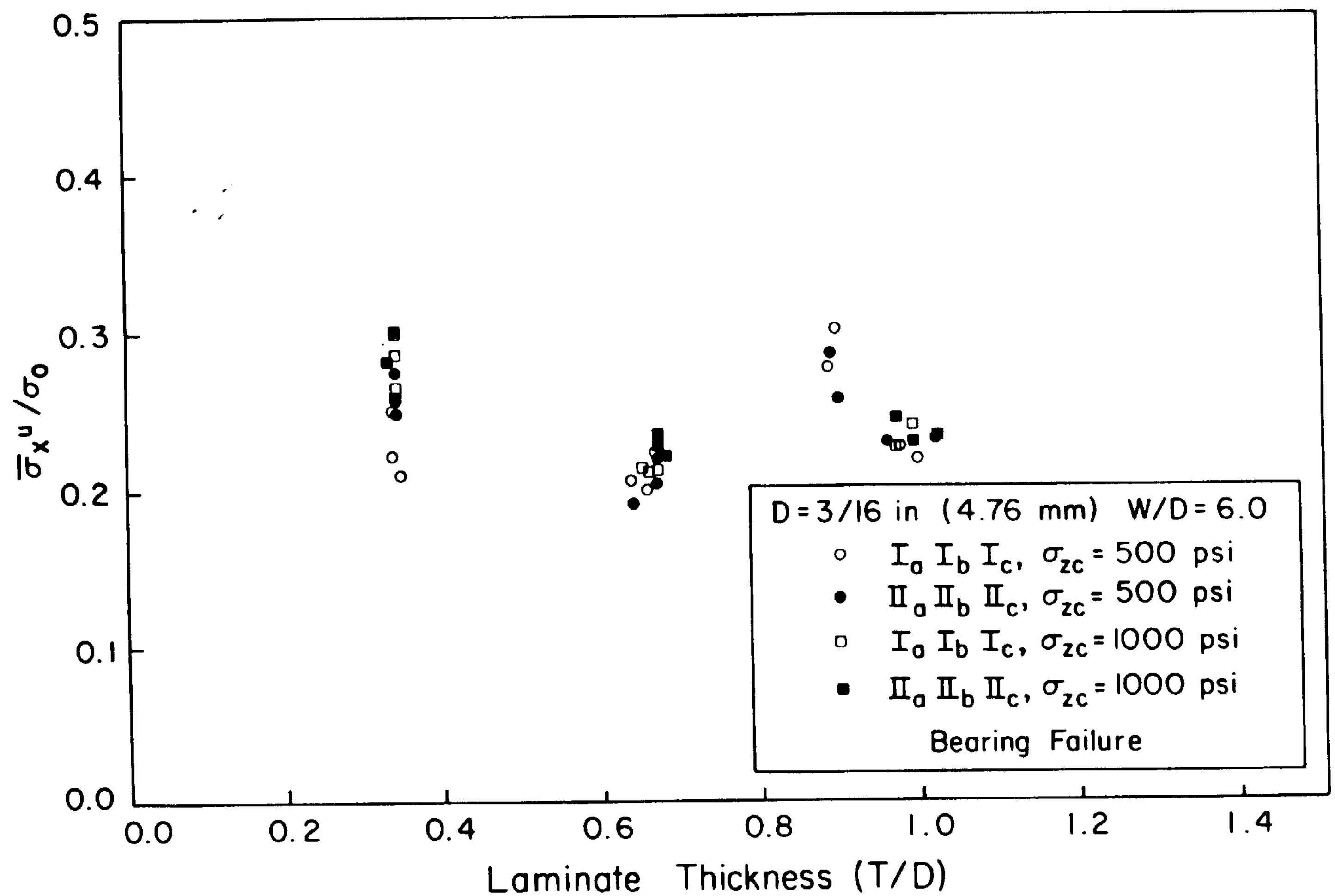

Figure 4.3-19 Plot Of Strength Versus Laminate Thickness For D=3/16, w/D=6.0.

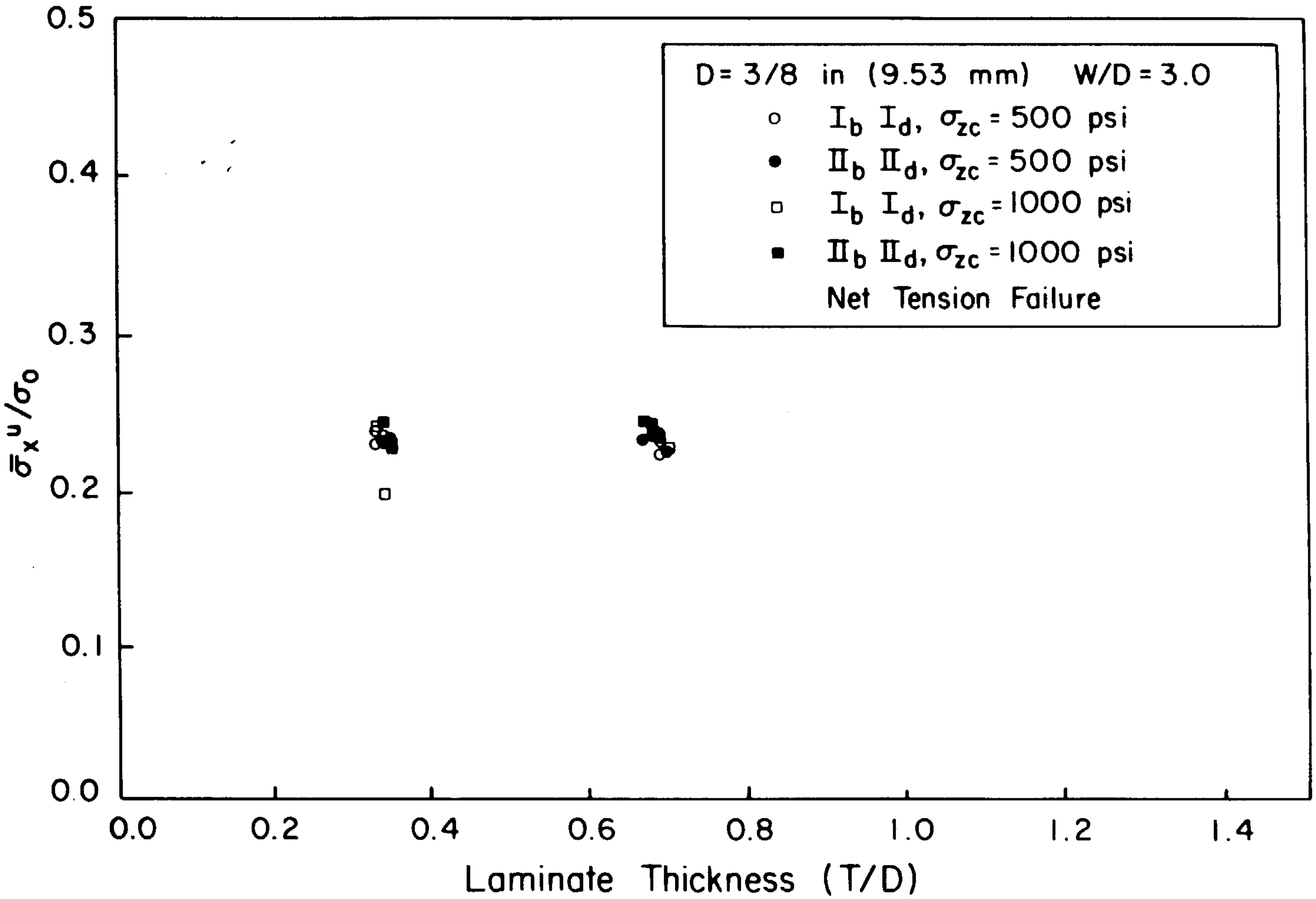

Figure 4.3-20 Plot Of Strength Versus Laminate Thickness For D=3/18, w/D=3.0.

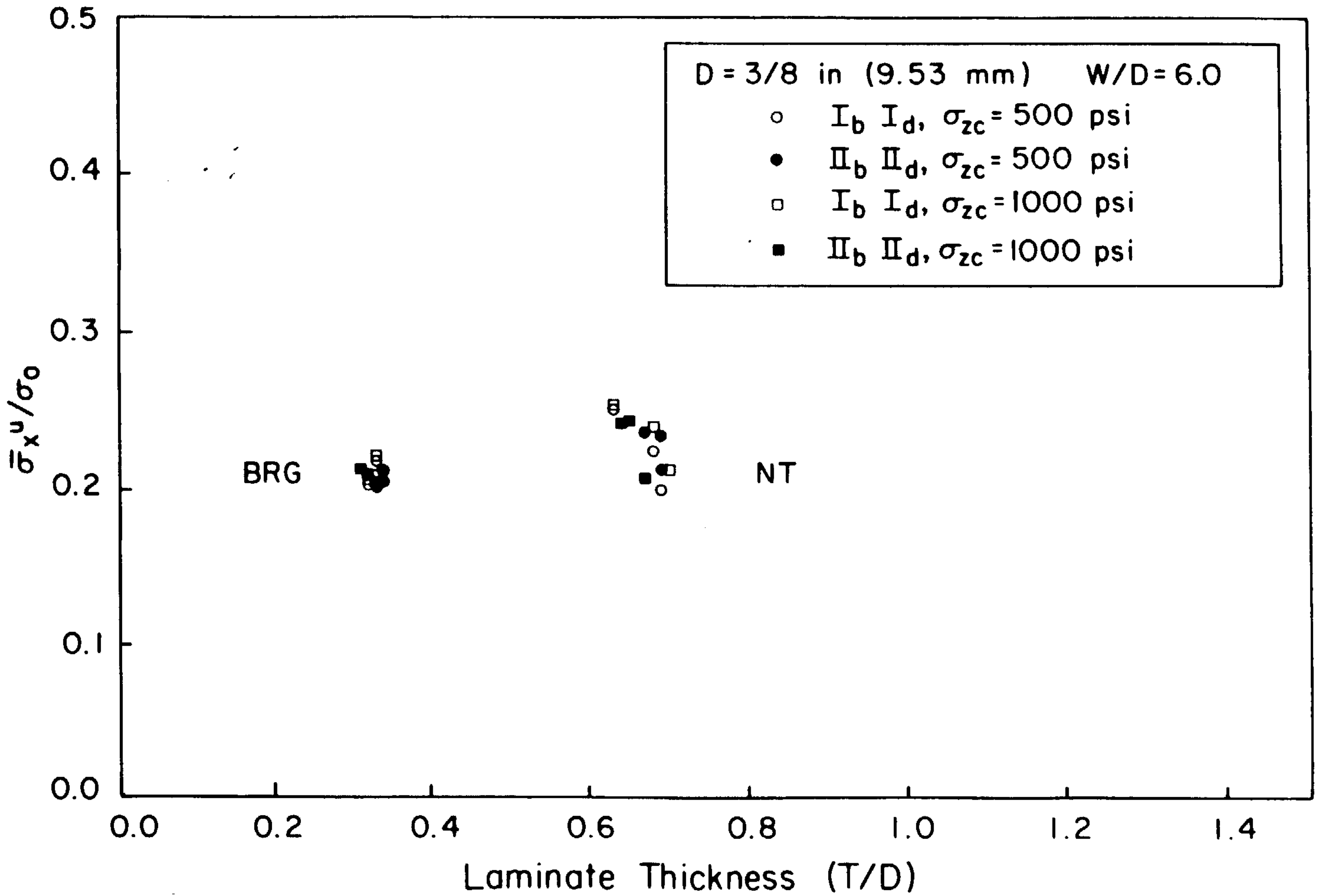

Figure 4.3-21 Plot Of Strength Versus Laminate Thickness For D=3/18, w/D=6.0.

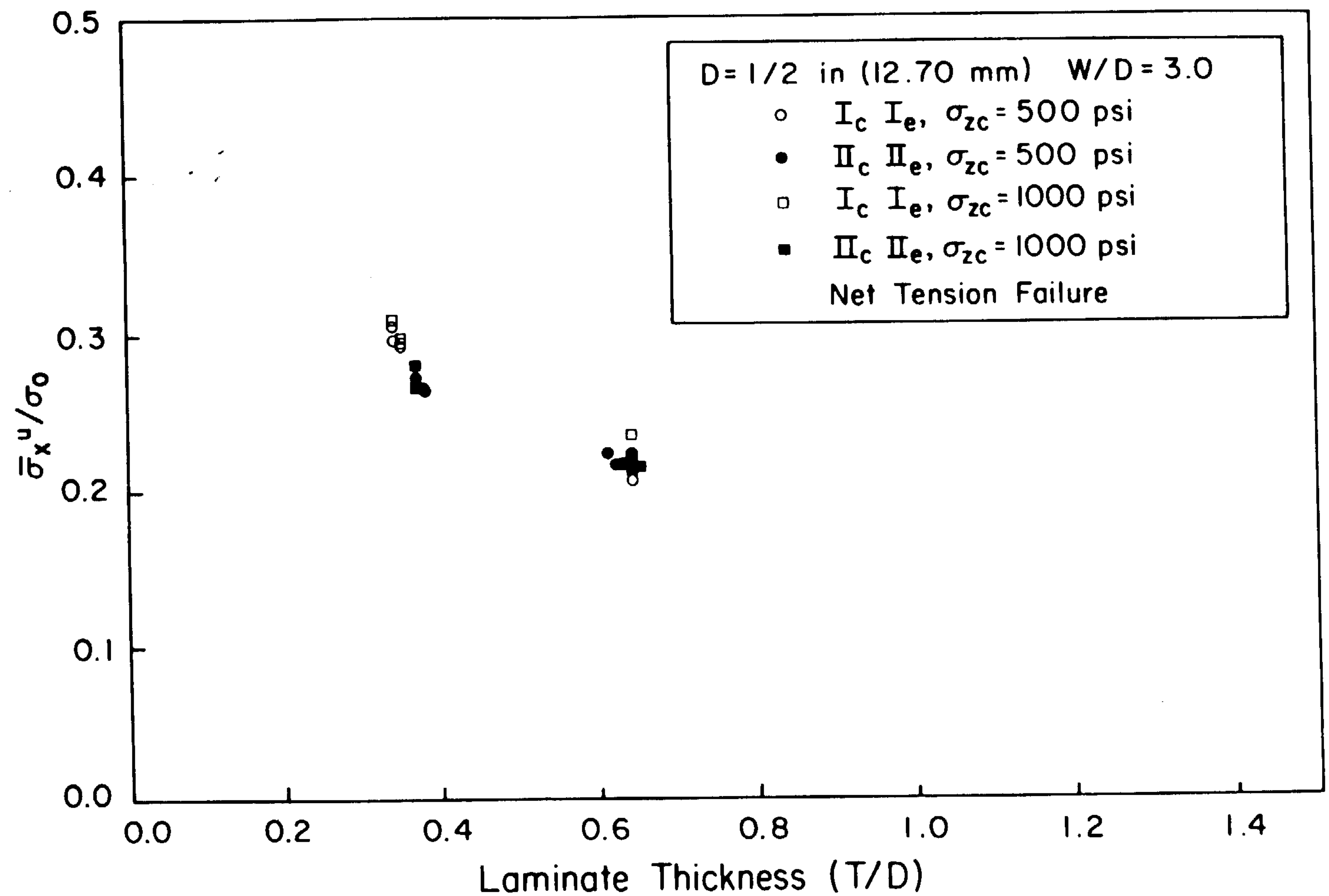

Figure 4.3-22 Plot Of Strength Versus Laminate Thickness for D=1/2, w/D=3.0.

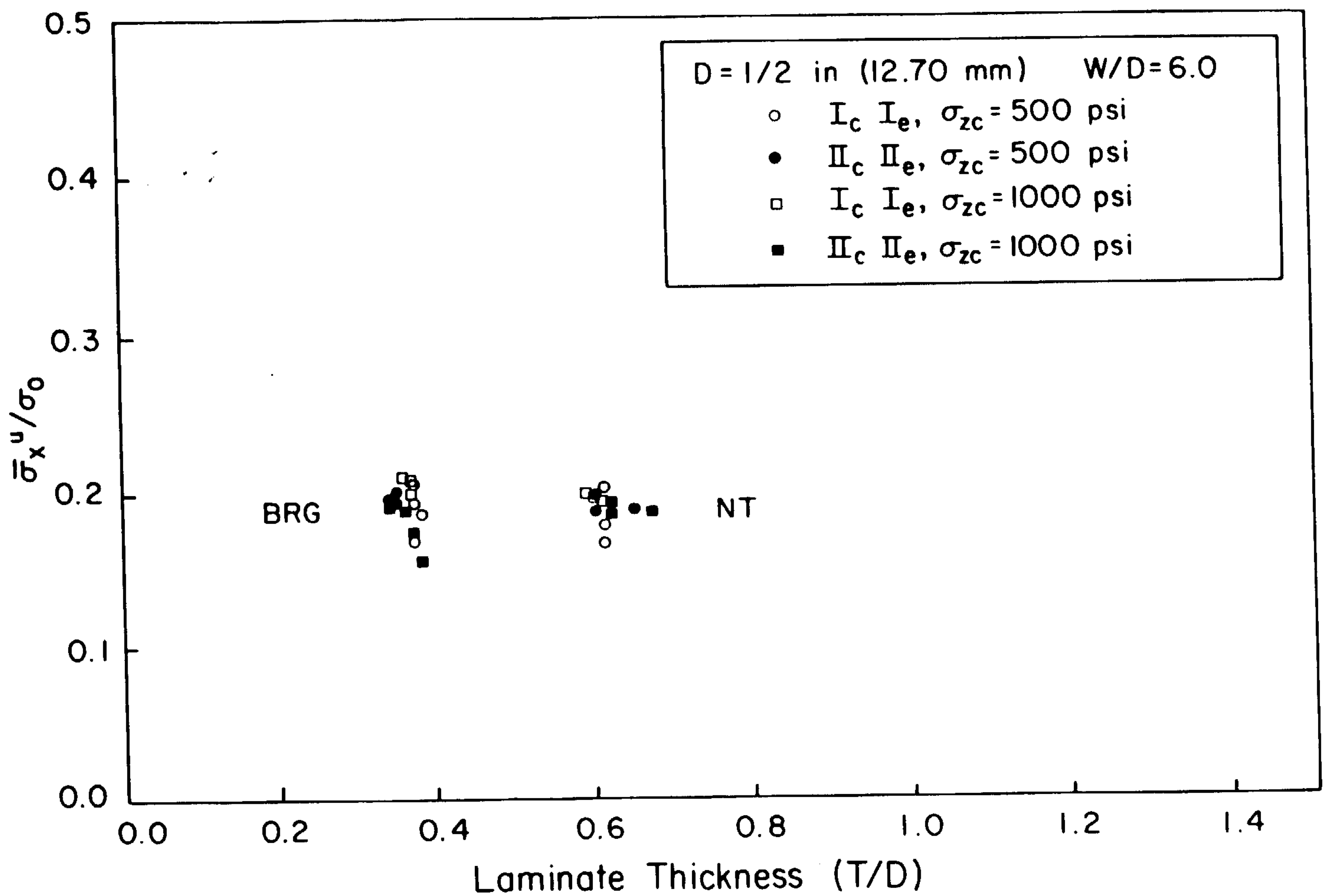

Figure 4.3-23 Plot Of Strength Versus Laminate Thickness For D=1/2, w/D=6.0.

decrease in strength with increasing t/D was measured. There are some interesting observations concerning failure modes. All laminates tested with w/D=3.0 failed in net tension through the hole for all values of t/D tested. The 3/16 in. fastener failed in bearing for all values of t/D investigated at w/D=6.0. The 3/8 in. and the 1/2 in. fasteners shifted from bearing to net tension at t/D increased. This occurred independent of stacking sequence and fastener preload. This may be due to the fact that the increase in cross-sectional area of the net tension plane is constant for w/D constant whereas the bearing area increases as a function of D, thus the increase in bearing area shifts the critical failure mode to net tension for increasing t/D.

Bearing Failure Mechanics

A series of tests were run with a woven fabric material of similar weave geometry but composed of a different resin system. The method employed compression tests on single fastener double lap joints to insure bearing failures. The purpose was to test the applicability of a failure model described by Collings [24] for predicting bearing failure strength of composite laminates in the $[0_{\ell}/\pm 45_n/90_m]_s$ family to woven fabric laminates.

Collings' model attempts to account for the dominant modes of failure under constrained compression loading in each basic lamina of the laminate and requires data for constrained compression properties in each lamina. In a fabric this translates to the properties of 0/90 laminate units and ±45° lamina units. These properties were measured and are given in table 4.3-1. One important characteristic of bearing failures in woven fabric composites consisting of varying amounts of ±45° plies is the associated change in the load deflection curve with increasing percentage of ±45° plies. Pure 0/90 laminates of woven fabric bearing failure resulted in linear loading to first failure followed by load redistribution and reloading to a level higher than the initial load after which ultimate failure occurred. Placing ±45° plies in the system softened the laminate and resulted in a psuedoplastic response after first ply failure. Many similar configurations for continuous fiber composites will not continue to carry loads equal to no greater than the first failure load.

Strength versus fastener diameter was determined for laminates consisting of 0, 25, 50, 75 and 100 per cent ±45° plies, the balance being (0/90) lamina. Results are shown in figure 4.3-24 with the far field bearing stress normalized by laminate ultimate compressive strength. Notice that increasing the ratio of ±45° plies from 0 to 100 per cent increases the strength efficiency of the joint by approximately a factor of two for D=0.25 inches. The

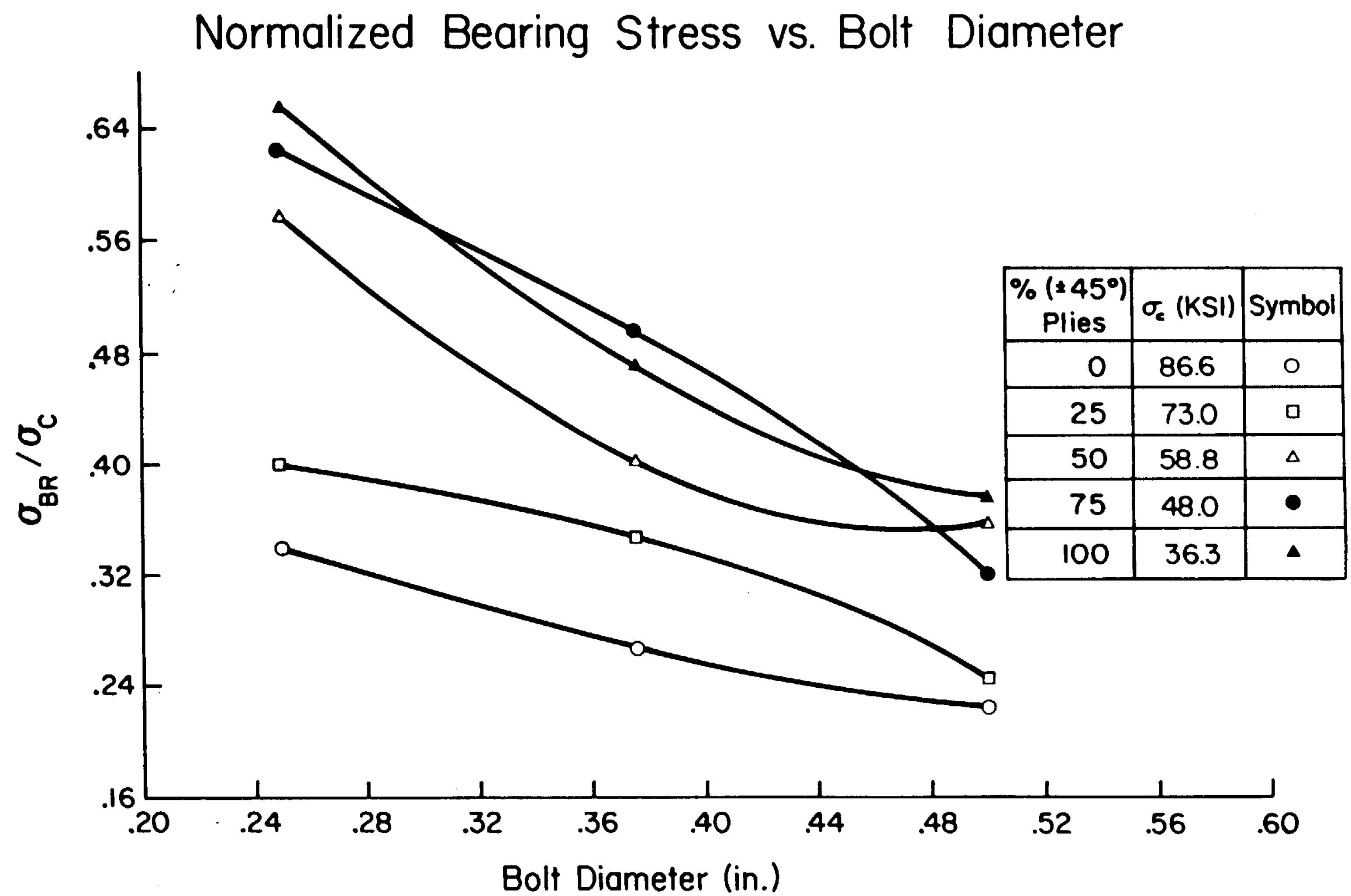

Figure 4.3-24 Plot Of Normalized Strength Versus Bolt Diameter For Different Percentages of $\pm 45°$ Plies.

increase in effeciency decreases slightly with increasing fastener size. This data along with the basic property data form the basis for the bearing failure model discussed in section 5.2.

The damage zone formed at first failure was investigated by ultrasonic c-scan and by sectioning and microscopy. Figure 4.3-25 shows the interlaminar damage zone patterns developed for [0/90], [$\pm$45] and [(0/90)/($\pm$45) laminates. The interlaminar damage pattern strongly reflects the orientation of the plies. One specimen was sectioned along the planes illustrated in figure 4.3-26 and studied microscopically. The damage observed directly in front to the fastener is typical of a compression shear type failure. A higher magnification along one of the shear cracks shows microbuckling failure of the fiber boundles (figure 4.3-27). Also visable in figure 4.2-28 are indications of local crushing of the fibers at the hole boundary. It was interesting to note that along the plane located at the 45° position the same type of compression failures in the fibers were observed in the +45° plies on one side of the hole and in the -45 plies on the opposing side.

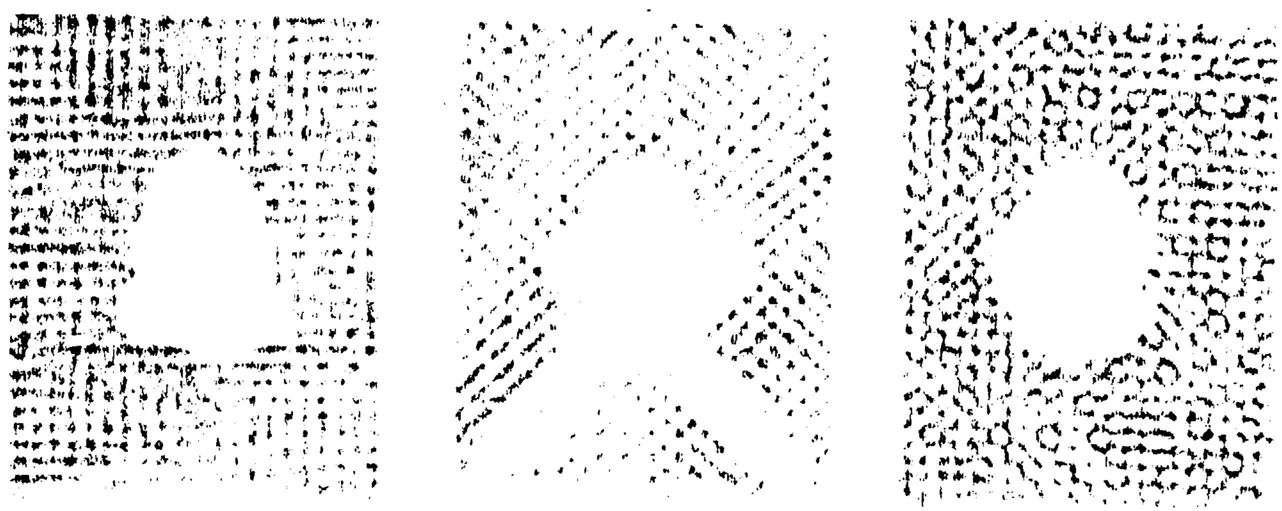

Figure 4.3-25 Ultrasonic C-Scans Of Delamination Damage Developed In The Bearing Tests of [0/90], [±45] and [(0/90)/(±45)] Laminates.

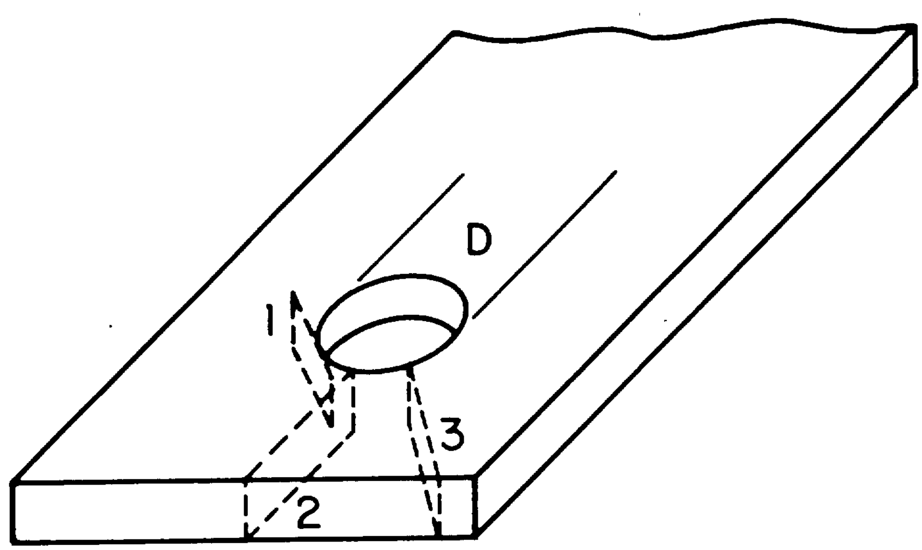

Location of Photomicrograph Sections

Figure 4.3-26 Location And Orientation Of Photomicrographs Taken Of Failed Bearing Specimen.

Figure 4.3-27 Photomicrograph Of Microbuckling Failure Of Fiber Bundles Due To Bearing Failure.

Figure 4.3-28 Photomicrograph Of Local Crushing In The Laminate At The Fastener-Laminate Interface.

5.0 ANALYTICAL RESULTS AND DISCUSSION

The experimental findings discussed in section 4.0 were used to evaluate the applicability of a phenomenological strength model based on the application of the Tsai-Hill failure criterion at a critical distance from the hole boundary and to assess the bearing failure model concept proposed by Collings.

5.1 Bolted Joint Strength Model

The mechanical properties experimentally determined for the fabric were used as input for the stress analysis. Assuming the critical distance d_0 was constant with angular position around the loaded portion of the hole, a series of parametric studies was performed in which the relationships between fastener diameter, critical distance, fastener half spacing and strength were characterized for the fabric laminate. Comparison of the experimentally determined bolted joint strengths with the analytically generated parametric curves was used to define the function, $f(D,\theta)$, for d_0 in the woven fabric laminate.

Figures 5.1-1 and 5.1-2 summarize the predicted strength of a $[(0/90)/\pm45/\pm45/(0/90)]$ woven fabric laminate as a function of critical distance parameter for the three fastener sizes investigated and for w/D=3.0 and 6.0 respectively. The plots were developed using the ply properties

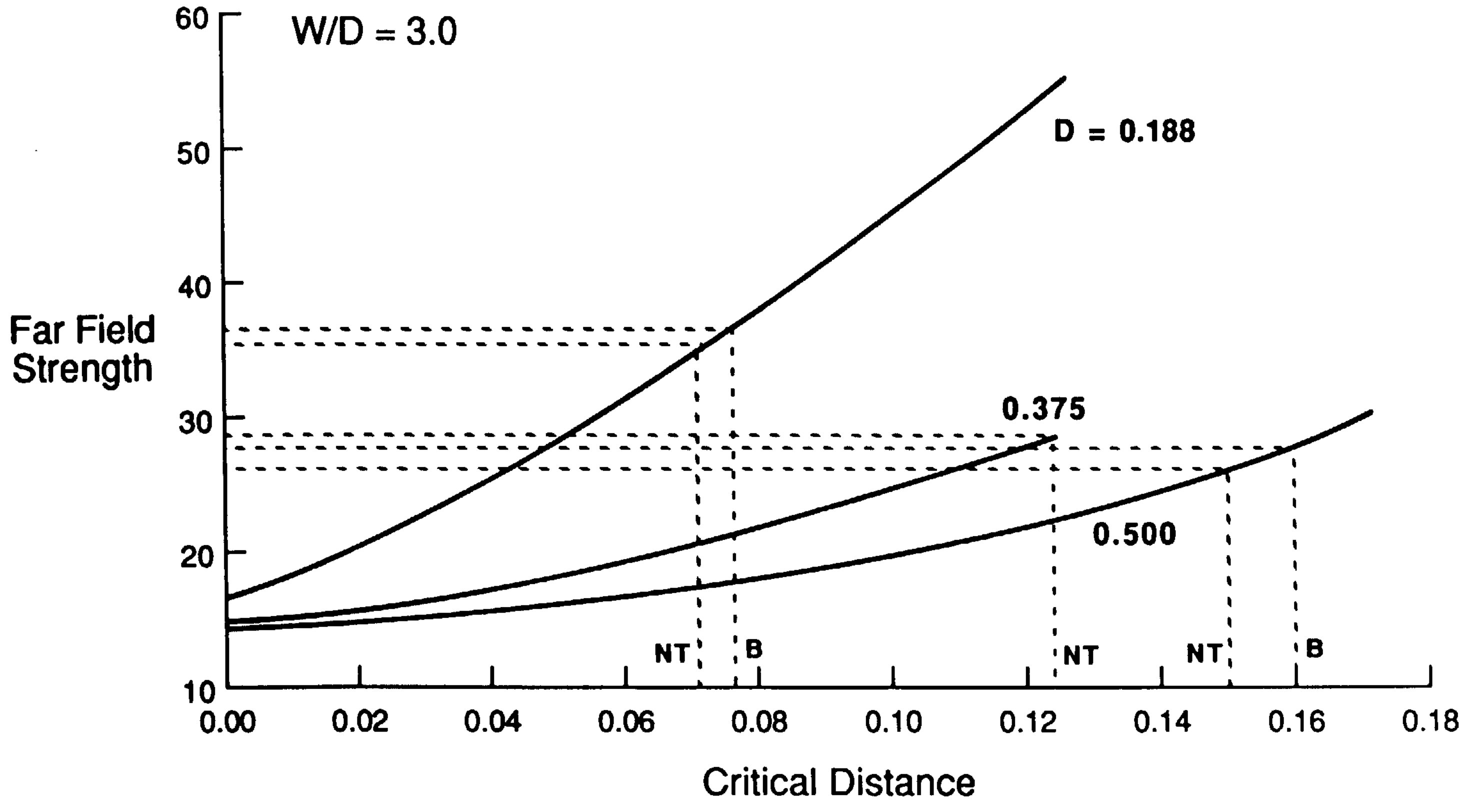

Figure 5.1-1 Plot Of The Predicted Strength Versus Critical Distance Parameter For w/D=3.0.

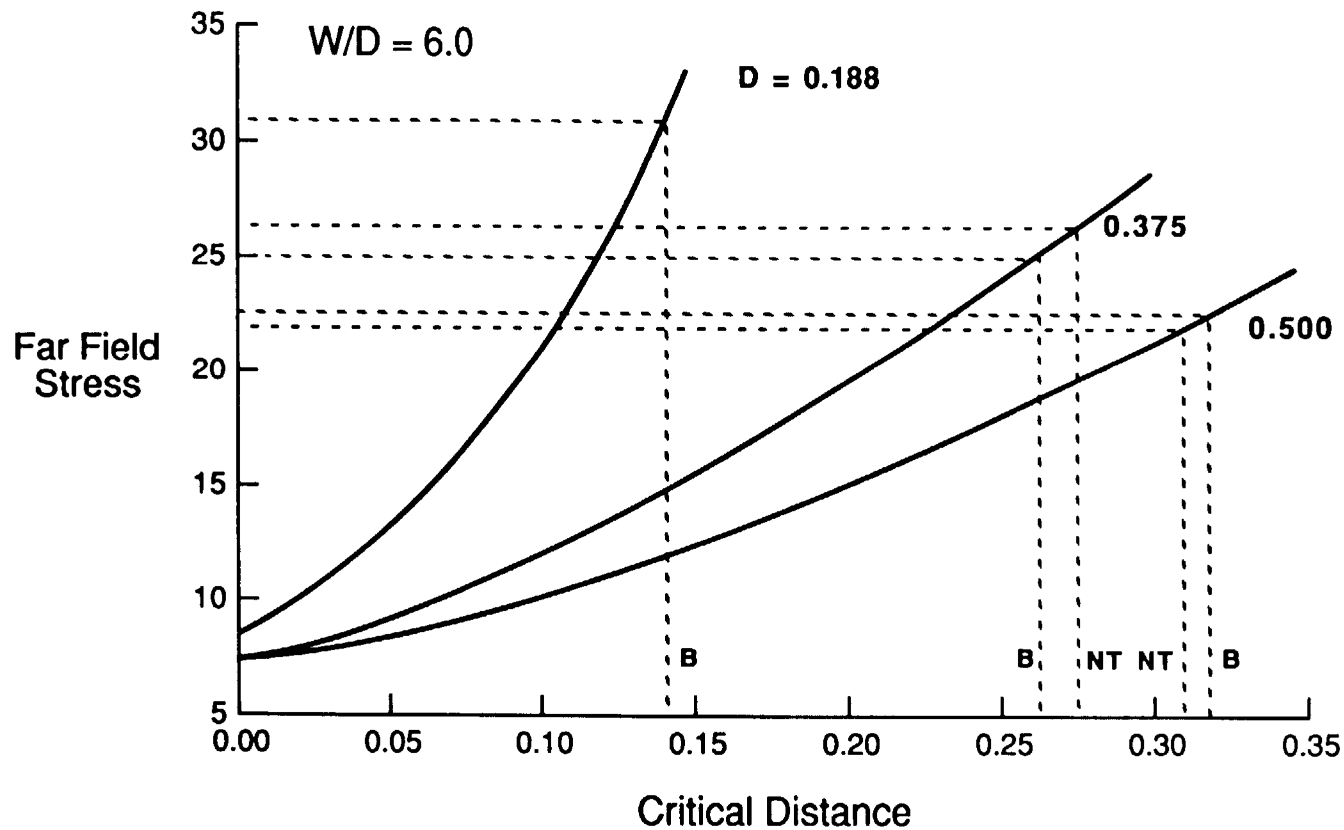

Figure 5.1-2 Plot Of The Predicted Strength Versus Critical Distance Parameter for w/D=6.0.

given in table 4.1-1 and assumed that d_0 was constant for $0<\theta<90$. All failures for this laminate configuration and for the two w/D's investigated were predicted to occur at the 0° location which suggests consistant bearing failures. A similar analysis with w/D=2.0 did result in the prediction of net tension failures. The results in Figures 5.1-1 and 5.1-2 show that for a constant d_0 the predicted strength decreases significantly with increasing fastener size and also that increasing w/D at d_0 constant results in decreasing predicted strength.

The superposition of experimental bolted joint results onto these figures is represented by the labelled constant strength lines, the intersection of these lines with the analytical curves determines the critical distance parameter values for each fastener diameter failure mode and w/D. Two failure modes were observed experimentally for both w/D values, bearing and net tension. The critical distance is similar for both failure modes at constant fastener diameter. Taking average values of the critical distance for the two failure modes figure 5.1-3 shows the relationship between critical distance and fastener diameter for the two w/D values investigated. The relationship is nearly linear in each case but the slopes are different for the different values of w/D.

The finding that critical distance is similar for both net tension and bearing failures implies that the

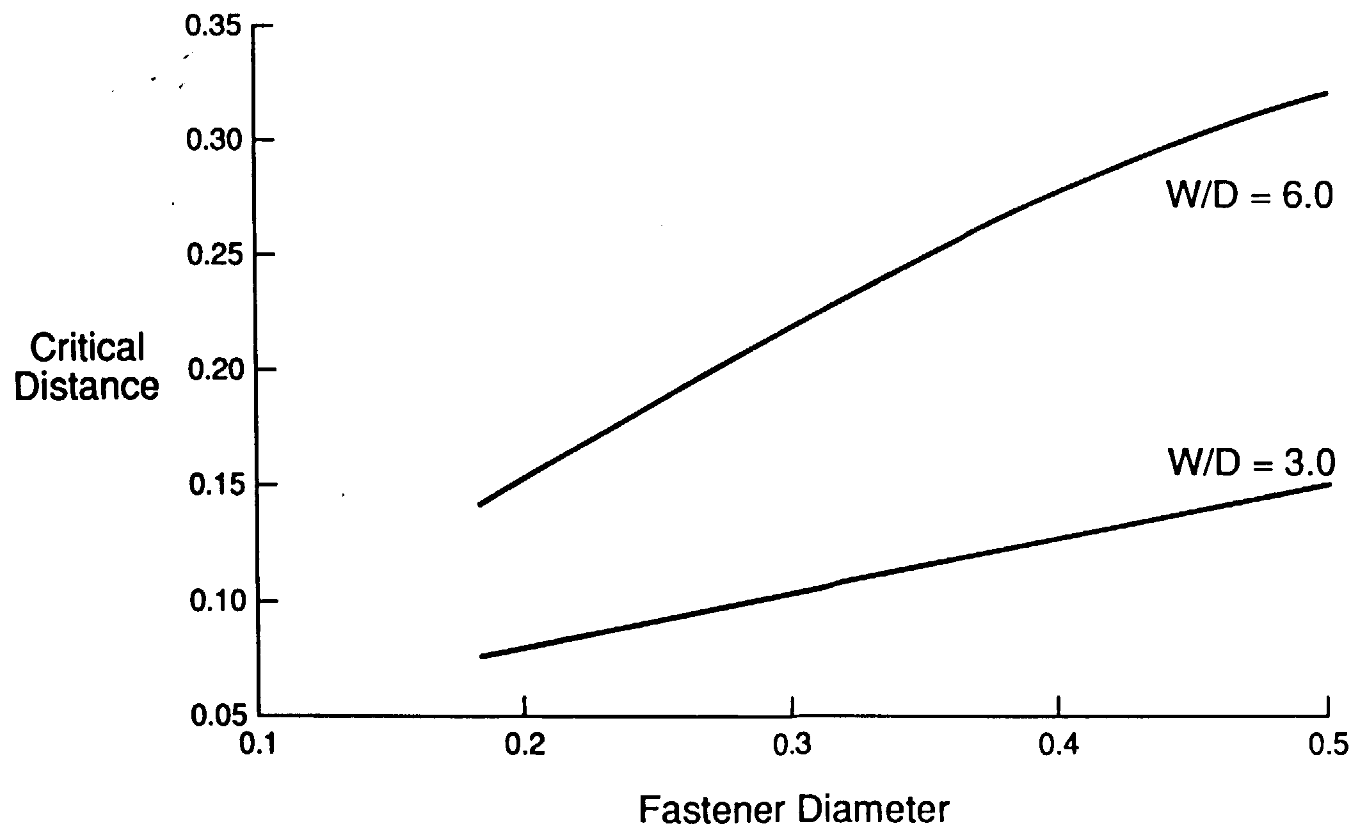

Figure 5.1-3 Plot of Critical Distance Parameter As A Function Of Fastener Diameter.

parameter d_0 is constant with location θ around the hole for the conditions investigated. This finding is a key difference in behavior from that reported for continuous fiber laminates where d_0 is a function of location and where failures are predicted in the 30-36° location most of the time. The data suggest linear functions of fastener diameter for the description of d_0 but there is not enough data for different values of w/D to describe the width dependence.

5.2 Bearing Failure Model

The ply bearing factor (K) curves as a function of percent 45° plies for the 0.250, 0.375, and the 0.500 in. diameter fasteners are given in figure 5.2-1. As can be seen the relationships are linear but with different slope for each fastener size. Using these K calibration curves bearing strength predictions as a function of percent 45° plies were determined as shown in figure 5.2-2. The symbols represent actual data from the experiments. The correlation is good considering that the calibration of the model was based on limited data and the scatter in the experimental results large. It is important to note that the maximum predicted and measured strength occurred for a laminate with a 50% composition of 45° plies. Thus for maximum bolted joint strength for a laminate made from plain weave fabric 50% of the plies should be oriented at 45°.

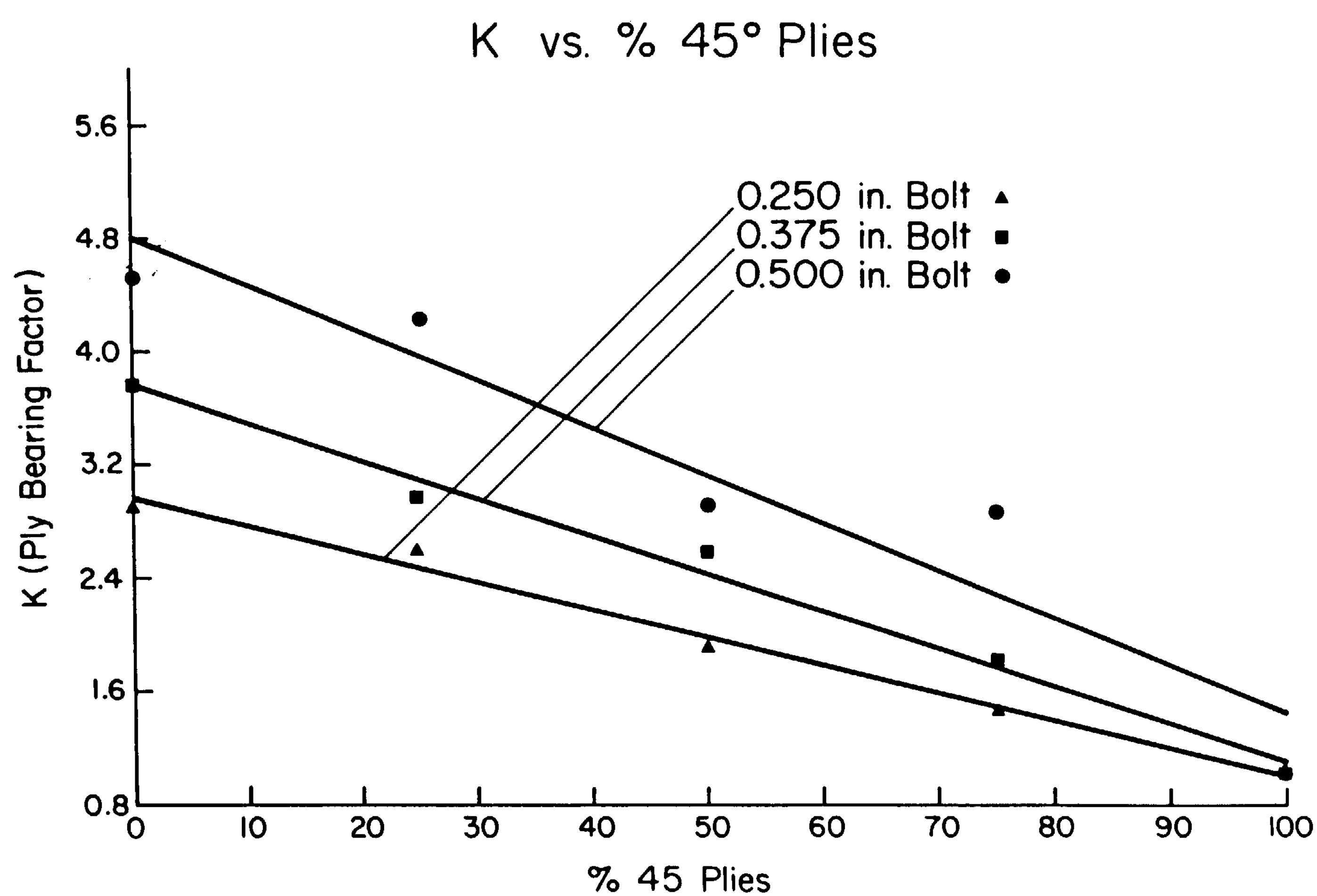

Figure 5.2-1 Plot Of The Ply Bearing Factor As A Function Of The Percentage Of +45° Plies In The Laminate For 0.25, 0.375 and 0.500 In. Fastener Diameters.

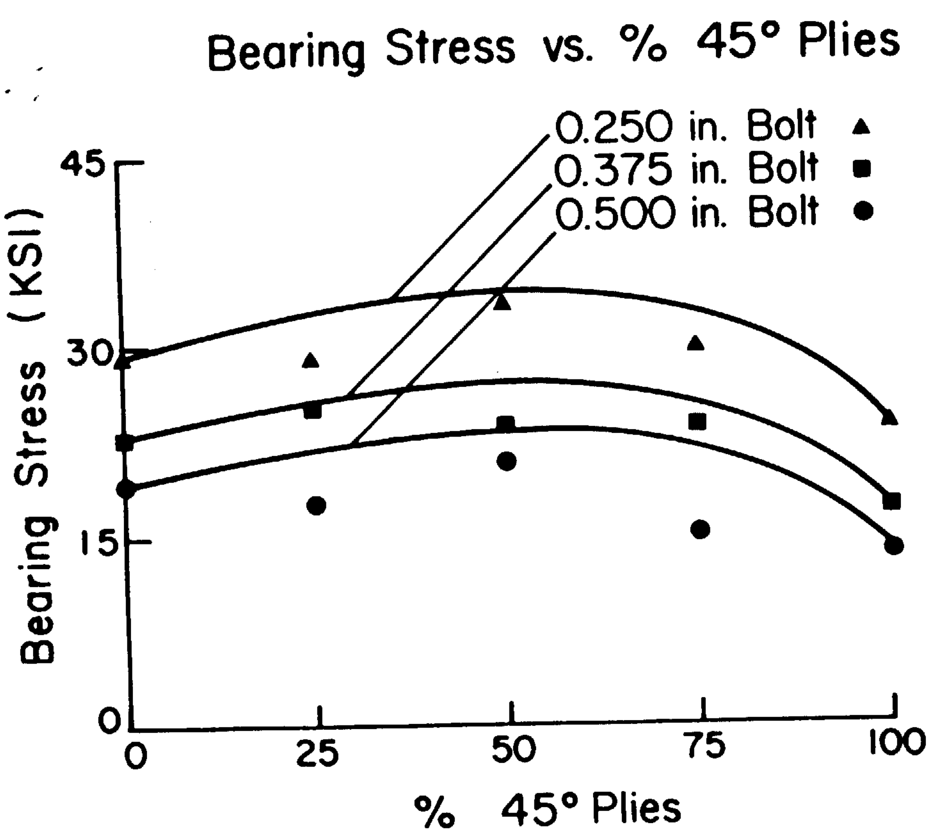

Figure 5.2-2 Comparison Of The Predicted And Experimentally Determined Values Of Bearing Strength As A Function Of Percentages Of $\pm 45°$ Plies In The Laminate.

6.0 CONCLUSIONS

In general the woven fabric bolted joints exhibited a joint efficiency ranging between 0.2 to 0.35 where the joint efficiency is defined as the ratio of bolted joint ultimate far field stress to unnotched tensile strength. While joint strength was shown to decrease with increasing fastener size the influences of clamping pressure, w/D, t/D and stacking sequence on strength were minimal for the laminate configuration investigated. Only bearing and net tension failures were observed and often both modes were observed for the same specimen geometry. Where both failure modes occurred for the same geometry the strengths as determined by ultimate far field stress were similar for the two failure modes.

The phenomenological bolted joint strength analysis works for the fabric laminate investigated and the functions describing the critical distance were defined for the two W/D ratios investigated. The critical distance parameter was found to be a linear function of fastener size for W/D constant, not the usual power law configuration assumed by the point stress criterion. Also the critical distance was not found to be a function of location around the loaded boundary of the hole for the material and conditions investigated. Since only two w/D ratios were studied experimentally the functional relationship of critical distance to w/D could not be adequately defined.

The Collings bearing failure model concept was shown to work for fabric based laminates with varying composition of 45° oriented plies and it was shown that the ply bearing factor is a function of fastener size. The experimental study showed that the highest joint efficiency for bearing failures was achieved for laminate configurations with 50 percent 45° oriented plies. Fractographic analysis of failed specimens revealed that damage in the 45° plies was similar to that observed in the 0° oriented plies; the damage consisted of matrix and fiber compression failure which extended to locations up to 0.1-0.2 inches from the hole boundary.

While the Collings based bearing strength model works for bearing failures it was shown that for the woven fabric laminates tested in this research program, failure mode is not predicable based on geometry. Therefore one canot always know appiori what the failure mode will be and hence know when the model is applicable. The phenomenological strength analysis can be calibrated to accurately model strength but is not very general since geometry affects the function for the critical distance parameter. The model is therefore not much more economical to use than the traditional empirical analyses.

APPENDIX A

Notched Strength Data

Table 1a - Notched Strength Results For I_b $[(0/90/\pm45/\pm45/(0/90)]_{2S}$ Laminate Configuration

US CUSTOMARY UNITS

SPEC ID	HOLE DIAMETER (IN)	SPECIMEN WIDTH (IN)	SPECIMEN THICKNESS (IN)	FAILURE LOAD (LB)	FAILURE STRESS (Ksi)
1A	0.125	2.003	0.129	14107	54.6
2A	0.127	1.994	0.130	14250	55.0
3A	0.120	2.000	0.132	14865	56.3
1B	0.251	2.002	0.129	11859	45.9
2B	0.258	2.015	0.132	12235	46.0
3B	0.257	1.992	0.131	12898	49.4
1C	0.382	2.004	0.130	11175	42.9
2C	0.385	2.004	0.127	10990	43.2
3C	0.382	2.004	0.130	10862	41.7
1D	0.493	1.990	0.126	9880	39.4
*2D	0.508	2.000	0.117	10720	45.8
*3D	0.507	2.009	0.117	10043	42.7
*4D	0.505	1.997	0.115	10774	46.9

*Cut from a different panel

Table 1b - Notched Strength Results for I_b $[(0/90)/\underline{+}45/\underline{+}45/0/90)]_{2S}$ Laminate Configuration

S.I. UNITS

SPEC ID	HOLE DIAMETER (mm)	SPECIMEN WIDTH (mm)	SPECIMEN THICKNESS (mm)	FAILURE LOAD (kg)	FAILURE STRESS MPa
1A	3.175	50.876	3.277	6412	376.4
2A	3.226	50.648	3.302	6477	379.2
3A	3.048	50.800	3.353	6757	388.2
1B	6.375	50.851	3.277	5390	316.5
2B	6.553	51.181	3.353	5561	317.1
3B	6.528	50.597	3.327	5863	340.6
1C	9.703	50.902	3.302	5080	295.8
2C	9.779	50.902	3.226	4996	297.8
3C	9.703	50.902	3.302	4937	287.5
1D	12.522	50.546	3.200	4491	271.6
2D	12.903	50.800	2.972	4873	315.8
3D	12.878	51.029	2.972	4565	294.4
4D	12.827	50.724	2.921	4897	323.3

Table 2a - Notched Strength Results for II_b, $[\pm 45/(0/90)/(0/90)/\pm 45]_{2S}$

Laminate Configuration

US CUSTOMARY UNITS

SPEC ID	HOLE DIAMETER (IN)	SPECIMEN WIDTH (IN)	SPECIMEN THICKNESS (IN)	FAILURE LOAD (LB)	FAILURE STRESS (Ksi)
1A	0.129	2.007	0.120	14166	58.8
2A	0.125	1.996	0.119	14798	62.3
3A	0.124	2.034	0.120	15175	62.2
1B	0.256	1.999	0.120	11902	49.6
2B	0.250	2.003	0.119	12574	52.8
3B	0.248	2.000	0.118	11965	50.7
N6C	0.375	1.993	0.111	10099	45.7
N5C	0.374	1.980	0.112	10311	46.4
N3B	0.373	1.999	0.112	9527	42.5
2C	0.385	1.988	0.120	10963	46.0
3C	0.379	2.008	0.119	11036	46.2
1D	0.505	1.998	0.121		39.8
N4B	0.497	1.996	0.112	9364	41.9
N2A	0.496	1.999	0.111	10043	45.3
N1A	0.494	2.005	0.111	9186	41.3

Table 2b - Notched Strength Results for IIb, $[\pm45/(0/90)/(0/90)/\pm45]_{2S}$ Laminate Configuration

METRIC UNITS

SPEC ID	HOLE DIAMETER (mm)	SPECIMEN WIDTH (mm)	SPECIMEN THICKNESS (mm)	FAILURE LOAD (kg)	FAILURE STRESS MPa
1A	3.277	50.978	3.048	6439	405.4
2A	3.175	50.698	3.023	6726	429.5
3A	3.150	51.664	3.048	6898	428.8
1B	6.502	50.775	3.048	5410	342.0
2B	6.350	50.876	3.023	5715	364.0
3B	6.300	50.800	2.997	5439	349.5
N6C	9.525	50.622	2.819	4581	314.9
N5C	9.499	50.292	2.845	4677	320.7
N3B	9.583	50.775	2.845	4321	293.5
2C	9.779	50.495	3.048	4983	317.1
3C	9.627	51.003	3.023	5016	318.5
1D	12.827				
N4B	12.624	50.698	2.845	4247	288.9
N2A	12.598	50.775	2.819	4555	312.2
N1A	12.548	50.927	2.819	4167	284.7

Table 3a - Notched Strength Results for I_f, $[(0/90)/\pm45/\pm45/(0/90)]_{6S}$ Laminate Specimens

US CUSTOMARY UNITS

SPEC ID	HOLE DIAMETER (IN)	SPECIMEN WIDTH (IN)	SPECIMEN THICKNESS (IN)	FAILURE LOAD (LB)	FAILURE STRESS (Ksi)
1A	0.130	1.991	0.381	43750	57.7
3A	0.129	2.015	0.385	43650	56.3
1B	0.259	2.004	0.383	34050	44.4
2B	0.257	2.013	0.380	35870	46.9
3B	0.259	1.994	0.382	33980	44.6
1C	0.380	2.005	0.382	32440	42.4
2C	0.380	1.984	0.381	31840	42.1
3C	0.383	1.992	0.383	32610	42.7
1D	0.506	1.989	0.383	29270	38.4
2D	0.505	2.000	0.383	28550	37.3
3D	0.514	2.000	0.382	29770	39.0
2A -	Not drilled,bit broke				

Table 3b - Notched Strength Results for I_f, $[(0/90/\pm45/\pm45/(0/90]_{6S}$ Laminate Configuration

METRIC UNITS

SPEC ID	HOLE DIAMETER (mm)	SPECIMEN WIDTH (mm)	SPECIMEN THICKNESS (mm)	FAILURE LOAD (kg)	FAILURE STRESS MPa
1A	3.302	50.571	9.677	19886	197.8
3A	3.277	51.181	9.779	19841	388.2
1B	6.579	50.902	9.728	15477	306.1
2B	6.528	51.130	9.652	16305	323.3
3B	6.579	50.648	9.703	15445	307.4
1C	9.652	50.927	9.703	14745	292.3
2C	9.652	50.394	9.677	14473	290.3
3C	9.728	50.597	9.728	14823	294.4
1D	12.852	50.521	9.728	13305	264.7
2D	12.827	50.800	9.728	12977	257.2
3D	13.056	50.800	9.703	13532	268.9

Table 4a - Notched Strength Results for II_f, $[\pm 45/(0/90)/(0/90)/\pm 45]_{6S}$ Laminate Configuration

US CUSTOMARY UNITS

SPEC ID	HOLE DIAMETER (IN)	SPECIMEN WIDTH (IN)	SPECIMEN THICKNESS (IN)	FAILURE LOAD (LB)	FAILURE STRESS (Ksi)
N11'	0.135	1.990	0.394	37920	48.4
N9'	0.131	2.002	0.391	40140	51.3
N12'	0.137	2.001	0.400	38290	47.8
N8	0.245	2.031	0.389	33980	43.0
N2	0.257	2.001	0.401	31600	39.4
N7	0.252	1.949	0.374	31910	43.8
N3	0.373	1.937	0.399	26520	34.3
N5	0.374	2.010	0.396	28060	35.3
N1	0.372	1.996	0.384	27550	35.9
N10'	0.497	1.948	0.383	26530	35.6
N15'	0.495	1.998	0.384	27250	35.5
N16'	0.497	2.009	0.402	28910	35.8

'from different panel

Table 4b - Notched Strength Results for II_f, $[\pm 45/(0/90)/(0/90)/\pm 45]_{6S}$ Laminate Configuration

		METRIC UNITS			
SPEC ID	HOLE DIAMETER (mm)	SPECIMEN WIDTH (mm)	SPECIMEN THICKNESS (mm)	FAILURE LOAD (kg)	FAILURE STRESS MPa
N11'	3.429	50.546	10.008	17200.22	333.56
N9'	3.327	50.851	9.931	18207.20	353.69
N12'	3.480	50.825	10.610	17368.05	329.95
N8	6.223	51.587	9.881	15413.07	296.63
N2	6.274	50.825	10.185	14333.07	271.63
N7	6.401	49.505	9.510	14474.13	301.60
N3	9.474	49.200	10.135	12029.27	236.66
N5	9.499	51.054	10.058	12727.80	243.15
N1	9.449	50.698	9.754	12496.47	247.90
N10'	12.624	50.668	9.728	12033.81	239.50
N15'	12.573	50.749	9.754	12360.39	244.96
N16'	12.624	51.029	10.211	13113.36	246.89

APPENDIX B

Bolted Joint Test Data

Table 5a - Bolted Joint Data For I_a $[(0/90)/\underline{+}45/\underline{+}45/(0/90)]_S$

US CUSTOMARY UNITS

SPEC ID	WIDTH (IN)	THICKNESS (IN)	HOLE DIAMETER (IN)	t/D	W/D	EDGE DISTANCE (IN)	e/D	BOLT DIAMETER (IN)	FASTNER TORQUE (IN)	BEARING DAMAGE LOAD (LB)	BEARING DAMAGE STRESS (Ksi)	FAILURE LOAD	FAILURE STRESS (Ksi)	FAILURE MODE
1A	0.497	0.064	0.195	0.33	2.55	0.757	3.88	0.182	25	1310	41.2	1317	41.4	NT
2A	0.498	0.064	0.195	0.33	2.55	0.757	3.88	0.182	25	1285	40.3	1354	42.5	NT
3A	0.495	0.065	0.195	0.33	2.54	0.757	3.88	0.182	25	1250	38.9	1277	39.7	NT
1B	0.496	0.064	0.194	0.33	2.56	0.757	3.90	0.183	50	620	19.5	1322	41.6	NT
2B	0.495	0.064	0.193	0.33	2.56	0.752	3.90	0.183	50	785	24.8	1238	39.1	NT
3B	0.496	0.065	0.194	0.34	2.56	0.751	3.87	0.183	50	1220	37.8	1230	38.2	NT
1C	0.995	0.065	0.192	0.34	5.18	0.756	3.94	0.182	25	-	-	1931	29.9	BRG
2C	0.993	0.066	0.191	0.35	5.20	0.752	3.94	0.182	25	-	-	1642	25.1	BRG
3C	0.997	0.065	0.193	0.34	5.17	0.753	3.90	0.182	25	-	-	1723	26.6	BRG
1D	0.973	0.065	0.193	0.34	5.04	0.753	3.90	0.183	50	-	-	2258	35.7	BRG
2D	0.995	0.065	0.192	0.34	5.18	0.752	3.92	0.183	50	-	-	2208	34.1	BRG
3D	0.984	0.065	0.192	0.34	5.13	0.751	3.91	0.183	50	-	-	2021	31.6	BRG

Table 5b - Bolted Joint Data For I_a $[(0/90)/\underline{+}45/\underline{+}45/(0/90)]_S$

METRIC UNITS

SPEC ID	WIDTH (mm)	THICKNESS (mm)	HOLE DIAMETER (mm)	t/D	W/D	EDGE DISTANCE (mm)	e/D	BOLT DIAMETER (mm)	FASTNER TORQUE (Nm)	BEARING DAMAGE LOAD (Kg)	BEARING DAMAGE STRESS (MPa)	FAILURE LOAD (Kg)	FAILURE STRESS (MPa)	FAILURE MODE
1A	12.624	1.626	4.953	0.33	2.55	19.228	3.88	4.623	2.82	595.5	283.9	598.6	285.5	NT
2A	12.649	1.626	4.953	0.33	2.55	19.228	3.88	4.623	2.82	585.1	278.0	615.5	292.9	NT
3A	12.573	1.651	4.953	0.33	2.54	19.228	3.88	4.623	2.82	568.2	267.8	580.5	273.6	NT
1B	12.598	1.626	4.928	0.33	2.56	19.228	3.90	4.648	5.65	281.8	134.7	600.9	287.1	NT
2B	12.573	1.626	4.902	0.33	2.56	19.101	3.90	4.648	5.65	356.8	170.8	562.7	269.4	NT
3B	12.598	1.651	4.928	0.34	2.56	10.075	3.87	4.648	5.65	554.5	260.9	559.1	263.0	NT
1C	25.273	1.651	4.877	0.34	5.18	10.202	3.94	4.623	2.82	-	-	877.7	205.8	BRG
2C	25.222	1.676	4.851	0.35	5.20	19.101	3.94	4.623	2.82	-	-	746.4	172.7	BRG
3C	25.323	1.651	4.902	0.34	5.17	19.126	3.90	4.623	2.82	-	-	783.2	183.3	BRG
1D	24.714	1.651	4.902	0.34	5.04	19.126	3.90	4.648	5.65	-	-	1026.4	246.1	BRG
2D	25.273	1.651	4.877	0.34	5.18	19.101	3.92	4.648	5.65	-	-	1003.6	235.4	BRG
3D	24.994	1.651	4.877	0.34	5.13	19.075	3.91	4.648	5.65	-	-	918.6	217.8	BRG

Table 6a - Bolted Joint, Test Data for II_a $[(\pm 45)/0/90)/(0/90)/\pm 45)]_S$ US CUSTOMARY UNITS

SPEC ID	WIDTH (IN)	THICKNESS (IN)	HOLE DIAMETER (IN)	t/D	W/D	EDGE DISTANCE (IN)	e/D	BOLT DIAMETER (IN)	FASTNER TORQUE (IN)	BEARING DAMAGE LOAD (LB)	BEARING DAMAGE STRESS (Ksi)	FAILURE LOAD (LB)	FAILURE STRESS (Ksi)	FAILURE MODE
1A	0.497	0.065	0.194	0.34	2.56	0.754	3.87	0.182	25	1263	39.1	1328	41.1	NT
2A	0.497	0.064	0.193	0.33	2.58	0.754	3.91	0.182	25	1285	40.4	1285	40.4	NT
3A	0.495	0.060	0.188	0.32	2.63	0.754	4.01	0.182	25	-	-	1183	39.8	NT
1B	0.496	0.064	0.193	0.33	2.57	0.754	3.91	0.182	50	1250	39.4	1278	40.3	NT
2B	0.496	0.064	0.195	0.33	2.54	0.755	3.87	0.182	50	1075	33.9	1321	41.6	NT
3B	0.497	0.064	0.194	0.33	2.56	0.753	3.88	0.182	50	1081	34.0	1251	39.3	NT
1C	0.988	0.064	0.189	0.34	5.23	0.750	3.97	0.184	25	-	-	2055	32.5	BRG
2C	0.981	0.066	0.192	0.34	5.11	0.751	3.91	0.184	25	-	-	1970	30.4	BRG
3C	0.983	0.064	0.190	0.34	5.17	0.750	3.95	0.184	25	-	-	1856	29.5	BRG
1D	0.983	0.065	0.192	0.34	5.12	0.752	3.92	0.183	50	-	-	2295	35.9	BRG
2D	0.992	0.064	0.193	0.33	5.14	0.754	3.91	0.183	50	-	-	2140	33.7	BRG
3D	0.968	0.065	0.191	0.34	5.07	0.752	3.94	0.183	50	-	-	1944	30.9	BRG

Table 6b - Bolted Joint Data for II_a $[(\pm 45)/(0/90)/(0/90)/\pm 45]_S$ METRIC UNITS

SPEC ID	WIDTH (mm)	THICKNESS (mm)	HOLE DIAMETER (mm)	t/D	W/D	EDGE DISTANCE (mm)	e/D	BOLT DIAMETER (mm)	FASTNER TORQUE (Nm)	BEARING DAMAGE LOAD (Kg)	BEARING DAMAGE STRESS (MPa)	FAILURE LOAD (Kg)	FAILURE STRESS (MPa)	FAILURE MODE
1A	12.624	1.651	4.928	0.34	2.56	19.152	3.87	4.623	2.82	574.1	269.5	603.6	283.4	NT
2A	12.624	1.626	4.902	0.33	2.58	19.152	3.91	4.623	2.82	584.1	278.5	584.1	278.5	NT
3A	12.573	1.524	4.775	0.32	2.63	19.152	4.01	4.623	2.82	-	-	537.7	274.6	NT
1B	12.598	1.626	4.902	0.33	2.57	19.152	3.91	4.623	5.65	568.2	271.5	580.9	277.6	NT
2B	12.598	1.626	4.953	0.33	2.54	19.177	3.87	4.623	5.65	488.6	233.5	600.5	286.9	NT
3B	12.624	1.626	4.928	0.33	2.56	19.126	3.88	4.623	5.65	491.4	234.3	568.6	271.2	NT
1C	25.095	1.626	4.801	.034	5.23	19.050	3.97	4.674	2.82	-	-	934.1	224.1	BRG
2C	24.917	1.676	4.877	0.34	5.11	19.075	3.91	4.674	2.82	-	-	895.5	209.8	BRG
3C	24.968	1.626	4.826	0.34	5.17	19.050	3.95	4.674	2.82	-	-	843.6	203.4	BRG
1D	24.968	1.651	4.877	0.34	5.12	19.101	3.92	4.648	5.65	-	-	1043.2	247.6	BRG
2D	25.197	1.626	4.902	0.33	5.14	19.152	3.91	4.648	5.65	-	-	972.7	232.4	BRG
3D	24.587	1.651	4.851	0.34	5.07	19.101	3.94	4.648	5.65	-	-	883.6	213.0	BRG

Table 7a - Bolted Joint Test Data for I_b $[(0/90)/\pm45/\pm45/(0/90)]_{2S}$ US CUSTOMARY UNITS

SPEC ID	WIDTH (IN)	THICKNESS (IN)	HOLE DIAMETER (IN)	t/D	W/D	EDGE DISTANCE (IN)	e/D	BOLT DIAMETER (IN)	FASTNER TORQUE (IN)	BEARING DAMAGE LOAD (LB)	BEARING DAMAGE STRESS (Ksi)	FAILURE LOAD (LB)	FAILURE STRESS (Ksi)	FAILURE MODE
1B	1.060	0.127	0.377	0.34	2.81	1.5	3.98	0.373	50	-	-	3807	28.3	NT
2B	1.117	0.125	0.378	0.33	2.96	1.5	3.97	0.373	50	-	-	3997	28.6	NT
3B	1.117	01.25	0.381	0.33	2.93	1.5	3.94	0.373	50	-	-	3853	27.6	NT
4B	1.123	0.125	0.379	0.33	2.96	1.5	3.96	0.373	100	-	-	4080	29.1	NT
5B	1.110	0.127	0.378	0.34	2.94	1.5	3.97	0.373	100	-	-	3377	24.0	NT
6B	1.112	0.128	0.381	0.34	2.92	1.5	3.94	0.373	100	-	-	3964	27.9	NT
1A	2.246	0.124	0.385	0.32	5.83	1.5	3.90	0.373	50	6170	22.2	6763	24.3	BRG
2A	2.245	0.122	0.374	0.33	6.00	1.5	4.01	0.373	50	6370	23.3	7142	26.1	BRG
3A	2.245	0.123	0.376	0.33	5.97	1.5	3.99	0.373	50	5960	21.6	6642	24.1	BRG
4A	2.248	0.122	0.379	0.32	5.93	1.5	3.96	0.373	100	6350	23.2	6778	24.7	NT
5A	2.246	0.124	0.375	0.33	5.99	1.5	4.00	0.373	100	6590	23.7	7464	26.4	BRG
6A	2.248	0.123	0.376	0.33	5.98	1.5	3.99	0.373	100	6470	23.4	6903	25.0	BRG

Table 7b - Bolted Joint Data for I_b $[(0/90)/\underline{+}45/\underline{+}45/(0/90)]_{2S}$

METRIC UNITS

SPEC ID	WIDTH (mm)	THICKNESS (mm)	HOLE DIAMETER (mm)	t/D	W/D	EDGE DISTANCE (mm)	e/D	BOLT DIAMETER (mm)	FASTNER TORQUE (Nm)	BEARING DAMAGE LOAD (Kg)	BEARING DAMAGE STRESS (MPa)	FAILURE LOAD (Kg)	FAILURE STRESS (MPa)	FAILURE MODE
1B	26.924	3.226	9.576	0.34	2.81	38.1	3.98	9.474	5.65	-	-	1726.8	195.1	NT
2B	28.372	3.175	9.601	0.33	2.96	38.1	3.97	9.474	5.65	-	-	1813.0	197.5	NT
3B	28.372	3.175	9.677	0.33	2.93	38.1	3.94	9.474	5.65	-	-	1747.7	190.4	NT
4B	28.524	3.175	9.627	0.33	2.96	38.1	3.96	9.474	11.30	-	-	1850.7	200.5	NT
5B	28.194	3.226	9.601	0.34	2.94	38.1	3.97	9.474	11.30	-	-	1531.8	165.3	NT
6B	28.245	3.251	9.677	0.34	2.92	38.1	3.94	9.474	11.30	-	-	1789.0	192.2	NT
1A	57.048	3.150	9.779	0.32	5.83	38.1	3.90	9.474	5.65	2798.7	152.9	3067.6	167.5	BRG
2A	57.023	3.100	9.499	0.33	6.00	38.1	4.01	9.474	5.65	2889.4	160.5	3239.6	179.9	BRG
3A	57.023	3.124	9.550	0.33	5.97	38.1	3.99	9.474	5.65	2703.4	148.9	3012.8	165.9	BRG
4A	57.099	3.100	9.627	0.32	5.93	38.1	3.96	9.474	11.30	2880.3	159.8	3074.5	170.5	NT
5A	57.048	3.150	9.525	0.33	5.99	38.1	4.00	9.474	11.30	2989.2	163.3	3340.3	182.4	BRG
6A	57.099	3.124	9.550	0.33	5.98	38.1	3.99	9.474	11.30	2934.7	161.4	3131.2	172.3	BRG

Table 8a - Bolted Joint, Test Data for I_b $[(0/90)/\underline{+}45/\underline{+}45/(0/90)]_{2S}$ US CUSTOMARY UNITS

SPEC ID	WIDTH (IN)	THICKNESS (IN)	HOLE DIAMETER (IN)	t/D	W/D	EDGE DISTANCE (IN)	e/D	BOLT DIAMETER (IN)	FASTNER TORQUE (IN)	BEARING DAMAGE LOAD (LB)	BEARING DAMAGE STRESS (Ksi)	FAILURE LOAD (LB)	FAILURE STRESS (Ksi)	FAILURE MODE
*1D	0.560	0.125	0.192	0.65	2.92	0.75	3.91	0.184	25	-	-	2316	33.1	NT
3D	0.562	0.125	0.190	0.66	2.96	0.75	3.95	0.184	25	-	-	2503	35.6	NT
4D	0.562	0.125	0.186	0.67	3.02	0.75	4.03	0.184	25	-	-	2233	31.8	NT
5D	0.563	0.125	0.189	0.66	2.98	0.75	3.97	0.184	50	-	-	2445	34.7	NT
5D	0.571	0.125	0.189	0.66	3.02	0.75	3.97	0.184	50	-	-	2405	33.7	NT
7D	0.559	0.125	0.193	0.65	2.90	0.75	3.89	0.184	50	-	-	2307	33.0	NT
8D	0.559	0.125	0.190	0.66	2.94	0.75	3.95	0.184	50	-	-	2193	31.4	NT
7C	1.060	0.127	0.188	0.67	5.64	0.75	3.99	0.187	25	2918	21.7	3597	26.7	BRG
*8C	1.118	0.124	0.189	0.66	5.91	0.75	3.97	0.187	25	2045	14.8	3308	23.9	BRG
9C	1.121	0.122	0.189	0.64	5.93	0.75	3.97	0.187	25	3239	23.7	3364	24.6	BRG
10C	1.117	0.125	0.189	0.66	5.91	0.75	3.97	0.187	50	-	-	3507	25.1	BRG
11C	1.119	0.125	0.187	0.67	5.98	0.75	4.01	0.187	50	3285	23.5	3534	25.3	BRG
12C	1.118	0.126	0.193	0.65	5.79	0.75	3.89	0.187	50	3310	23.5	3581	25.4	BRG

Table 8b - Bolted Joint Data for I_b $[(0/90)/\underline{+}45/\underline{+}45/0/90)]_{2S}$

METRIC UNITS

SPEC ID	WIDTH (mm)	THICKNESS (mm)	HOLE DIAMETER (mm)	t/D	W/D	EDGE DISTANCE (mm)	e/D	BOLT DIAMETER (mm)	FASTNER TORQUE (Nm)	BEARING DAMAGE LOAD (Kg)	BEARING DAMAGE STRESS (MPa)	FAILURE LOAD (Kg)	FAILURE STRESS (MPa)	FAILURE MODE
*1D	14.224	3.175	4.877	0.65	2.92	19.05	3.91	4.674	2.82	-	-	1050.5	228.3	NT
3D	14.275	3.175	4.826	0.66	2.96	19.05	3.95	4.674	2.82	-	-	1135.3	245.8	NT
4D	14.275	3.175	4.724	0.67	3.02	10.05	4.03	4.674	2.82	-	-	1012.9	219.3	NT
5D	14.300	3.175	4.801	0.66	2.98	19.05	3.97	4.674	5.65	-	-	1109.0	239.7	NT
6D	14.503	3.175	4.801	0.66	3.02	19.05	3.97	4.674	5.65	-	-	1090.9	232.5	NT
7D	14.199	3.175	4.902	.065	2.90	19.05	3.89	4.674	5.65	-	-	1046.4	227.8	NT
8D	14.199	3.175	4.826	0.66	2.94	10.05	3.95	4.674	5.65	-	-	994.7	216.5	NT
7C	26.924	3.226	4.775	0.67	5.64	19.05	3.99	4.750	2.82	1323.6	149.6	1631.6	184.4	BRG
*8C	28.397	3.150	4.801	0.66	5.91	19.05	3.97	4.750	2.82	927.6	101.8	1500.5	164.6	BRG
9C	28.473	3.099	4.801	0.64	5.93	19.05	3.97	4.750	2.82	1469.2	163.4	1525.9	169.7	BRG
10C	28.372	3.175	4.801	0.66	5.91	19.05	3.97	4.750	5.65	-	-	1590.7	173.3	BRG
11C	28.423	3.175	4.750	.067	5.98	19.05	4.01	4.750	5.65	1490.1	162.0	1603.0	174.3	BRG
12C	28.397	3.200	4.902	0.65	5.79	19.05	3.89	4.750	5.65	1501.4	162.1	1624.3	175.4	BRG

*tested w/o end tabs

Table 9a - Bolted Joint, Test Data for II_b $[\pm 45/(0/90)/(0/90)/\pm 45]_{2S}$ US CUSTOMARY UNITS

SPEC ID	WIDTH (IN)	THICKNESS (IN)	HOLE DIAMETER (IN)	t/D	W/D	EDGE DISTANCE (IN)	e/D	BOLT DIAMETER (IN)	FASTNER TORQUE (IN)	BEARING DAMAGE LOAD (LB)	BEARING DAMAGE STRESS (Ksi)	FAILURE LOAD (LB)	FAILURE STRESS (Ksi)	FAILURE MODE
5D	0.562	0.125	0.192	0.65	2.93	0.75	3.91	0.184	25	-	-	2416	34.3	NT
6D	0.564	0.130	0.193	0.67	2.92	0.75	3.87	0.184	25	-	-	2368	32.3	NT
7D	0.563	0.124	0.192	0.65	2.93	0.75	3.91	0.184	25	-	-	2365	33.9	NT
8D	0.565	0.130	0.192	0.68	2.94	0.75	3.91	0.184	25	-	-	2298	31.3	NT
1DD	0.566	0.124	0.190	0.65	2.98	0.75	3.95	0.184	50	-	-	2722	38.8	NT
2DD	0.567	0.125	0.189	0.66	3.00	0.75	3.97	0.184	50	-	-	2436	34.4	NT
3DD	0.566	0.123	0.190	0.65	2.98	0.75	3.95	0.184	50	-	-	2511	36.1	NT
4DD	0.567	0.124	0.190	0.65	2.98	0.75	3.95	0.184	50	-	-	2392	24.0	NT
8E	1.080	0.123	0.192	0.64	5.63	0.75	3.91	0.187	25	-	-	2997	22.6	BRG
9E	1.133	0.128	0.191	0.67	5.93	0.75	3.93	0.187	25	2570	17.7	3493	24.1	BRG
10E	1.126	0.129	0.192	0.67	5.86	0.75	4.04	0.187	25	-	-	3775	26.0	BRG
11E	1.081	0.130	0.194	0.67	5.57	0.75	3.87	0.185	50	-	-	3951	28.1	BRG
12E	1.133	0.129	0.189	0.68	5.99	0.75	3.97	0.185	50	3026	20.7	3870	26.5	BRG
14E*	1.082	0.130	0.194	0.67	5.61	0.75	3.89	0.184	50	-	-	3836	27.3	BRG

*bolt failure

Table 9b - Bolted Joint Data for II_b $[\underline{+}45/(0/90)(0/90)/\underline{+}45]_{2S}$ METRIC UNITS

SPEC ID	WIDTH (mm)	THICKNESS (mm)	HOLE DIAMETER (mm)	t/D	W/D	EDGE DISTANCE (mm)	e/D	BOLT DIAMETER (mm)	FASTNER TORQUE (Nm)	BEARING DAMAGE LOAD (Kg)	BEARING DAMAGE STRESS (MPa)	FAILURE LOAD (Kg)	FAILURE STRESS (MPa)	FAILURE MODE
5D	14.275	3.175	4.877	0.65	2.93	19.05	3.91	4.674	2.82	-	-	1096	236.9	NT
6D	14.326	3.302	4.902	0.67	2.92	19.05	3.87	4.674	2.82	-	-	1074	222.8	NT
7D	14.300	3.150	4.877	0.65	2.93	19.05	3.91	4.674	2.82	-	-	1073	233.7	NT
8D	14.351	3.302	4.877	0.68	2.94	19.05	3.91	4.674	2.82	-	-	1042	215.9	NT
10D	14.376	3.150	4.826	0.65	2.98	19.05	3.95	4.674	5.65	-	-	1235	267.6	NT
2DD	14.402	3.175	4.801	0.66	3.00	19.05	3.97	4.674	5.65	-	-	1105	237.1	NT
3DD	14.376	3.124	4.826	0.65	2.98	19.05	3.95	4.674	5.65	-	-	1139	248.9	NT
4DD	14.402	3.150	4.826	0.65	2.98	19.05	3.95	4.674	5.65	-	-	1085	234.7	NT
8E	28.778	3.124	4.877	0.64	5.63	19.05	3.91	4.750	2.82	-	-	1359	155.7	BRG
9E	28.600	3.251	4.851	0.67	5.93	19.05	3.93	4.750	2.82	1165.73	122.27	1584	166.2	BRG
10E	27.457	3.277	4.877	0.67	5.86	19.05	4.04	4.750	2.82	-	-	1712	179.3	BRG
11E	27.457	3.302	4.928	0.67	5.57	19.05	3.87	4.699	5.65	1741.79	188.53	1792	194.0	BRG
12E	28.778	3.277	4.801	0.68	5.99	19.05	3.97	4.699	5.65	1372.57	142.85	1755	182.7	BRG
*14E	27.483	3.302	4.902	0.67	5.61	19.05	3.89	4.674	5.65	-	-	1740	188.2	BRG

*Bolt Failure

Table 10a - Bolted Joint, Test Data for II_b $[\pm 45/(0/90)/(0/90)/\pm 45]_{2S}$ US CUSTOMARY UNITS

SPEC ID	WIDTH (IN)	THICKNESS (IN)	HOLE DIAMETER (IN)	t/D	W/D	EDGE DISTANCE (IN)	e/D	BOLT DIAMETER (IN)	FASTNER TORQUE (IN)	BEARING DAMAGE LOAD (LB)	BEARING DAMAGE STRESS (Ksi)	FAILURE LOAD (LB)	FAILURE STRESS (Ksi)	FAILURE MODE
1B	1.128	0.129	0.376	0.34	3.00	1.5	3.99	0.373	50	-	-	4068	28.0	NT
2B	1.128	0.130	0.378	0.34	2.98	1.5	3.97	0.373	50	-	-	4133	28.2	NT
3B	1.128	0.130	0.376	0.35	3.00	1.5	3.99	0.373	50	-	-	4135	28.2	NT
5B	1.121	0.127	0.376	0.34	2.98	1.5	3.99	0.373	100	-	-	4154	29.2	NT
6B	1.126	0.130	0.376	0.35	2.99	1.5	3.99	0.373	100	-	-	4013	27.5	NT
7B	1.127	0.130	0.375	0.35	3.00	1.5	4.00	0.373	100	-	-	4080	27.8	NT
4C	2.185	0.128	0.375	0.34	5.83	1.5	4.00	0.373	50	6683	24.0	7120	25.5	NT
5C	2.257	0.126	0.377	0.33	5.99	1.5	3.98	0.373	50	6320	22.2	6878	24.2	BRG
6C	2.255	0.127	0.376	0.34	6.00	1.5	3.99	0.373	50	5880	20.5	7058	24.6	BRG
10CC	2.244	0.120	0.376	0.32	5.97	1.5	3.99	0.373	100	5730	21.3	6772	25.1	BRG
11CC	2.250	0.123	0.378	0.33	5.95	1.5	3.97	0.373	100	6120	22.1	6788	24.5	BRG
12CC	2.244	0.118	0.377	0.31	5.95	1.5	3.98	0.373	100	6130	23.2	6777	25.6	BRG

*CC from a different cured panel

Table 10b - Bolted Joint Data for II_b $[\pm 45/(0/90)/(0/90)/\pm 45]_{2S}$ METRIC UNITS

SPEC ID	WIDTH (mm)	THICKNESS (mm)	HOLE DIAMETER (mm)	t/D	W/D	EDGE DISTANCE (mm)	e/D	BOLT DIAMETER (mm)	FASTNER TORQUE (Nm)	BEARING DAMAGE LOAD (Kg)	BEARING DAMAGE STRESS (MPa)	FAILURE LOAD (Kg)	FAILURE STRESS (MPa)	FAILURE MODE
1B	28.651	3.277	9.550	0.34	3.00	38.1	3.99	9.474	5.65	-	-	1845	192.9	NT
2B	28.651	3.302	9.601	0.34	2.98	38.1	3.97	9.474	5.65	-	-	1875	194.5	NT
3B	28.651	3.302	9.550	0.35	3.00	38.1	3.99	9.474	5.65	-	-	1876	194.6	NT
5B	28.473	3.226	9.550	0.34	2.98	38.1	3.99	9.474	11.30	-	-	1884	201.3	NT
6B	28.600	3.302	9.550	0.35	2.99	38.1	3.99	9.474	11.30	-	-	1820	189.7	NT
7B	28.626	3.302	9.525	0.35	3.00	38.1	4.00	9.474	11.30	-	-	1851	192.1	NT
4C	55.499	3.251	9.525	0.34	5.83	38.1	4.00	9.474	5.65	3031	164.9	3230	175.6	NT
5C	57.328	3.200	9.576	0.33	5.99	38.1	3.98	9.474	5.65	2867	153.3	3120	166.9	BRG
6C	57.277	3.226	9.550	0.34	6.00	38.1	3.99	9.474	5.65	2667	141.7	3201	170.0	BRG
10CC	56.998	3.048	9.550	0.32	5.97	38.1	3.99	9.474	11.30	2599	146.8	3072	173.5	BRG
11CC	57.150	3.124	9.601	0.33	5.95	38.1	3.97	9.474	11.30	2776	152.6	3079	169.2	BRG
12CC	56.998	2.997	9.576	0.31	5.95	38.1	3.98	9.474	11.30	2781	159.7	3074	176.6	BRG

*CC fram a different cured panel

Table 11a - Bolted Joint Data For I_c $[(0/90)/\pm45/\pm45/(0/90)]_{3S}$ US CUSTOMARY UNITS

SPEC ID	WIDTH (IN)	THICKNESS (IN)	HOLE DIAMETER (IN)	t/D	W/D	EDGE DISTANCE (IN)	e/D	BOLT DIAMETER (IN)	FASTNER TORQUE (IN)	BEARING DAMAGE LOAD (LB)	BEARING DAMAGE STRESS (Ksi)	FAILURE LOAD (LB)	FAILURE STRESS (Ksi)	FAILURE MODE
1A	0.496	0.174	0.195	0.89	2.31	0.759	3.90	0.184	25	-	-	3772	43.7	NT
2A	0.495	0.173	0.195	0.89	2.54	0.763	3.91	0.184	25	-	-	3404	39.8	NT
3A	0.497	0.193	0.195	0.99	2.55	0.756	3.88	0.183	25	2640	27.5	3261	34.0	NT
1B	0.497	0.174	0.196	0.89	2.54	0.759	3.87	0.183	50	-	-	3442	39.8	NT
2B	0.497	0.194	0.194	1.00	2.56	0.758	3.91	0.184	50	-	-	3464	35.9	NT
3B	0.493	0.173	0.195	0.89	2.53	0.759	3.89	0.184	50	-	-	3602	42.2	NT
*1C	0.980	0.171	0.193	0.89	5.08	0.751	3.89	0.189	25	-	-	5535	33.0	BRG
*2C	0.963	0.172	0.192	0.90	5.02	0.750	3.91	0.189	25	-	-	5939	35.9	BRG
53B	1.132	0.192	0.192	1.00	5.90	0.770	4.01	0.187	25	-	-	5672	26.1	BRG
54B	1.125	0.190	0.193	0.98	5.83	0.769	3.98	0.187	25	-	-	5742	26.9	BRG
52A	1.128	0.190	0.195	0.97	5.78	0.774	3.97	0.187	50	-	-	5755	26.9	BRG
54A	1.119	0.190	0.191	0.99	5.86	0.767	4.02	0.187	50	-	-	6084	28.6	BRG

* Bolt Bent

Table 11b - Bolted Joint Data for I_c $[(0/90)/\pm 45/\pm 45/(0/90)]_{3S}$

METRIC UNITS

SPEC ID	WIDTH (mm)	THICKNESS (mm)	HOLE DIAMETER (mm)	t/D	W/D	EDGE DISTANCE (mm)	e/D	BOLT DIAMETER (mm)	FASTNER TORQUE (Nm)	BEARING DAMAGE LOAD (Kg)	BEARING DAMAGE STRESS (MPa)	FAILURE LOAD (Kg)	FAILURE STRESS (MPa)	FAILURE MODE
1A	12.598	4.419	4.953	0.89	2.31	19.279	3.90	4.674	2.82	-	-	1714.5	301.3	NT
2A	12.573	4.394	4.953	0.89	2.54	19.380	3.91	4.674	2.82	-	-	1547.3	274.1	NT
3A	12.624	4.902	4.953	0.99	2.55	19.202	3.88	4.648	2.82	1200.00	189.7	1482.3	234.4	NT
1B	12.624	4.419	4.978	0.89	2.54	19.279	3.87	4.648	5.65	-	-	1564.5	274.4	NT
2B	12.624	4.928	4.928	1.00	2.56	19.253	3.91	4.674	5.65	-	-	1574.5	247.7	NT
3B	12.522	4.394	4.953	0.89	2.53	19.279	3.89	4.674	5.65	-	-	1637.3	291.2	NT
1C	24.892	4.343	4.902	0.89	5.08	19.075	3.89	4.801	2.82	-	-	2515.9	227.7	BRG
2C	24.460	4.369	4.877	0.90	5.02	19.050	3.91	4.801	2.82	-	-	2699.5	247.2	BRG
S3B	28.753	4.877	4.877	1.00	5.90	19.558	4.01	4.750	2.82	-	-	2572.8	179.9	BRG
S4B	28.575	4.826	4.902	0.98	5.83	19.533	3.98	4.750	2.82	-	-	2604.5	185.5	BRG
S2A	28.651	4.826	4.953	0.97	5.78	19.660	3.97	4.750	5.65	-	-	2610.4	185.5	BRG
S4A	28.423	4.826	4.851	0.99	5.86	19.482	4.02	4.750	5.65	-	-	2759.7	197.2	BRG

Table 12a - Bolted Joint Data For I_c $[(0/90)/\underline{+}45/\underline{+}45/(0/90)]_S$ US CUSTOMARY UNITS

SPEC ID	WIDTH (IN)	THICKNESS (IN)	HOLE DIAMETER (IN)	t/D	W/D	EDGE DISTANCE (IN)	e/D	BOLT DIAMETER (IN)	FASTNER TORQUE (IN)	BEARING DAMAGE LOAD (LB)	BEARING DAMAGE STRESS (Ksi)	FAILURE LOAD (LB)	FAILURE STRESS (Ksi)	FAILURE MODE
1E	1.516	0.171	0.508	0.34	2.98	2.000	3.94	0.499	100	8250	31.8	9107	35.1	NT
2E	1.493	0.170	0.507	0.34	2.94	1.996	3.49	0.499	100	6700	26.4	9134	36.1	NT
3E	1.500	0.177	0.511	0.35	2.94	1.998	3.91	0.499	100	6723	25.3	9198	34.6	NT
1F	1.495	0.176	0.509	0.35	2.94	1.998	3.93	0.499	200	7831	29.8	9350	35.5	NT
2F	1.497	0.176	0.508	0.35	2.95	1.997	3.93	0.499	200	7553	28.7	9267	35.2	NT
3F	1.498	0.174	0.508	0.34	2.95	1.996	3.93	0.499	200	7695	29.5	9626	36.9	NT
1G	2.991	0.191	0.507	0.38	5.90	2.010	3.96	0.498	100	-	-	12580	22.0	BRG
2G	2.992	0.187	0.507	0.37	5.90	2.010	3.96	0.498	100	-	-	10980	19.6	BRG
3G	2.958	0.190	0.508	0.37	5.82	2.010	3.96	0.498	100	-	-	13680	24.3	BRG
1H	2.995	0.187	0.507	0.37	5.91	2.010	3.96	0.498	100	-	-	12800	22.9	BRG
S1B	2.984	0.184	0.507	0.36	5.89	2.030	4.00	0.497	200	-	-	13098	23.9	BRG

Table 12b - Bolted Joint Data for I_c $[(0/90)/\pm 45/\pm 45/(0/90)]_{3S}$ METRIC UNITS

SPEC ID	WIDTH (mm)	THICKNESS (mm)	HOLE DIAMETER (mm)	t/D	W/D	EDGE DISTANCE (mm)	e/D	BOLT DIAMETER (mm)	FASTNER TORQUE (Nm)	BEARING DAMAGE LOAD (Kg)	BEARING DAMAGE STRESS (MPa)	FAILURE LOAD (Kg)	FAILURE STRESS (MPa)	FAILURE MODE
1E	38.506	4.343	12.903	0.34	2.98	50.800	3.94	12.675	11.30	3750.0	219.4	4139.5	242.2	NT
2E	37.922	4.318	12.878	0.34	2.94	50.698	3.94	12.674	11.30	3045.5	182.0	4160.9	248.7	NT
3E	38.100	4.496	12.979	0.35	2.94	50.749	3.91	12.675	11.30	3055.9	174.4	4180.9	238.9	NT
1F	37.973	4.470	12.929	0.35	2.94	50.749	3.93	12.675	22.60	3559.5	205.2	4250.0	245.0	NT
2F	38.024	4.470	12.903	0.35	2.95	50.724	3.93	12.674	22.60	3433.2	197.6	4212.3	242.5	NT
3F	38.049	4.420	12.903	0.34	2.95	50.698	3.93	12.675	22.60	3497.7	203.5	4375.5	254.6	NT
1G	75.971	4.851	12.878	0.38	5.90	51.054	3.96	12.649	11.30	-	-	5718.2	151.8	BRG
2G	75.997	4.750	12.878	0.37	5.90	51.054	3.96	12.649	11.30	-	-	4990.9	135.3	BRG
3G	75.133	4.826	12.903	0.37	5.82	51.054	3.96	12.649	11.30	-	-	6218.2	167.8	BRG
1H	76.073	4.750	12.878	0.37	5.91	51.054	3.96	12.649	11.30	-	-	5818.2	157.6	BRG
S1B	75.794	4.674	12.878	0.36	5.89	51.562	4.00	12.624	22.60	-	-	6243.7	173.1	BRG
S1A	75.717	4.674	12.903	0.36	5.87	50.902	3.94	12.624	22.60	-	-	5941.1	164.8	BRG
S5B	74.854	4.724	12.878	0.37	5.81	50.952	3.96	12.624	22.60	5588.3	155.1	6191.1	171.7	BRG

Table 13a - Bolted Joint Data for II_c $[\pm 45/(0/90)/(0/90)/\pm 45]_{3S}$ US CUSTOMARY UNITS

SPEC ID	WIDTH (IN)	THICKNESS (IN)	HOLE DIAMETER (IN)	t/D	W/D	EDGE DISTANCE (IN)	e/D	BOLT DIAMETER (IN)	FASTNER TORQUE (IN)	BEARING DAMAGE LOAD (LB)	BEARING DAMAGE STRESS (Ksi)	FAILURE LOAD (LB)	FAILURE STRESS (Ksi)	FAILURE MODE
1A	0.492	0.919	0.192	0.99	2.56	0.756	3.94	0.184	25	2050	21.8	3097	33.0	NT
2A	0.490	0.191	0.193	0.99	2.54	0.754	3.91	0.185	25	3175	33.9	3325	35.5	NT
3A	0.498	0.169	0.195	0.87	2.55	0.755	3.87	0.184	25	-	-	3781	44.9	NT
1B	0.485	0.192	0.195	0.98	2.49	0.755	3.87	0.187	50	-	-	3188	34.2	NT
2B	0.487	0.192	0.192	1.00	2.59	0.753	3.92	0.187	50	-	-	3002	32.1	NT
3B	0.497	0.171	0.194	0.88	2.56	0.757	3.90	0.187	50	-	-	3199	37.6	NT
1C	0.996	0.170	0.191	0.89	5.21	0.753	3.94	0.189	25	-	-	5734	33.9	BRG
2C	0.994	0.173	0.192	0.90	5.18	0.751	3.91	0.185	25	-	-	5233	30.4	BRG
S5C	1.140	0.184	0.191	0.96	5.97	0.746	3.91	0.187	25	-	-	5695	27.2	BRG
S3C	1.132	0.194	0.190	1.02	5.96	0.767	4.04	0.187	25	-	-	6010	27.4	BRG
S2D	1.124	0.193	0.194	0.99	5.79	0.772	3.98	0.187	50	-	-	5972	27.5	BRG
S3D	1.129	0.194	0.191	1.02	5.91	0.750	3.93	0.187	50	-	-	6116	27.9	BRG
S5D	1.134	0.184	0.191	0.97	5.97	0.765	4.03	0.187	50	-	-	6115	29.3	BRG

Table 13b - Bolted Joint Data for II_c $[\underline{+}45/(0/90)/(0/90)/\underline{+}45]_{3S}$ METRIC UNITS

SPEC ID	WIDTH (mm)	THICKNESS (mm)	HOLE DIAMETER (mm)	t/D	W/D	EDGE DISTANCE (mm)	e/D	BOLT DIAMETER (mm)	FASTNER TORQUE (Nm)	BEARING DAMAGE LOAD (Kg)	BEARING DAMAGE STRESS (MPa)	FAILURE LOAD (Kg)	FAILURE STRESS (MPa)	FAILURE MODE
1A	12.497	4.851	4.877	0.99	2.56	19.202	3.94	4.674	2.82	931.8	150.4	1407.7	227.2	NT
2A	12.446	4.851	4.902	0.99	2.54	19.152	3.91	4.699	2.82	1443.2	233.9	1511.4	244.9	NT
3A	12.649	4.293	4.953	0.87	2.55	19.177	3.87	4.674	2.82	-	-	1718.6	309.7	NT
1B	12.319	4.877	4.953	0.98	2.49	19.177	3.87	4.750	5.65	-	-	1449.1	236.0	NT
2B	12.370	4.877	4.877	1.00	2.59	19.126	3.92	4.750	5.65	-	-	1364.5	221.3	NT
3B	12.624	4.343	4.928	0.88	2.56	19.228	3.90	4.750	5.65	-	-	1454.1	259.5	NT
1C	25.298	4.318	4.851	0.89	5.21	19.126	3.94	4.801	2.82	-	-	2606.4	233.5	BRG
2C	25.248	4.394	4.877	0.90	5.18	19.075	3.91	4.699	2.82	-	-	2378.6	209.8	BRG
S5C	28.956	4.674	4.851	0.96	5.97	18.948	3.91	4.750	2.82	-	-	2583.2	187.5	BRG
S3C	28.753	4.928	4.826	1.02	5.96	19.482	4.04	4.750	2.82	-	-	2726.1	188.9	BRG
S2D	28.550	4.902	4.928	0.99	5.79	19.609	3.98	4.750	5.65	-	-	2708.9	189.6	BRG
S3D	28.677	4.928	4.851	1.02	5.91	19.050	3.93	4.750	5.65	-	-	2774.2	192.4	BRG
S5D	28.802	4.764	4.826	0.97	5.97	19.431	4.03	4.750	5.65	-	-	2773.7	202.1	BRG

Table 14a - Bolted Joint Data for II_c $[\pm 45/(0/90)/(0/90)/\pm 45]_{3S}$

US CUSTOMARY UNITS

SPEC ID	WIDTH (IN)	THICKNESS (IN)	HOLE DIAMETER (IN)	t/D	W/D	EDGE DISTANCE (IN)	e/D	BOLT DIAMETER (IN)	FASTNER TORQUE (IN)	BEARING DAMAGE LOAD (LB)	BEARING DAMAGE STRESS (Ksi)	FAILURE LOAD (LB)	FAILURE STRESS (Ksi)	FAILURE MODE
1E	1.490	0.191	0.508	0.38	2.93	1.996	3.93	0.498	100	7500	26.4	8940	31.4	NT
2E	1.483	0.190	0.508	0.37	2.92	1.994	3.93	0.498	100	7200	25.6	9120	32.4	NT
3E	1.484	0.191	0.508	0.38	2.92	1.999	3.94	0.498	100	7300	25.8	8950	31.6	NT
1F	1.470	0.189	0.509	0.37	2.89	2.004	3.93	0.498	200	7400	26.6	8780	31.6	NT
2F	1.491	0.190	0.508	0.37	2.94	1.998	3.93	0.498	200	7600	26.8	8980	31.7	NT
3F	1.495	0.190	0.509	0.37	2.94	1.996	3.92	0.498	200	7700	27.1	9450	33.3	NT
1G	2.992	0.176	0.506	0.35	5.91	2.009	3.97	0.498	100	-	-	12610	23.9	BRG
2G	2.990	0.175	0.507	0.35	5.90	2.010	3.96	0.498	100	-	-	12020	23.0	BRG
3G	2.898	0.172	0.507	0.34	5.72	2.010	3.96	0.498	100	-	-	11970	23.3	BRG
1H	2.992	0.173	0.505	0.34	5.92	2.009	39.8	0.498	200	-	-	11780	22.8	BRG
S1C	2.999	0.182	0.506	0.36	5.93	2.005	3.96	0.497	200	-	-	12259	22.5	NT
S1D	2.999	0.186	0.506	0.37	5.93	2.004	3.96	0.497	200	-	-	11682	20.9	NT
S4C	3.013	0.191	0.508	0.38	5.93	2.006	3.95	0.497	200	-	-	10757	18.7	NT

Table 14b - Bolted Joint Data for II_c $[\pm 45/(0/90)/(0/90)/\pm 45]_{3S}$ METRIC UNITS

SPEC ID	WIDTH (mm)	THICKNESS (mm)	HOLE DIAMETER (mm)	t/D	W/D	EDGE DISTANCE (mm)	e/D	BOLT DIAMETER (mm)	FASTNER TORQUE (Nm)	BEARING DAMAGE LOAD (Kg)	BEARING DAMAGE STRESS (MPa)	FAILURE LOAD (Kg)	FAILURE STRESS (MPa)	FAILURE MODE
1E	37.846	4.851	12.903	0.38	2.93	50.698	3.93	12.649	11.30	3409.1	181.7	4063.6	216.6	NT
2E	37.668	4.826	12.903	0.37	2.92	50.648	3.93	12.649	11.30	3272.7	176.2	4145.5	223.1	NT
3E	37.694	4.851	12.903	0.38	2.92	50.775	3.94	12.649	11.30	3318.2	177.6	4068.2	217.7	NT
1F	37.338	4.801	12.929	0.37	2.89	50.902	3.93	12.649	22.60	3363.6	183.6	3990.9	217.9	NT
2F	37.871	4.826	12.903	0.37	2.94	50.749	3.93	12.649	22.60	3454.5	185.0	4081.8	218.5	NT
3F	37.973	4.826	12.929	0.37	2.94	50.698	3.92	12.649	22.60	3500.0	186.9	4295.5	229.4	NT
1G	75.997	4.470	12.852	0.35	5.91	51.029	3.97	12.649	11.30	-	-	5731.8	165.1	BRG
2G	75.946	4.445	12.878	0.35	5.90	51.054	3.96	12.649	11.30	-	-	5463.6	158.4	BRG
3G	75.921	4.369	12.878	0.34	5.72	51.054	3.96	12.649	11.30	-	-	5440.9	160.5	BRG
1H	75.997	4.394	12.878	0.34	5.92	51.029	3.98	12.649	22.60	-	-	5354.5	156.9	BRG
S1C	76.175	4.623	12.852	0.36	5.93	50.927	3.96	12.624	22.60	-	-	5560.6	155.1	NT
S1D	76.175	4.724	12.852	0.37	5.93	50.902	3.96	12.624	22.60	-	-	5289.9	144.1	NT
S4C	76.530	4.851	12.903	0.38	5.93	50.953	3.95	12.624	22.60	-	-	4879.3	128.9	NT

Table 15a - Bolted Joint Data For I_d $[(0/90)/\pm45/(0/90)]_{4S}$

US CUSTOMARY UNITS

SPEC ID	WIDTH (IN)	THICKNESS (IN)	HOLE DIAMETER (IN)	t/D	W/D	EDGE DISTANCE (IN)	e/D	BOLT DIAMETER (IN)	FASTNER TORQUE (IN)	BEARING DAMAGE LOAD (LB)	BEARING DAMAGE STRESS (Ksi)	FAILURE LOAD (LB)	FAILURE STRESS (Ksi)	FAILURE MODE
4C	1.115	0.260	0.375	0.69	2.97	1.511	4.03	0.372	60	-	-	8078	27.9	NT
5C	1.124	0.258	0.375	0.69	3.00	1.508	4.02	0.372	50	-	-	7773	26.8	NT
6C	1.124	0.254	0.375	0.68	3.00	1.509	4.02	0.372	50	-	-	8065	28.3	NT
4D	1.122	0.261	0.375	0.70	2.99	1.508	4.02	0.372	100	-	-	8034	27.4	NT
5D	1.123	0.255	0.375	0.68	2.99	1.509	4.02	0.372	100	-	-	8215	28.7	NT
6D	1.124	0.255	0.376	0.68	2.99	1.505	4.00	0.372	100	-	-	8186	28.6	NT
1C	2.298	0.237	0.376	0.63	6.11	1.474	3.92	0.372	50	-	-	16306	29.9	NT
2C	2.251	0.254	0.372	0.68	6.05	1.516	4.08	0.372	50	-	-	15302	26.8	NT
3C	2.264	0.259	0.375	0.69	6.04	1.514	4.04	0.372	50	-	-	14892	25.4	NT
1D	2.298	0.239	0.377	0.63	6.10	1.472	3.90	0.372	100	-	-	16655	30.3	NT
2D	2.246	0.253	0.373	0.68	6.02	1.517	4.07	0.372	100	-	-	16281	28.6	NT
3D	2.261	0.260	0.374	0.70	6.05	1.501	4.01	0.372	100	-	-	14906	25.4	NT

Table 15b - Bolted Joint Data For I_d $[(0/90)/\underline{+}45/\underline{+}45/(0/90)]_{4S}$ METRIC UNITS

SPEC ID	WIDTH (mm)	THICKNESS (mm)	HOLE DIAMETER (mm)	t/D	W/D	EDGE DISTANCE (mm)	e/D	BOLT DIAMETER (mm)	FASTNER TORQUE (Nm)	BEARING DAMAGE LOAD (Kg)	BEARING DAMAGE STRESS (MPa)	FAILURE LOAD (Kg)	FAILURE STRESS (MPa)	FAILURE MODE
4C	28.321	6.604	9.525	0.69	2.97	38.379	4.03	9.449	5.65	-	-	3664	192.19	NT
5C	28.550	6.553	9.525	0.69	3.00	38.303	4.02	9.449	5.65	-	-	3526	184.87	NT
6C	28.550	6.452	9.525	0.68	3.00	38.329	4.02	9.449	5.65	-	-	3658	194.82	NT
4D	28.499	6.629	9.525	0.70	2.99	38.303	4.02	9.449	11.30	-	-	3644	189.23	NT
5D	28.524	6.477	9.525	0.68	2.99	38.329	4.02	9.449	11.30	-	-	3726	197.86	NT
6D	28.550	6.477	9.550	0.68	2.99	38.227	4.00	9.449	11.30	-	-	3713	196.98	NT
1C	58.369	6.020	9.550	0.63	6.11	37.440	3.92	9.449	5.65	-	-	7396	206.49	NT
2C	57.175	6.452	9.449	0.68	6.05	38.506	4.08	9.449	5.65	-	-	6941	184.58	NT
3C	57.506	6.579	9.525	0.69	6.04	38.456	4.04	9.449	5.65	-	-	6755	175.15	NT
1D	58.369	6.071	9.576	0.63	6.10	37.389	3.90	9.449	11.30	-	-	7555	209.14	NT
2D	57.048	6.426	9.474	0.68	6.02	39.532	4.07	9.449	11.30	-	-	7385	197.62	NT
3D	57.429	6.604	9.590	0.70	6.05	38.125	4.01	9.449	11.30	-	-	6761	174.89	NT

Table 16a - Bolted Joint Data For II_d $[\pm45/(0/90)/(0/90)/\pm45]_{4S}$

US CUSTOMARY UNITS

SPEC ID	WIDTH (IN)	THICKNESS (IN)	HOLE DIAMETER (IN)	t/D	W/D	EDGE DISTANCE (IN)	e/D	BOLT DIAMETER (IN)	FASTNER TORQUE (IN)	BEARING DAMAGE LOAD (LB)	BEARING DAMAGE STRESS (Ksi)	FAILURE LOAD (LB)	FAILURE STRESS (Ksi)	FAILURE MODE
6A	1.124	0.263	0.376	0.70	2.99	1.516	4.03	0.373	50	-	-	8054	27.2	NT
7A	1.126	0.258	0.376	0.69	2.99	1.516	4.03	0.373	50	-	-	8311	28.6	NT
8A	1.128	0.253	0.376	0.67	3.00	1.514	4.03	0.373	50	-	-	8018	28.1	NT
6B	1.125	0.260	0.375	0.69	3.00	1.516	4.04	0.373	100	-	-	8211	28.1	NT
7B	1.126	0.257	0.376	0.68	2.99	1.503	4.00	0.373	100	-	-	8399	29.0	NT
8B	1.130	0.251	0.376	0.67	3.01	1.519	4.04	0.373	100	-	-	8275	29.2	NT
2A	2.252	0.252	0.376	0.67	5.99	1.508	4.01	0.373	50	-	-	16131	28.4	NT
3A	2.263	0.261	0.376	0.69	6.02	1.506	4.01	0.373	50	-	-	16584	28.1	NT
3B	2.262	0.261	0.376	0.69	6.02	1.516	4.03	0.373	50	-	-	14158	24.0	NT
9B	2.266	0.245	0.376	0.65	6.03	1.516	4.03	0.373	100	-	-	16247	29.3	NT
1B	2.255	0.240	0.375	0.64	6.01	1.493	3.98	0.373	100	-	-	15732	29.1	NT
2B	2.248	0.253	0.376	0.67	5.98	1.507	4.01	0.373	100	-	0	14141	24.9	NT

Table 16b - Bolted Joint Data for II_d $[\underline{+}45/(0/90)/(0/90)/\underline{+}45]_{4S}$ METRIC UNITS

SPEC ID	WIDTH (mm)	THICKNESS (mm)	HOLE DIAMETER (mm)	t/D	W/D	EDGE DISTANCE (mm)	e/D	BOLT DIAMETER (mm)	FASTNER TORQUE (Nm)	BEARING DAMAGE LOAD (Kg)	BEARING DAMAGE STRESS (MPa)	FAILURE LOAD (Kg)	FAILURE STRESS (MPa)	FAILURE MODE
6A	28.550	6.680	9.550	0.70	2.99	38.506	4.03	9.474	5.65	-	-	3653.2	187.5	NT
7A	28.600	6.553	9.550	0.69	2.99	38.506	4.03	9.474	5.65	-	-	3769.8	197.2	NT
8A	28.651	6.426	9.550	0.67	3.00	38.456	4.03	9.474	5.65	-	-	3636.9	193.7	NT
6B	28.575	6.604	9.525	0.69	3.00	38.506	4.04	9.474	11.30	-	-	3724.4	193.7	NT
7B	28.600	6.528	9.550	0.68	2.99	38.176	4.00	9.474	11.30	-	-	3809.7	199.9	NT
8B	28.702	6.375	9.550	0.67	3.01	38.583	4.04	9.474	11.30	-	-	3753.5	201.3	NT
2A	57.201	6.401	9.550	0.67	5.99	38.303	4.01	9.474	5.65	-	-	7316.9	195.8	NT
3A	57.480	6.629	9.550	0.69	6.02	38.252	4.01	9.474	5.65	-	-	7522.4	193.7	NT
3B	57.455	6.629	9.550	0.69	6.02	38.506	4.03	9.474	5.65	-	-	6422.0	165.5	NT
9B	57.556	6.629	9.550	0.65	6.03	38.506	4.03	9.474	11.30	-	-	7369.5	202.0	NT
1B	57.277	6.096	9.525	0.64	6.01	37.922	3.98	9.474	11.30	-	-	7135.9	200.6	NT
2B	57.099	6.426	9.550	0.67	5.98	38.278	4.01	9.474	11.30	-	-	6414.2	171.7	NT

Table 17a - Bolted Joint Data For I_e $[(0/90)/\pm 45/\pm 45/(0/90)]_{5S}$

US CUSTOMARY UNITS

SPEC ID	WIDTH (IN)	THICKNESS (IN)	HOLE DIAMETER (IN)	t/D	W/D	EDGE DISTANCE (IN)	e/D	BOLT DIAMETER (IN)	FASTNER TORQUE (IN)	BEARING DAMAGE LOAD (LB)	BEARING DAMAGE STRESS (Ksi)	FAILURE LOAD (LB)	FAILURE STRESS (Ksi)	FAILURE MODE
2A	1.498	0.324	0.505	0.64	2.97	1.989	3.94	0.497	100	-	-	11737	24.2	NT
2B	1.496	0.324	0.503	0.64	2.97	2.004	3.98	0.497	100	-	-	12673	26.1	NT
3A	1.492	0.323	0.504	0.64	2.96	2.004	3.98	0.497	100	-	-	12058	25.0	NT
3B	1.493	0.324	0.506	0.64	2.95	2.002	3.96	0.497	200	-	-	12302	25.4	NT
4A	1.504	0.318	0.503	0.63	2.99	2.002	3.98	0.497	200	-	-	12228	25.6	NT
4B	1.504	0.317	0.499	0.64	3.01	2.001	4.01	0.497	200	-	-	13276	27.8	NT
1A	3.018	0.307	0.507	0.61	5.95	1.989	3.92	0.497	100	22.35K	24.1	18.25K	19.7	NT
1B	3.016	0.307	0.504	0.61	5.98	1.998	3.96	0.497	100	18.58K	20.1	19.49K	21.1	BRG
5A	3.002	0.308	0.505	0.61	5.94	1.998	3.96	0.497	100	21.30K	23.0	22.21K	24.0	NT
5B	3.007	0.307	0.504	0.61	5.97	1.990	3.95	0.497	200	-	-	21.42K	23.2	NT
6A	2.999	0.297	0.503	0.59	5.96	1.995	3.97	0.497	200	17.10K	19.2	21.19K	23.8	NT
6B	2.998	0.297	0.505	0.60	5.94	2.023	4.01	0.497	200	12.30K	13.8	20.81K	23.5	NT

Table 17b - Bolted Joint Data For I_e $[(0/90)/\underline{+}45/\underline{+}45/(0/90)]_{5S}$

METRIC UNITS

SPEC ID	WIDTH (mm)	THICKNESS (mm)	HOLE DIAMETER (mm)	t/D	W/D	EDGE DISTANCE (mm)	e/D	BOLT DIAMETER (mm)	FASTNER TORQUE (Nm)	BEARING DAMAGE LOAD (Kg)	BEARING DAMAGE STRESS (MPa)	FAILURE LOAD (Kg)	FAILURE STRESS (MPa)	FAILURE MODE
2A	38.049	8.230	12.827	0.64	2.97	50.521	3.94	12.624	11.30	-	-	5324	166.8	NT
2B	37.998	8.230	12.776	0.64	2.97	50.902	3.98	12.624	11.30	-	-	5748.	180.3	NT
3A	37.897	8.204	12.802	0.64	2.96	50.902	3.98	12.624	11.30	-	-	5469.4	172.6	NT
3B	37.922	8.230	12.852	0.64	2.95	50.851	3.96	12.624	22.60	-	-	5580.	175.4	NT
4A	38.202	8.077	12.776	0.63	2.99	50.851	3.98	12.624	22.60	-	-	5547	176.3	NT
4B	38.202	8.052	12.675	0.64	3.01	50.825	4.01	12.624	22.60	-	-	6022	192.1	NT
1A	76.657	7.798	12.878	0.61	5.95	50.521	3.92	12.624	11.30	10138	166.4	8278.	135.8	NT
1B	76.606	7.798	12.802	0.61	5.98	50.749	3.96	12.624	11.30	8428	138.4	8841	145.2	NT
5A	76.251	7.823	12.837	0.61	5.94	50.749	3.96	12.624	11.30	9662	159.0	10074.	165.7	NT
5B	76.378	7.798	12.802	0.61	5.97	50.546	3.95	12.624	22.60	-	-	9716	160.0	NT
6A	76.175	7.544	12.776	0.59	5.96	50.673	3.97	12.624	22.60	7756	132.4	9612	164.1	NT
6B	76.149	7.544	12.827	0.60	5.94	51.384	4.01	12.624	22.60	5579	95.3	9485	162.0	NT

Table 18a - Bolted Joint Data For II_e $[\underline{+}45/(0/90)/(0/90)/\underline{+}45]_{5S}$

US CUSTOMARY UNITS

SPEC ID	WIDTH (IN)	THICKNESS (IN)	HOLE DIAMETER (IN)	t/D	W/D	EDGE DISTANCE (IN)	e/D	BOLT DIAMETER (IN)	FASTNER TORQUE (IN)	BEARING DAMAGE LOAD (LB)	BEARING DAMAGE STRESS (Ksi)	FAILURE LOAD (LB)	FAILURE STRESS (Ksi)	FAILURE MODE
2C	1.514	0.308	0.502	0.61	3.02	1.975	3.93	0.497	100	-	-	12333	26.5	NT
2D	1.513	0.311	0.501	0.62	3.02	1.979	3.95	0.497	100	-	-	12038	25.6	NT
3C	1.491	0.314	0.502	0.63	2.97	1.999	3.98	0.497	100	-	-	11989	25.6	NT
3D	1.491	0.319	0.500	0.64	2.98	2.005	4.01	0.497	200	-	-	12486	26.3	NT
4C	1.500	0.321	0.501	0.64	2.99	1.991	3.97	0.497	200	-	-	12039	25.0	NT
4D	1.502	0.327	0.503	0.65	2.99	2.014	4.00	0.497	200	-	-	12461	25.4	NT
1C	3.001	0.302	0.503	0.60	5.97	1.997	3.97	0.497	100	12.60K	13.9	21.37K	23.6	NT
1D	2.999	0.303	0.501	0.60	5.99	1.995	3.98	0.497	100	13.10K	14.4	20.25K	22.3	NT
5C	2.997	0.325	0.503	0.65	5.96	.1997	3.97	0.497	100	13.70K	14.1	21.84K	22.4	NT
5D	2.993	0.334	0.502	0.67	5.97	.1999	3.98	0.497	200	14.10K	14.1	22.41K	22.4	NT
6C	2.944	0.310	0.501	0.62	5.88	1.995	3.98	0.497	200	13.20K	14.5	20.26K	22.2	NT
6D	2.945	0.310	0.502	0.62	5.87	1.998	3.98	0.497	200	12.60K	13.8	21.20K	23.2	NT

REFERENCES

1. Hartsmith, L. J., "Bolted Joints in Graphite-Epoxy Composites", Douglas Aircraft Company, NASA Contract Report NASA CR-144899, June 1976.

2. Van Siclen, R. C., "Evaluation of Bolted Joints in Graphite Epoxy", Proceedings of the Army Symposium on Solid Mechanics, AMMRC-MS-74-8, September, 1984. pp. 120-138.

3. "Mechanically Fastened Joints", in Structural Design Guide for Advanced Composite Applications, 3rd ed., Vol. 2, Section 2.42, Air Force Materials laboratory, 1976.

4. DeJong, T., "Stresses Around Pin-Loaded Holes in Elastically Orthotropic or Isotropic Plates", Journal of Composite Materials, Vol. 11, July 1977, pp. 313-331.

5. Oplinger, D. W. and Gandhi, D. R., "Stresses in Mechanically Fastened Orthotropic Laminates", Proceedings of the 2nd Conference on Fibrous Composites in Flight Vehicle Design, May 1974, pp 813-834.

6. Harris, H. G. and Ojalvo, I.U., "Simplified 3-D Analysis of Mechanically Fastened Joints", AMMRC-MS-74-8, Army Materials and Mechanics Research Center, Watertown, MA, Sept. 1974, pp. 177-192.

7. Waszczak, J.P. and Cruse, T. A., "Failure Mode and Strength Predictions of Anisotropic Bolt Bearing Specimens", Journal of Composite Materials, Vol. 5, July 1971, pp. 421-425.

8. Wilson, D. W. and Pipes, R. B., "Analysis of the Shearout Failure Mode in Composite Bolted Joints", Proceedings of the 1st International Conference on Composite Structures, Paisley College of Technology, Scotland, (1981), pp. 34-49.

9. York, J. L., Wilson, D. W. and Pipes, R. B., "Analysis of Net Tension Failure in Composite Bolted Joints", J. of Reinforced Plastics and Composites, Vol. 1, (1982), pp. 141-153.

10. Ramkumar, R. L., "Bolted Joint Design", Test Methods and Design Allowables for Fibrous Composites, STP 734, American Society for Testing and Materials, Philadlephia, 1981, pp. 376-395.

11. Garbo, S. P. and Ogonowski, J. M., "Effect of Variances and Manufacturing Tolerances on the Design Strength and Life of Mechanically Fastened Composite Joints", AFWAL-TR-81-3041, Air Force Wright Aeronautical Laboratory, Dayton, OH, Vol 1 and 2, April 1982.

12. Chang, F. K., Scott, R. A. and Springer, G. S., "Strength of Mechanically Fastened Composite Joints", J. of Composite Materials, Vol. 16, pp.470-493, (1982).

13. Chang, F. K., Scott, R. A. and Springer, G. S., "Failure of Composite Laminates Containing Pin Loaded Holes-Method of Solution", J. of Composite Materials, Vol. 18, pp. 255-278, (1984).

14. Chang, F. K., Scott, R. A. and Springer, G. S., "Failure Strength of Nonlinearly Elastic Composite Laminates", J. of Composite Materials, Vol. 18, pp. 464-475, (1984).

15. Lekhnitskii, S. G., Anisotropic Plates, English Edition (Translated by S. W. Tsai and T. Cheron), Gordon and Breach, London, 1968.

16. Zhang, K. D. and Ueng, C. E., "Stresses Around A Pin Loaded Hole in Orthotropic Plates", Journal of Composite Materials, Vol. 18, Sept. 1984, pp. 432-446.

17. Hyer, M. W.,and Chang, E. C.,, "Contact Stresses in Pin Loaded Orthotropic Plates", Virginia Polytechnic Institute and State University, Report No. VPI-E-84-14, Blacksburg, VA 1984.

18. Soni, S. R., "Failure Analysis of Composite Laminates with a Fastened Hole", Journal of Composite Materials, STP 749, American Society for Testing and Materials, Philadelphia, PA, 1981, pp. 145-164.

19. Matthews, F. L., Wang, C. M. and Chryssafitis, S., "Stress Distribution Around a Single Bolt in Fibre Reinforced Plastic", Composites, Vol. 13, No. 3, July 1982 pp. 316-322.

20. Tsujimoto, Y. and Wilson, D. W., "Elasto-Plastic Failure Analysis of Composite Bolted Joints", Journal of Composite Bolted Joints", Journal of Composite Materials, in press.

21. Wilson, D. W. and Tsujimoto, Y., "On Phenomological Failure Criteria for Composite Bolted Joint Analysis", in review.

22. Whitney, J. M. and Nuismer, R. J., "Stress Fracture Criteria for Laminated Composites Containing Stress

Concentrations", Journal of Composite Materials, Vol. 8, July 1974, p. 253-265.

23. Pipes, R. B., Wetherhold, R. C. and Gillesipe, J. W., Jr., "Notched Strength of Composite Materials", Journal of Composite Materials, Vol. 13, April 1979, pp. 148-160.

24. Collings, T. A., "On the Bearng Strength of CFRP Laminates", Composites, july 1982, pp. 241-252.

25. Jurf, R. A., private communication.